# Post-transcriptional regulation by UNR: insights into histone mRNA metabolism and cellular senescence

Marta Inglés Ferrándiz

TESI DOCTORAL UPF / 2018

Thesis supervisor

Dra. Fátima Gebauer

GENE REGULATION, STEM CELLS AND CANCER PROGRAMME

CENTRE FOR GENOMIC REGULATION

Universitat Pompeu Fabra Barcelona

A l'Àvia

A mi madre y a mi padre

*It is our choices that show what we truly are,*
*far more than our abilities.*
J.K. Rowling

# Abstract

RNA-binding proteins guide post-transcriptional control of gene expression and are emerging as important regulators in disease. UNR (CSDE1) is a conserved RNA-binding protein that regulates mRNA stability and translation. In melanoma, UNR promotes metastasis and binds to around 1500 transcripts which encode, among other proteins, pro-metastatic regulators, histones and SASP (senescence associated secretory phenotype) factors. Here we study two separate aspects of UNR: its potential role in regulation of histone transcripts and its role in senescence.

UNR binds to mature histone transcripts upstream of the 3' UTR stem-loop, the main regulatory *cis* element of these mRNAs. RNA-Seq experiments revealed that histone mRNA levels are reduced upon UNR depletion. As UNR is mostly cytoplasmic we hypothesized that UNR might be regulating stabilization and/or translation in this cell compartment. Several approaches were undertaken to elucidate the molecular function of UNR in this context. However, we could not detect any specific role of UNR on histone mRNAs. If any, a non-specific effect of UNR in transcription was detected.

SASP factors are activated upon senescence induction. Using primary mouse keratinocytes (PMK) we explored the role of UNR in oncogene-induced senescence (OIS) and unveiled novel tumour suppressive properties of UNR. Depletion of UNR leads to senescence bypass, proliferation and immortalization. In addition, UNR contributes to modulation of the microenvironment through the SASP. RNA-seq analysis indicates that senescence bypass occurs concomitant with activation of cancer-related pathways, and without significant changes in the levels of cell cycle inhibitors. Our data suggest that UNR is an important regulator of the post-transcriptional senescent program. Further studies are necessary to elucidate the crucial UNR targets and/or partners in OIS.

# Resum

Les proteïnes d'unió a l'ARN guien el control posttranscripcional de l'expressió gènica i estan sorgint com a reguladors importants de malalties. UNR (CSDE1) és una proteïna conservada d'unió a l'ARN que regula l'estabilitat i la traducció de ARNs missatgers (ARNm). En melanoma, UNR promou la metàstasi i uneix al voltant de 1500 ARNm que codifiquen, entre d'altres proteïnes, per factors metastàtics, histones i factors SASP (fenotip secretor associat a la senescència). En aquesta tesi s'han estudiat dos funcions independents de UNR: el seu potencial paper en la regulació del metabolisme dels ARNm d'histones i el seu paper en la senescència cel·lular.

UNR s'uneix als ARNm madurs d'histones just per sobre de l'estructura anomenada *stem-loop*, a la part no traduïda 3'. Aquesta estructura és el principal element regulador en *cis* d'aquests ARNm. Gràcies a experiments de seqüenciació d'ARN vam observar que els nivells d'ARNm d'histones es redueixen quan es depleciona UNR de les cèl·lules. Com que UNR és majoritàriament citoplasmàtica, hem plantejat com a hipòtesi que UNR podria estar regulant l'estabilització i/o la traducció d'aquests ARNm en aquest compartiment cel·lular. Es van adoptar diversos enfocaments experimentals per aclarir la funció molecular de UNR en aquest context. No obstant això, no hem estat capaços de detectar quina és la funció específica que exerceix UNR en els ARNm d'histona. En qualsevol cas, es va detectar un efecte inespecífic de UNR en la transcripció.

Els factors SASP s'activen després de la inducció de senescència. Utilitzant queratinòcits primaris de ratolí (PMK), hem estudiat el paper de UNR en la senescència induïda per oncogens (OIS) i els nostres resultats suggereixen que UNR exerceix funcions de supressió tumoral. La depleció de UNR condueix a l'evasió de la senescència, la proliferació i la immortalització cel·lular. A més, UNR contribueix a la modulació de l'ambient extracel·lular a través dels factors SASP. L'anàlisi de

seqüenciació d'ARN suggereix que l'evasió de la senescència es produeix per l'activació de vies relacionades amb el càncer. Aquests canvis, però, es donen sense alterar els nivells de proteïnes inhibidores del cicle cel·lular. Les nostres dades suggereixen que UNR és un regulador posttranscriptional important del programa de senescència. Més estudis ajudaran a dilucidar tant els complexes com la identitat dels gens crucials regulats per UNR durant la OIS.

## Table of contents

# Abbreviations

| | |
|---|---|
| **aa** | amino acid |
| **ATP** | adenosine triphosphate |
| **ATR** | ataxia telangiectasia and rad3-related protein |
| **bp** | base pair |
| **BrdU** | 5-bromo-2-desoxiuridina |
| **CaCl2** | calcium chloride |
| **CBP80/20** | cap-binding protein complex 80/20 |
| **CCL** | cc chemokine ligands |
| **CDK** | cyclin-dependent kinases |
| **CFA** | colony forming assays |
| **CHK1/2** | checkpoint kinase 1/2 |
| **CM** | conditioned medium |
| **cpm** | counts per minute |
| **CPSF73** | cleavage and polyadenylation specificity factor 73 KDa subunit |
| **CSD** | cold-shock domain |
| **CSDE1** | cold shock domain-containing protein E1 |
| **CTIF** | cbp80/20-dependent translation initiation factor |
| **CTP** | cytidine triphosphate |
| **CXCL** | chemokine (c-x-c motif) ligand |
| **Cys or C** | cysteine |
| **DCC** | dosage compensation complex |
| **DDR** | dna damage response |
| **DMEM** | dulbecco's modified eagle's medium |
| **DNA** | deoxyribonucleic acid |
| **dNTPs** | deoxyribonucleotides |
| **dpi** | days post infection |
| **dsRBD** | double stranded RNA-binding domain |
| **DTT** | dithiothreitol |
| **E2F** | transcription factor 2F |
| **ECM** | extracellular matrix |
| **EGF** | epidermal growth factor |
| **EGTA** | ethylene glycol-bis(2-aminoethylether)-n,n,n′,n′-tetraacetic acid |
| **eIF4E** | eukaryotic translation initiation factor 4E |
| **eIF4G** | eukaryotic translation initiation factor 4G |
| **EMEM** | eagle's minimum essential medium |
| **EMSA** | electrophoretic mobility shift assays |
| **EMT** | epithelial–mesenchymal transition |
| **ERK** | extracellular regulated kinases |
| **FACS** | fluorescence activated cell sorting |
| **FBS** | fetal bovine serum |
| **FCS** | forward scatter |
| **Fw** | forward |
| **G-CSF** | granulocyte colony-stimulating factor |

| | |
|---|---|
| **GFP** | green fluorescent protein |
| **GM-CSF** | granulocyte-macrophage colony-stimulating factor |
| **GTP** | guanosine triphosphate |
| **HCC** | histone cleavage complex |
| **HDE** | histone downstream element |
| **HEPES** | 4-(2-hydroxyethyl)-1-piperazineethanesulfonic acid |
| **hESC** | human embryonic stem cells |
| **HGF** | hepatocyte growth factor |
| **HLB** | histone locus body |
| **HRV-2** | human rhinovirus 2 |
| **ICAM** | intercellular adhesion molecule |
| **iCLIP** | individual nucleotide resolution UV-crosslink and immunoprecipitation |
| **IGFBP** | insulin-like growth factor-binding protein |
| **IL** | interleukin |
| **iPMK** | immortal primary mouse keratinocytes |
| **IPTG** | isopropyl β-d-1-thiogalactopyranoside |
| **IRES** | internal ribosome entry site |
| **ITAF** | IRES *trans*-acting factors |
| **KCl** | potassium chloride |
| **KH** | k-homology domain |
| **KO** | knockout |
| **Luc** | luciferase |
| **M** | mitosis |
| **MAPK** | mitogen-activated protein kinases |
| **MCP** | monocyte chemoattractant proteins |
| **MDM2** | murine double minute 2 |
| **mESC** | mouse embryonic stem cells |
| **Met or M** | methionine |
| **MgCl2** | magnesium chloride |
| **MIP** | macrophage inflammatory proteins |
| **miRNA** | microRNA |
| **MMP** | matrix metalloproteinase |
| **MnSOD** | manganese-dependent superoxide dismutase |
| **mRNA** | messenger RNA |
| **msl-2** | male-specific lethal 2 |
| **mTOR** | mammalian target of rapamycin |
| **$Na_2HPO_4$** | disodium hydrogen phosphate |
| **NaCl** | sodium chloride |
| **NCBI** | national centre for biotechnology information |
| **NMD** | nonsense-mediated mRNA decay |
| **NO CM** | no conditioned medium |
| **NP-40** | nonidet p-40 |
| **NR** | nucleoplasmic reticulum |

| | |
|---|---|
| **nt** | nucleotide |
| **NTC** | normal termination codon |
| **OIS** | oncogene-induced senescence |
| **ORF** | open reading frame |
| **PABP** | poly(a)-binding protein |
| **PBS** | phosphate-buffered saline |
| **PCR** | polymerase chain reaction |
| **PI3K** | phosphatidylinositol-4,5-bisphosphate 3-kinase |
| **PMK** | primary mouse keratinocytes |
| **PMSF** | phenylmethanesulfonyl fluoride |
| **pRB** | retinoblastoma protein |
| **PTB** | poly pyrimidine tract-binding protein |
| **PTC** | premature termination codon |
| **PTEN** | phosphatase and tensin homolog |
| **PUMA** | p53 upregulated modulator of apoptosis |
| **PVDF** | polyvinylidene difluoride |
| **qPCR** | quantitative pcr |
| **RBD** | RNA-binding domain |
| **RBP** | RNA-binding protein |
| **Rev** | reverse |
| **RFP** | red fluorescent protein |
| **RNP** | ribonucleoprotein complexes |
| **ROS** | reactive oxygen species |
| **RRM** | RNA recognition motif |
| **RT** | retro-transcription |
| **RT-qPCR** | real-time polymerase chain reaction |
| **SA-b-Gal** | senescence-associated beta-galactosidase |
| **SAHF** | senescence-associated heterochromatin foci |
| **SASP** | senescence-associated secretory phenotype |
| **SDS** | sodium dodecyl sulphate |
| **SDS-PAGE** | SDS-polyacrylamide gel |
| **shCtrl** | short hairpin control |
| **shLuc** | short hairpin luciferase |
| **shRNA** | short hairpin RNA |
| **SLBP** | stem-loop binding protein |
| **SLIP1** | stem-loop interacting protein 1 |
| **SSC** | side scatter |
| **STRAP** | serine/threonine kinase receptor-associated protein |
| **SV40** | simian virus 40 |
| **SXL** | sex-lethal |
| **TGF-b** | transforming growth factor beta |
| **TIMP** | tissue inhibitors of metalloproteinases |
| **TNF** | tumour necrosis factor |
| **TUT7** | terminal uridylyl transferase 7 |

| | |
|---|---|
| **U7 snRNP** | U7 Small Nuclear Ribonucleoprotein |
| **UNR** | upstream of N-ras |
| **UNRIP** | UNR-interacting protein |
| **UPF1** | up-frameshift suppressor 1 homolog |
| **UTP** | uridine triphosphate |
| **UTR** | untranslated region |
| **UV** | ultraviolet |
| **VEGF** | vascular endothelial growth factor |
| **VIM** | vimentin |
| **WT** | wild type |

# Introduction

## 1. Post-transcriptional regulation and RNA-binding proteins: an overview

Post-transcriptional regulation involves all steps in the gene expression cascade that occur downstream of transcription. These comprise events in both the nucleus and the cytoplasm including splicing, 5' capping, 3' end formation, editing, RNA modification, nucleocytoplasmic transport, stability, translation, degradation and intracellular localization. Post-transcriptional regulation greatly contributes to expand the complexity of our genome, and plays key roles in virtually all biological processes.

The master orchestrators of post-transcriptional regulation are the RNA-binding proteins or RBPs. These proteins recognize sequence or structural *cis*-acting elements in the RNA and form ribonucleoprotein complexes (RNPs) that direct RNA fate (Gerstberger et al., 2014a; Glisovic et al., 2008; Keene, 2001; Mitchell and Parker, 2014). The combination of *cis*-regulatory elements in a given RNA dictates its particular post-transcriptional metabolism. In messenger RNA (mRNA), most *cis* elements reside in the 5' and 3' untranslated regions (UTRs), which serve as "platforms" for the binding of *trans*-acting regulatory factors that include not only RBPs but also non-coding RNAs (particularly microRNAs or miRNAs) (Fabian et al., 2010; Gebauer et al., 2012; Iadevaia and Gerber, 2015; Mayr, 2017). The reasons for this biased localization of regulatory elements are unclear, but the fact that the open reading frame (ORF) has been subjected to higher evolutionary pressure might have played a role.

RNPs are dynamic, they change in time and space depending on cellular environmental conditions. Key to these changes is the capacity of RBPs to recognize RNA and to interact with other factors forming flexible, moldable complexes (Achsel and Bagni, 2016). RBPs bind mRNA through their RNA-binding domains (RBDs). There are more than 30 identified RBDs, the best known being the RNA recognition motif (RRM), the cold-shock domain (CSD), the K-homology domain (KH), double stranded RNA

binding domain (dsRBD), Arginine-rich domain, zinc finger, PAZ and PIWI domains (Gerstberger et al., 2014a, 2014b). In addition, recent reports based on unbiased, high-throughput approaches have revealed unconventional RNA binding motifs, such as patches of positive amino acids, rossmann-fold domains or disordered regions (Baltz et al., 2012; Castello et al., 2012, 2016). These and other studies have tripled the number of known RBPs, which reach an estimated number of ~1400 in human cells (Albihlal and Gerber, 2018; Beckmann et al., 2016; Hentze et al., 2018).

The large number of RBPs, together with the fact that each RBP can bind hundreds of mRNAs, gives an idea of the enormous impact of post-transcriptional gene regulation. RBPs form regulatory networks that are finely tuned to keep cell homeostasis. In these networks, RBPs regulate groups of functionally-related transcripts termed “RNA regulons” (Imig et al., 2012; Keene, 2007). Cooperation between RBPs and combinatorial control lay at the basis of gene expression. Thus, an RBP cannot be considered in isolation, but in a given molecular and cellular environment. In addition, RBPs may come in multiple isoforms, with different capacities to interact with protein partners and RNA targets. Together, this may explain why, despite the fact that RBPs are highly conserved and less that 10% are expressed in a tissue-specific fashion, their functions are highly context-dependent.

Considering that RBPs are main players in post-transcriptional regulation, their dysregulation or mutation can lead to a variety of diseases including cancer (Castello et al., 2013; Cooper et al., 2009; Darnell, 2010; Lukong et al., 2008).

Some of the most prominent examples of RBPs with functions in cancer are Sam68 (involved in alternative splicing and translation), eIF4E (important for cap-dependent translation and nucleocytoplasmic transport), La (mediates IRES-dependent translation initiation) and HuR (with roles at multiple steps of RNA metabolism). Their downstream targets encode factors involved in tumorigenesis, cell proliferation, inhibition of apoptosis, invasion, angiogenesis or EMT (reviewed in

Pereira et al., 2017; Wurth, 2012). The data illustrate that each step of post-transcriptional regulation is important and contribute to malignancy.
This study is based on previous work from our laboratory where we describe that the RBP UNR (also called CSDE1) is an oncogene which promotes melanoma metastasis (Wurth et al., 2016). UNR contributes to cancerous traits at least in part by downregulating the levels of the tumor suppressor PTEN and increasing the translation of the EMT markers Vimentin and RAC1. UNR, however, binds numerous other transcripts, as revealed by iCLIP studies (Wurth et al., 2016) including histones and senescence markers which are the object of this thesis.
In the following section, I describe in detail the current knowledge about UNR.

## 2. UNR (Upstream of N-ras)

### 2.1. The Unr gene

The *Unr* gene was originally identified as a transcriptional unit located immediately upstream of *N-ras* (hence its name) (Jeffers et al., 1990). In humans, the most 5' transcription start site of *N-RAS* is located only 18 base pairs downstream of the last exon of *UNR*, although each gene contains its own promoter. This gene arrangement is evolutionarily conserved, which suggested that some kind of transcriptional inter-regulation might exist between these two genes (Ferrer et al., 1999; Jacquemin-Sablon and Dautry, 1992). It was described transcriptional interference of *Unr* on *N-ras*, but database analysis of the expression of both genes in a variety of cells and tissues does not support this hypothesis (Boussadia et al., 1997).

*Unr* is essential for embryonic development, as the homozygous knockout is embryonic lethal in mice (Saltel et al., 2017). Mortality occurs after 10 days of gestation, suggesting that UNR is not indispensable for general cell viability or division but rather essential for specific stages of

differentiation. In addition, UNR is highly conserved from *Drosophila* to mammals, although it is absent in yeast. In *Drosophila*, hypomorph *Unr* mutants die shortly after eclosion from the pupae, and overexpression of UNR is lethal, indicating that appropriate dosage of UNR is important for organismal viability (Patalano et al., 2009).

## 2.2. UNR transcripts

*UNR* pre-mRNA is subject of alternative splicing giving rise to six spliced variants that differ in the inclusion of exons 2, 3 and 6 (out of 21 exons), yielding mature transcripts that differ in their 5' UTR and coding sequence (Figure 1). In addition, there are 3 alternative polyadenylation signals within the 3' UTR, which give rise to transcripts containing 3′UTRs of approximately 200, 900 and 1250 nt.

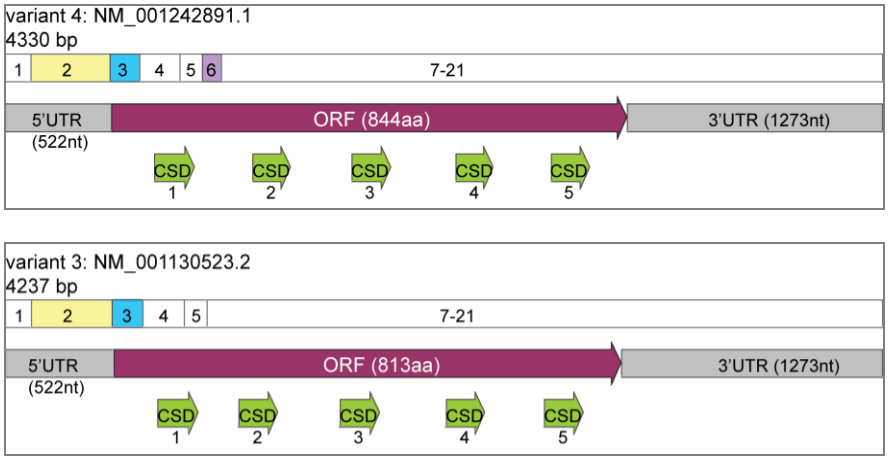

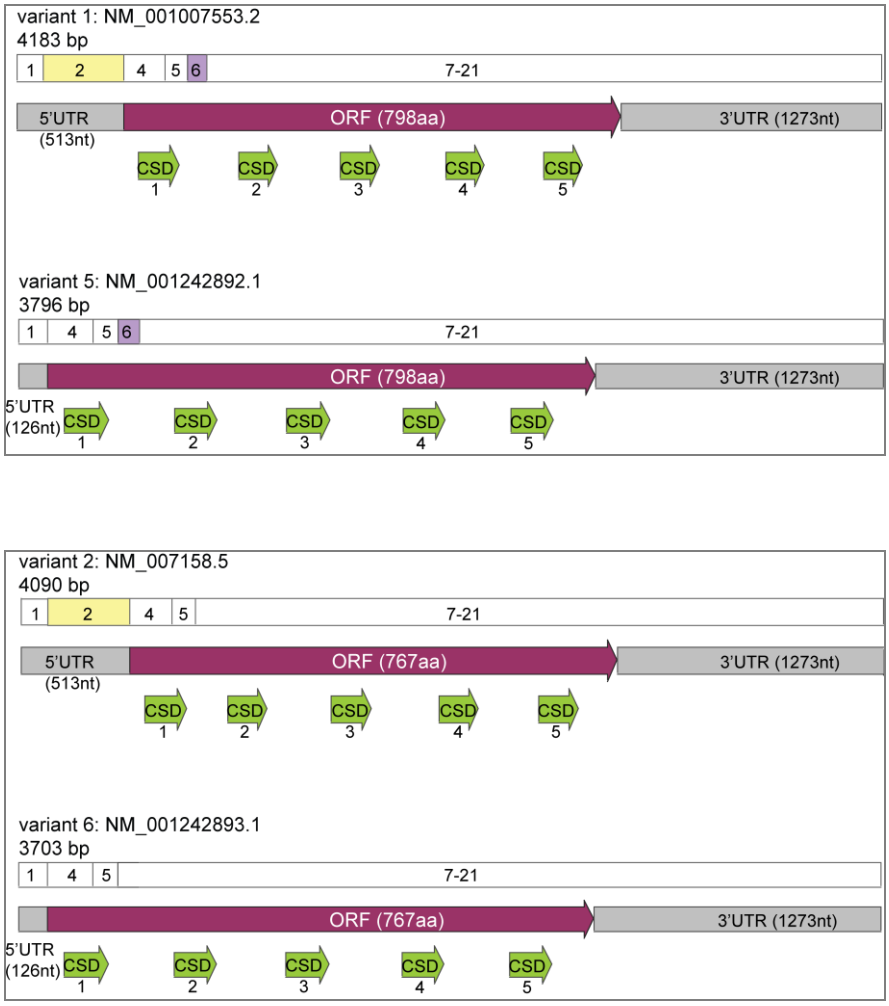


**Figure 1. UNR transcripts and protein variants.** Variants have been represented and numbered according to NCBI. The size of each transcript is shown below NCBI identifier. Numbered boxes represent exons. Transcript variants differ in the inclusion/exclusion of exons 2 (yellow), 3 (blue) and 6 (purple). Below are indicated the UTRs, the coding region and their corresponding sizes. Transcripts differing in the 3' UTR have not been drawn. Green arrows below ORFs represent the cold-shock domains.

## 2.3. UNR proteins

Alternative splicing yields four UNR protein isoforms (delimited in black rectangles in Figure 1), all of which contain five CSDs. CSDs are evolutionary conserved domains of approximately 70 amino acids found in bacteria and eukaryotes that allow binding to single stranded nucleic acids

(Graumann and Marahiel, 1998). CSDs present a beta-barrel fold with basic and aromatic amino acids that define the RNA-binding motifs RNP-1 and RNP-2 in the solvent exposed surface (Newkirk et al., 1994). In bacteria, CSD-containing proteins function as RNA-chaperones to modify RNA structure upon cold-stress (Graumann and Marahiel, 1998). In eukaryotes, CSDs are present in many proteins that – as UNR- do not necessarily function upon cold shock, and they are found either alone or in combination with other domains (Mihailovich et al., 2010). To the best of our knowledge, UNR is the only eukaryotic protein with such an arrangement of CSDs. The only other protein with a similar domain structure is bacterial ribosomal protein S1, which acts as an mRNA chaperone during bacterial translation (Duval et al., 2013).

## 2.4. Post-translational modifications

UNR is modified by phosphorylation and acetylation according to mass spectrometry analyses (see phosphosite database and Figure 2). While phosphorylation is found in unstructured regions, acetylation is most frequently found in CSDs. In addition, ubiquitylation, SUMOylation (small ubiquitin-like modifier), and arginine mono-methylation have been detected. The role of these modifications in UNR function have not been tested.

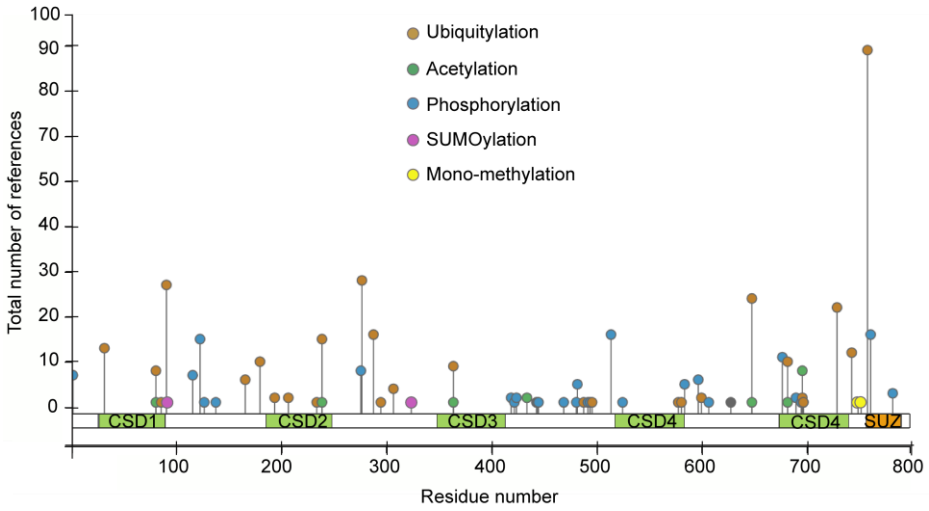


**Figure 2. Post-translation modifications of UNR according to Phosphosite.** Ubiquitylations, acetylations, phosphorylations, SUMOylations and mono-methylation are depicted in brown, green, blue, pink and yellow respectively.

## 2.5. UNR intracellular localization

UNR is a primarily cytoplasmic protein which has been found in the plasma membrane, the Golgi apparatus and a cytoplasmic structure called the nucleoplasmic reticulum (NR) (Saltel et al., 2017; Uhlen et al., 2015). More recently, also the mitochondrial inner membrane and stress granules have been associated to UNR (Youn et al., 2018; Zerbino et al., 2018). Unpublished data from our laboratory indicates that UNR co-localizes with a number of cytoplasmic structures in melanoma cells including the cytoskeleton (microtubules and intermediate filaments), the endoplasmic reticulum, the vesicle compartment and stress granules. However, we have been unable to confirm localization of UNR to the plasma membrane, the mitochondria or to the Golgi apparatus. In addition, a small amount of UNR can be found in the nucleus.

## 2.6. UNR expression in tissues

UNR plays a critical role in embryonic development in mice. Studies have shown that *Unr* knockout (KO) embryos die between E10.5 and E12.5. Up to E7.5 *Unr* KO are indistinguishable from their wild type counterparts. However, between E8.5 and E10.5 phenotypic differences start to arise (smaller embryos with delayed growth, incomplete closure of the neural tube or delayed heart maturation). A part from embryonic abnormalities, *Unr* deficient mice also present placental defects which are likely to be the cause of embryonic lethality (Saltel et al., 2017). In primary mouse erythroblasts UNR expression is increased compared to other hematopoietic lineages and exerts an important role in proliferation and differentiation (Moore et al., 2018).

In humans, UNR is almost ubiquitously expressed in adult tissues (Figure 3). A recent study demonstrates that UNR is highly expressed in hESC to keep their undifferentiated state and halt default neural fate (Lee et al., 2017).

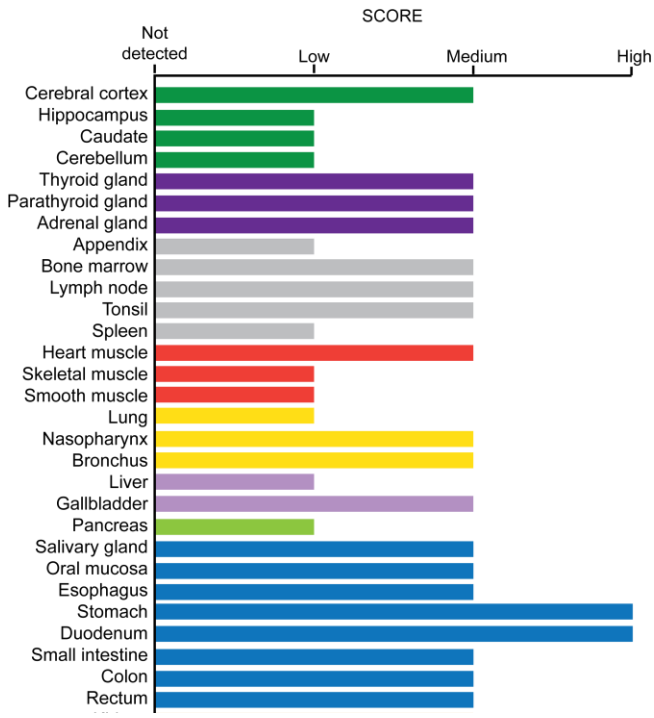

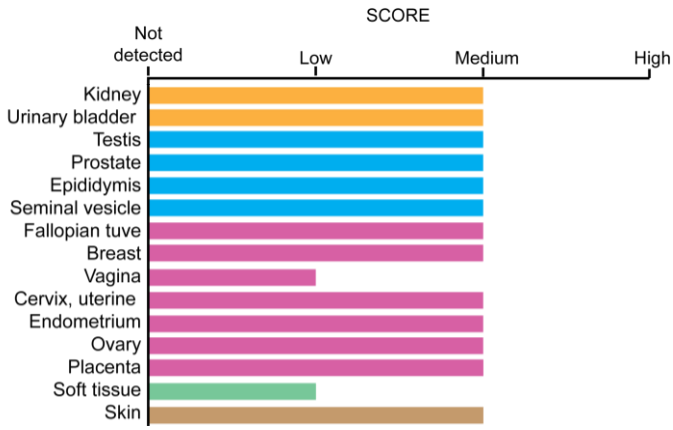


**Figure 3. UNR expression in human tissues according to The Human Protein Atlas.** Related organs are depicted with the same color.

## 2.7. Molecular functions of UNR

### 2.7.1. UNR as an IRES trans-acting factor (ITAF)

The most prevalent molecular function of UNR is that as a regulator of mRNA translation. Most mRNAs in the cell are translated by a mechanism whereby the $m^7G$ cap structure at the 5' end of the mRNA attracts the small ribosomal subunit during translation initiation. Cap-dependent translation is inhibited under stresses such as hypoxia, apoptosis, viral infection or amino acid starvation (Harvey and Willis, 2018). This allows global translation to be reduced, ameliorating the energetic burden in the cell until the stress situation is resolved. Transcripts encoding factors important in these conditions (e.g. those required to resolve stress) are usually translated by cap-independent mechanisms, such as that governed by IRESs (reviewed in Sriram et al., 2018). IRESs are long, structured regions usually located in the 5' UTR with the capacity to attract ribosomes in the absence of the cap (note, however, that small non-structured IRESs located throughout the mRNA have also been described [(Weingarten-Gabbay et al., 2016)]). IRES activity is modulated by RBPs that function as trans-acting factors (ITAFs).

UNR has been described as an ITAF in various contexts. UNR binds to human rhinovirus (HRV-2) and poliovirus type 1 IRESs (Boussadia et al., 2003; Hunt and Jackson, 1999; Hunt et al., 1999). All UNR CSD's are important to bind HRV-2 IRES as point mutation of a single CSD is enough to restrict translation stimulation *in vitro* (Brown, 2004). This suggests that UNR acts as an RNA-chaperone to maintain the IRES in an optimal conformation. In addition, UNR binds to the Apaf-1 IRES, where it has been shown to promote formation of an open structure that subsequently allows PTB binding and promotes ribosome landing (Mitchell et al., 2003).

Another context where UNR acts as ITAF is during mitosis. In that cell cycle phase UNR reaches its maximal expression and contributes to the synthesis of the CDK11/p58 PITSLRE protein through and IRES element in the ORF of the PITSLRE p100 mRNA (Tinton et al., 2005). The pattern of UNR expression during the cell cycle is, in fact, achieved via negative IRES-mediated autoregulation. In interphase, UNR binds to its own IRES and, together with PTB, inhibits its own expression (Cornelis, 2005; Dormoy-Raclet et al., 2005). Later, during G2/M, hnRNP C1/C2 competes with PTB binding, which in turn induces a conformational change in the IRES that displaces UNR, leading to active translation (Schepens et al., 2007).

### 2.7.2. Regulation of cap-dependent translation

UNR has been shown to repress cap-dependent translation of *Pabp1* mRNA. PABP1 itself stimulates UNR binding to the 5' UTR of its own transcript, establishing a negative auto-regulatory loop (Patel et al., 2005). Another extensively studied mechanism of negative regulation is that of *Drosophila msl-2* mRNA (Abaza, 2006; Duncan, 2006). Here, UNR and SXL bind cooperatively to the 3' UTR of *msl2* and impair the recruitment of the small ribosomal subunit to the mRNA (Gebauer et al., 2003; Hennig et al., 2014). PABP1 is also a partner of UNR in this case (Duncan et al., 2009), as well as Hrp48 (Szostak et al., 2018). Although the exact

mechanism of repression is still unclear, it seems to involve contacts of Hrp48 with the initiation factor eIF3d (Szostak et al., 2018).
In addition to regulating translation initiation, recent work from our group described a new function of UNR in promoting translation elongation of *VIM* and *RAC1* mRNAs in melanoma cells (Wurth et al., 2016).

In sum, UNR can have positive and negative roles in cap-dependent and cap-independent translation. How UNR interacts with the translation machinery to achieve these functions is not understood, but a role of UNR as an RNA chaperone may underlie many of these functions.

### 2.7.3. Regulation of mRNA stability

UNR has been shown to modulate RNA stability, both in a positive and negative manner. Perhaps the best known example pertains *c-Fos* mRNA. This transcript contains a region in the ORF termed “the major protein-coding region determinant of instability (mCRD)”, which is bound by a complex of UNR and PABP, among other proteins, connecting the mCRD with the poly(A) tail (Grosset et al., 2000). Prior to translation initiation, the complex protects the poly(A) tail from the attack of CCR4 (deadenylase protein). As the ribosome transits the mCRD, the complex is disrupted allowing CCR4 to access de poly(A) tail leading to deadenylation and decay (Chang, 2004). Thus, the case of *c-Fos* mRNA is a clear example of translation-dependent mRNA decay, unlike many other mRNAs where translation protects from degradation.
In addition to *c-Fos* mRNA, UNR has been reported to promote parathyroid hormone (PTH) mRNA stability by binding to the 3’ UTR together with the stability regulator AUF1 (Dinur et al., 2006).

Contrary to the cases described above, UNR promotes mRNA destabilization of *Gata6* mRNA in mouse embryonic stem cells (ESC), contributing to maintain their undifferentiated state (Elatmani et al., 2011). UNR regulates the steady-state levels of many transcripts in melanoma cells (Wurth et al., 2016) and hESC (Lee et al., 2017). In hESC, proper

stability assays have been performed to confirm either stabilization or destabilization of some of these transcripts.

## 2.8. UNR protein partners

As mentioned above, UNR can regulate a variety of mRNAs in several different aspects of their metabolism. This flexibility is achieved by the ability of UNR to interact with different protein partners. One of these is PABP1, an important partner in regulation of mRNA translation and stability, which interacts with UNR in humans (Grosset et al., 2000; Patel et al., 2005; Ray and Anderson, 2016) and in *Drosophila* (Duncan et al., 2009). PTB is also a functional partner of UNR in regulation of IRES-mediated translation, but no direct interactions have been described between the two proteins (Cornelis, 2005; Hunt et al., 1999; Mitchell et al., 2003). UNR interacts with the translational repressor 4E-T (an eIF4E-binding protein) but the functional relationship between these two proteins is unclear (Kamenska et al., 2016). In *Drosophila*, UNR interacts with the RNA helicase MLE to modify the structure of the lncRNA *roX2* (Militti et al., 2014) and with SXL and Hrp48 to regulate the translation of *msl-2* mRNA (Abaza, 2006; Duncan, 2006; Hennig et al., 2014; Szostak et al., 2018). These interactions allow UNR to regulate X-chromosome dosage compensation in a sex-specific manner.

The most prevalent complex partner of UNR is a 38 kDa WD40-family protein called UNRIP (for UNR-interacting protein) or STRAP (for Serine/Threonine kinase receptor-associated protein) (Hunt et al., 1999). Curiously, except for a minor role of UNRIP in the expression of select UNR targets in erythroid cells, it is unknown how UNRIP influences UNR function (Moore et al., 2018).

## 2.9. UNR binding specificity

SELEX (systematic evolution of ligands by exponential enrichment) was used to determine the RNA-binding specificity of UNR *in vitro* (Triqueneaux et al., 1999). In this study, two related consensus

sequences were identified, characterized by a conserved core motif AAGUA/G or AACG downstream of a purine stretch. A very similar motif was found *in vivo* in melanoma cells by using iCLIP (individual nucleotide resolution UV-crosslink and immunoprecipitation) (Wurth et al., 2016). Here, center of UNR binding peaks coincide with the motif in ORFs but not in UTRs, suggesting different rules governing UNR binding to these sections of the transcript.

Purine-rich sequences have been shown to bind UNR in the *c-Fos* mCRD (Grosset et al., 2000), PITSLRE (*CDK11/p58*) IRES (Tinton et al., 2005) and *UNR* IRES (Schepens et al., 2007), as well as in the lncRNA *roX2* (Militti et al., 2014). Altogether, it seems that despite the presence of a preferred purine-rich consensus binding motif, UNR binding specificity is relaxed and is increased by UNR protein partners. An illustrating example is that of UNR and SXL binding to *msl-2* 3' UTR. These two proteins bind cooperatively to adjacent sites on the mRNA: the affinity of SXL increases 10-fold in the presence of UNR, while that of UNR increases 1000-fold in the presence of SXL. The consequence is that UNR does not bind to *msl-2* mRNA unless i) SXL is present and ii) a SXL binding site is found in close proximity on the mRNA (Hennig et al., 2014).

## 2.10. Cellular and biological functions of UNR

One of the best characterized roles of UNR is that played in the regulation of X-chromosome dosage compensation in *Drosophila* (Graindorge et al., 2011). UNR has sex-specific opposite functions in this system: in females, it represses dosage compensation by inhibiting the translation of *msl-2*, which encodes a rate-limiting component of the dosage compensation complex (DCC) (Abaza, 2006; Duncan, 2006). Here, UNR forms a complex with SXL and Hrp48 on the 3' UTR of *msl-2*, leading to inhibition of recruitment of the small ribosomal subunit (Abaza, 2006; Hennig et al., 2014; Szostak et al., 2018). In males, UNR binds to two DCC components, the RNA helicase MLE and the lncRNA *rox2*, resulting in

*roX2* structural remodeling during initial steps of DCC assembly (Militti et al., 2014).

Even though conserved, mammalian UNR is not known to be involved in dosage compensation. However, UNR performs a variety of functions in mammalian cells. First, UNR can have positive or negative roles in apoptosis. In mESC cells, UNR promotes apoptosis upon ionizing radiation as clonogenic survival of *Unr* $^{-/-}$ cells was enhanced compare to wild type cells (Dormoy-Raclet et al., 2007). In contrast, UNR has an anti-apoptotic function in untreated and irradiated human hepatoma HuH7 cells (Dormoy-Raclet et al., 2007). Second, UNR is regulated in a cell-cycle dependent manner. UNR is highly expressed in G2/M, where it regulates the translation of CDK11/p58, a kinase required for spindle morphogenesis and centrosome maturation (Schepens et al., 2007). Consistent with these roles, depletion of UNR retards mitosis in HEK293T cells (Schepens et al., 2007). UNR is also involved in mouse erythroblast proliferation and differentiation, and is a factor altered in Diamond Blackfan Anemia (DBA) (Horos et al., 2012; Moore et al., 2018). It is unclear how UNR contributes to erythroblast biology, but a number of mRNAs have been shown to be bound by UNR in this system (Moore et al., 2018).

A third prevalent role of UNR is in preserving ESC stemness. UNR expression prevents differentiation of mESC into primitive endoderm (Elatmani et al., 2011). Similarly, UNR is highly expressed in hESC where it prevents their intrinsic neural differentiation (Lee et al., 2017). For both mESC and hESC, destabilization of specific mRNA targets by UNR (*Gata6* in the case of mESCs and *FABP7* and *VIM* in the case of hESCs) has been proposed to underlie the UNR effect.

Finally, UNR behaves as an oncogene in melanoma. UNR coordinates a set of mRNA regulons promoting invasion, anoikis resistance and metastasis (Wurth et al., 2016). In this work, UNR was found to bind hundreds of transcripts which were regulated in a coordinated manner at the levels of translation and mRNA steady state. In particular, regulation

of *VIM* and *RAC1* mRNA translation was shown to contribute to the tumorigenic properties of melanoma cells. Consistent with its role as an oncogene, UNR is overexpressed in primary and metastatic melanoma samples compared to benign nevi (Wurth et al., 2016). In contrast, high UNR expression was associated with longer progression-free survival after surgery in pancreatic ductal adenocarcinoma, suggesting a tumor suppressor role for UNR (Martinez-Useros et al., 2017). Thus, again, UNR can have diverse and even opposite roles depending on context.

In summary, UNR is key regulator of post-transcriptional gene expression that is involved in diverse biological processes by binding to RNAs depending on cellular context and through a variety of mRNP complexes.

Work in the lab has revealed that UNR binds to around 1500 transcripts in melanoma cells (Wurth et al., 2016). In addition to mRNAs encoding oncogenes and tumor suppressors, UNR binds to two other major RNA groups: those encoding histones and factors of the Senescence Associated Secretory Phenotype (SASP). This thesis aims to decipher the role of UNR in regulation of these transcripts. Therefore, in the next two sections I will briefly introduce the subjects of histone mRNA metabolism and senescence.

# 3. Histones

## 3.1. Histone proteins and their encoding transcripts

Histone proteins package approximately two meters of DNA inside the nucleus of each cell. An octamer of four histone core proteins constitute the basic chromatin unit, the nucleosome (H2A, H2B, H3 and H4). In addition, Histone H1, binds to the linker DNA regions between nucleosomes, as well as on the nucleosomes themselves (Li and Reinberg, 2011).

Histone proteins can be classified into replication-dependent (canonical) and replication-independent. Replication-dependent histones are

constituents of the nucleosome. They are mainly expressed during S phase to package the newly synthesized DNA. The mRNAs that code for each replication-dependent histone are highly similar in sequence and they do not contain introns. In addition, they are the only mRNAs in the cell that lack poly(A) tails (see below); instead, they contain a stem-loop structure in the 3' UTR which is crucial for all steps of histone mRNA metabolism (Marzluff and Koreski, 2017). Conversely, replication-independent histones are expressed throughout the cell cycle, can have significant differences in primary sequence, their mRNAs can contain introns and are often polyadenylated (Kouzarides, 2007; Marzluff et al., 2002). Some replication-independent variants can replace core histones, leading to different nucleosome composition depending on the cell type, differentiation or developmental stage, including diseased states such as cancer (Kamakaka, 2005; Maze et al., 2014).

### 3.2. Replication-dependent histone genes

In all metazoans, the replication-dependent histone genes are clustered together in the genome. In humans, clusters are located in three main loci: *HIST1*, located in chromosome 6, contains fifty-five genes; *HIST2* and *HIST3*, both located in chromosome 1, contain six and three histone genes, respectively. All clusters also contain several pseudogenes (Marzluff et al., 2002). All genes contain distinct promoters and 5'- 3' untranslated regions, but the sequence encoding the ORF of each core histone is highly similar. Thus, each individual gene contributes to a fraction of the total pool of histone proteins. It is not clear whether the variation existing between histone genes has any functional significance or is rather a residual variation that has been permitted by evolution (Marzluff et al., 2002). It is also unclear why histone genes have evolved remaining physically linked. As regulation of all histone genes requires common regulatory molecules, a possibility is that genomic linkage facilitates coordinate regulation (Marzluff et al., 2002).

The Histone Locus Body (HLB) is a specialized nuclear domain where replication-dependent histone mRNAs are processed. Proteins like NPAT (nuclear protein at the ataxia-telangiectasia locus), FLASH (FLICE-associated huge protein) and U7 snRNP (U7 small nuclear ribonucleoprotein) are required for HLB formation, creating and optimal environment for competent histone transcription and processing (Barcaroli et al., 2006a, 2006b; Frey and Matera, 1995; Ye et al., 2003). For more information about transcriptional regulation of these genes, please go to Marzluff and Koreski, 2017.

### 3.3. Post-transcriptional regulation of histone mRNAs

Histone mRNAs are expressed and regulated in a cell cycle-dependent manner. They accumulate during G1/S transition due to a dramatic increase in their transcription and pre-mRNA processing, giving rise to an overall ~35-fold increase in the percentage of mature histone mRNA that reach the cytoplasm (Marzluff and Koreski, 2017). During S phase, concomitant with DNA replication, histone mRNAs are highly translated. At the end of S phase, when DNA replication is inhibited, translationally active histone mRNAs are rapidly degraded to ensure a sharp inhibition of histone protein production (Kaygun and Marzluff, 2005a) (Figure 4).

The stem-loop binding protein (SLBP) is a cell cycle regulated protein that binds to the 5' side of the stem-loop structure in the 3' UTR of histone mRNAs (Brooks et al., 2015; Slevin et al., 2014). Similar to histone mRNAs, SLBP is synthesized when cells enter S phase and degraded at the end of the same phase. This protein is required for all steps of histone mRNA metabolism (Dominski et al., 1995; Mullen and Marzluff, 2008; Sanchez and Marzluff, 2002; Sullivan et al., 2009) (Figure 4). Despite the fact that histone mRNA levels parallel those of SLBP, their regulation is uncoupled. Cessation of DNA replication results in rapid degradation of histone mRNAs without affecting SLBP levels (Whitfield, 2004) and stabilization of SLBP does not prevent histone mRNA degradation at the end of S phase (Zheng et al., 2003).

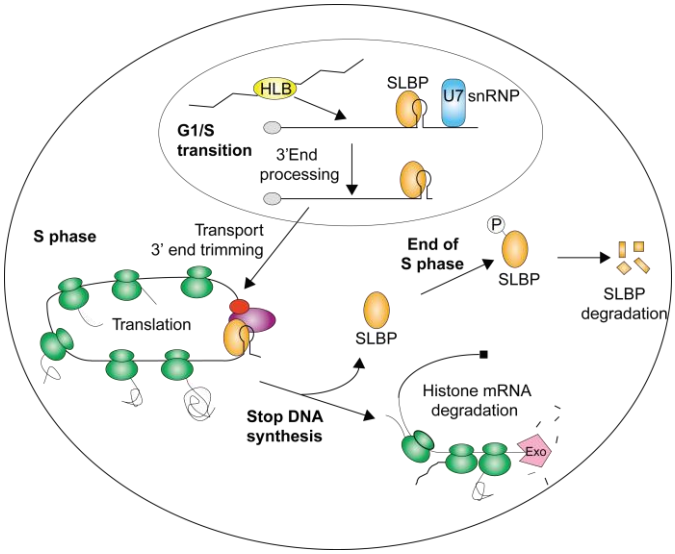


**Figure 4. Life cycle of histone mRNAs.** Histone mRNAs are transcribed in the. After 3' end processing in the nucleus, the 3' end is further trimmed in the cytoplasm where mRNAs are translated and degraded (see text for details). SLBP participates in all steps of the histone mRNA life cycle. Adapted from Marzluff and Duronio, 2002.

### 3.3.1. Histone 3' end formation

Because replication-dependent histone mRNAs do not contain introns, their co-transcriptional regulation basically consists of modulation of 3' end formation, that is, the endonucleolytic cleavage that gives rise to the 3' end of mature histone mRNAs. Two cis regulatory elements are essential for this process: the stem-loop and a downstream purine rich sequence termed Histone Downstream Element (HDE) (Dominski and Marzluff, 2007).

As soon as the 3' end is transcribed, SLBP binds to the stem-loop and the HDE base pairs with the 5' end of U7 snRNA (Marzluff and Koreski, 2017) (Figure 5). Apart from the U7 snRNA, the U7 snRNP contains five Sm proteins (SMB, SMD3, SMG, SME and SMF) and two Sm-like proteins LSM10 and LSM11 (Pillai, 2001, 2003). SLBP stabilizes the U7 snRNP on histone pre-mRNA through interactions with the protein FLASH (Skrajna

et al., 2017). Interaction of LSM11 with FLASH is essential to recruit the Histone Cleavage Complex (HCC) containing the Symplekin, CstF64, CPSF100 and the CPSF73 endonuclease, among other proteins (Sabath et al., 2013; Yang et al., 2013). Cleavage is catalyzed by CPSF73, the same protein that cleaves other pre-mRNAs during cleavage/polyadenylation (Dominski et al., 2005) (Figure 5).

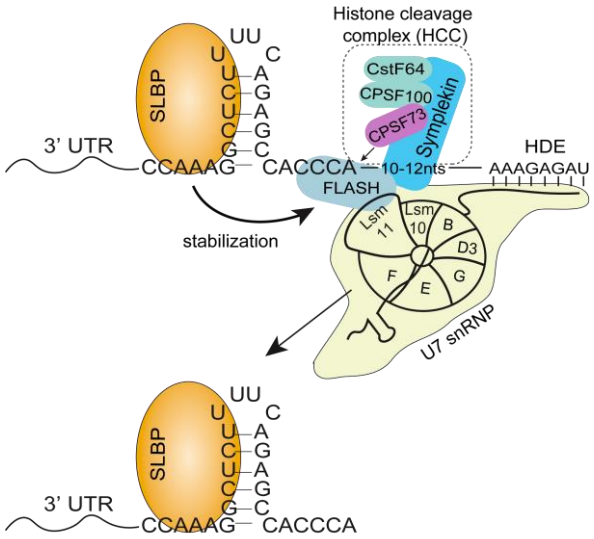


**Figure 5. Histone pre-mRNA 3' end formation.** Representation of the essential components of the processing reaction. CPSF73 cleaves the 3' UTR 5 nucleotides after the stem-loop structure. Adapted from Marzluff and Koreski, 2017.

Recently, the transcription elongation rate has been connected with histone pre-mRNA 3' end formation. Slow transcription leads to a defective stem-loop conformation, resulting in aberrant 3' end formation and accumulation of polyadenylated histone mRNA (Saldi et al., 2018).

After endonucleolytic cleavage, histone mRNAs are exported to the cytoplasm in a process that requires SLBP (Sullivan et al., 2009). Here, the 3' UTR is trimmed to 3 nucleotides after the stem-loop by the 3'hExo exonuclease, which binds to the 3' end of the stem-loop resulting in

mature mRNA (Tan et al., 2013; Yang et al., 2006). In case trimming proceeds further, the length of the mRNA is repaired by urydilation (Lackey et al., 2016).

### 3.3.2. Histone mRNA translation

During translation initiation of most mRNAs, ribosomes are recruited to the mRNA via interactions between translation initiation factors (eIFs), the mRNA and the small ribosomal subunit. Briefly, the cap binding complex (formed by the cap binding protein eIF4E, the scaffolding protein eIF4G and the RNA helicase eIF4A) binds to the 5' cap structure of the mRNA and, through interactions between eIF4G and ribosome-bound eIF3, ribosomes are recruited to the mRNA (reviewed in Merrick and Pavitt, 2018). Another factor, PABP, binds to the poly(A) tail and to eIF4G, leading to a closed-loop conformation of the mRNA which is thought to be optimal for translation (Figure 6a).

Histone mRNAs lack a poly(A) tail, but they have found alternative ways to achieve a closed-loop conformation. These transcripts seem to preferentially use the CPB80/20 complex (which recognizes the cap in the nucleus) for translation rather than the more typical cytoplasmic eIF4E complex (Choe et al., 2013). SLBP interacts with CTIF (CBP80/20-dependent translation interaction factor), effectively establishing a closed-loop and directly binging to eIF3 (Choe et al., 2013, 2014) (Figure 6b). SLBP also interacts with SLIP1 (Stem-loop interacting protein 1), a protein that is required for translation and interacts with eIF4G and eIF3 (Cakmakci et al., 2008; Neusiedler et al., 2012) (Figure 6b). Structures in the histone ORF and 3' UTR have been shown to contribute to translation regulation (Martin et al., 2011).

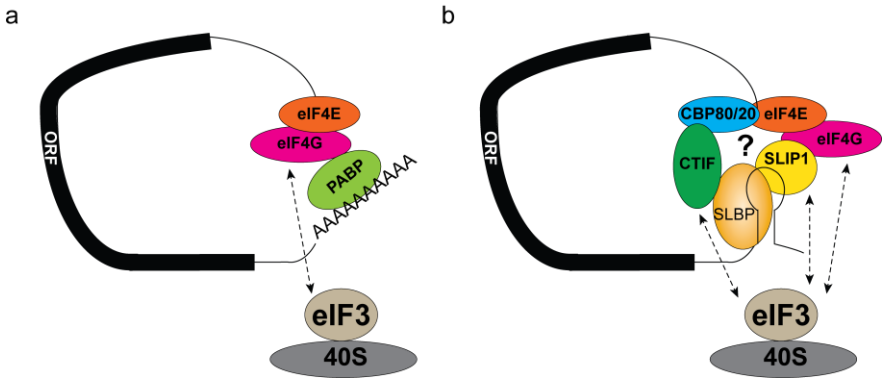


**Figure 6. Translation initiation models. (a)** Translation initiation model for non-histone mRNAs. **(b)** Histone mRNAs translation initiation strategy is has not yet been completely elucidated as several mechanisms implying different factors have been described. The two possible pathways concerning histone mRNA metabolism are not mutually exclusive. The main mechanism might vary depending on cell types.

### 3.3.3. Histone mRNA degradation

Nearly 30 years ago, it was suggested that active translation of histone mRNAs was required for their degradation (Graves, 1987). Later, it was shown that in addition to active translation, the presence of the stem-loop at a proper distance (30-70 nt) from the stop codon was required, suggesting a connection between translation termination and histone mRNA degradation (Kaygun and Marzluff, 2005a). As histone mRNA degradation in the cytoplasm occurs upon completion of DNA synthesis in the nucleus, an efficient crosstalk between these two cell compartments must exist. This crosstalk was proposed to be achieved by ATR and UPF1. ATR, a kinase activated during replication stress, phosphorylates UPF1, a protein originally identified a as a key factor in NMD (Non-sense Mediated Decay), which in turn interacts with SLBP and activates degradation (Kaygun and Marzluff, 2005b). A direct interaction of UPF1 with the mRNA just upstream of the stem-loop has been reported (Brooks et al., 2015). During degradation, 3'hExo trims the mRNA from the 3' end (Hoefig et al., 2013), generating degradation intermediates that are heavily uridylated by TUT7 (Lackey et al., 2016). Oligouridylated mRNAs

are bound by the Lsm1-7 complex, which promotes decapping with subsequent 5'-to-3' mRNA degradation (Marzluff and Koreski, 2017; Mullen and Marzluff, 2008; Slevin et al., 2014). (Figure 7)

However, the main mechanism of degradation involves 3'-to-5' exonucleolytic digestion of the mRNA by the exosome (Marzluff and Koreski, 2017; Mullen and Marzluff, 2008). Oligouridylated intermediates still have SLBP bound to the 3' UTR which this blocks further degradation. After 3'hExo digestion into the stem-loop, however, SLBP is removed, allowing further degradation by the exosome. Analysis of degradation intermediates is consistent with ribosomes periodically stalling, again indicating that degradation occurs on actively translating histone transcripts (Slevin et al., 2014).

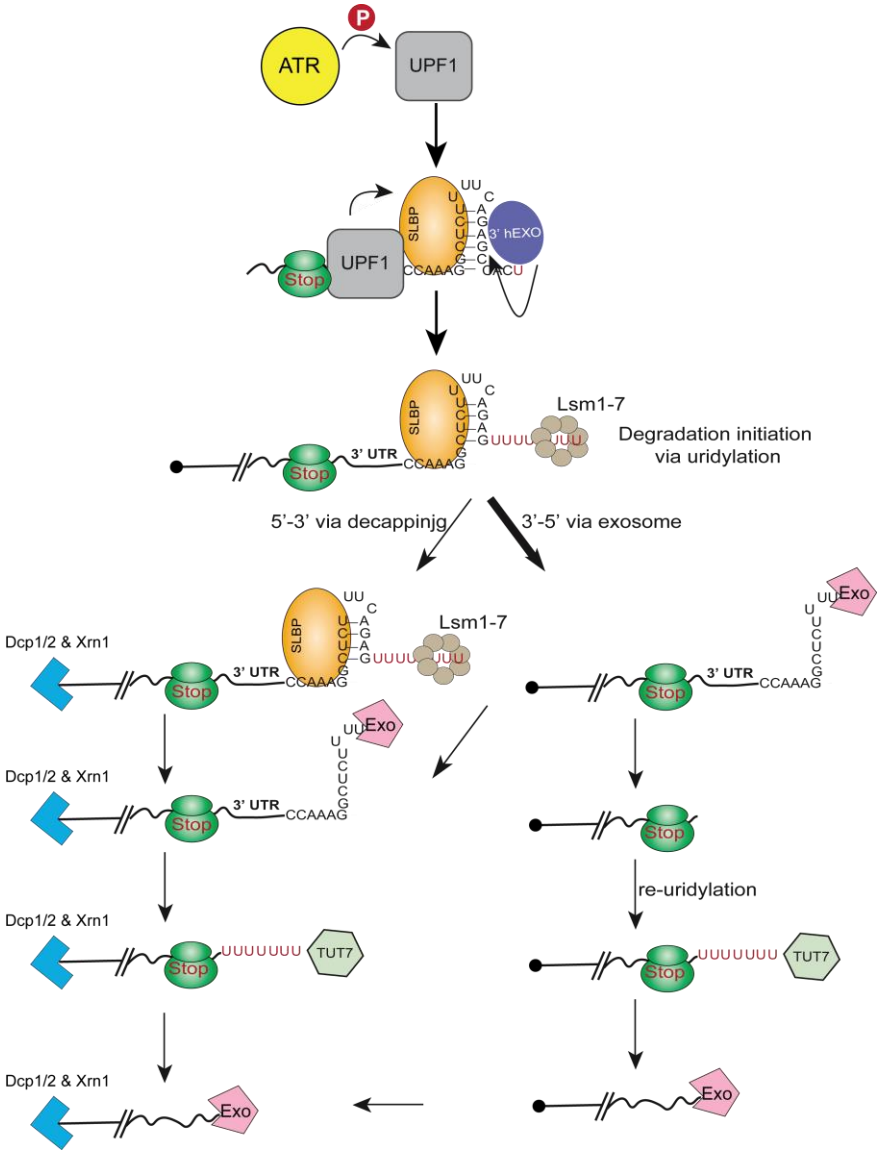


**Figure 7. Degradation of histone mRNAs.** The 3' end of histone mRNAs is trimmed by 3'hExo and oligouridylated by TUT7. Thereafter, two simultaneous degradation pathways (5'-to-3' and 3'-to-5) are activated to ensure rapid elimination of histone mRNAs. In the 5'-to-3' pathway, the mRNA is decapped followed by digestion by the ribonuclease Xrn1 (Slevin MK Mol. Cell 2014). The 3'-to-5' pathway relies on waves of degradation by the exosome (Exo) and re-uridylation by TUT7. The latter is the most active pathway (thick arrow). Adapted from Slevin et al., 2014.

### 3.4. Parallelism between NMD and histone mRNA degradation

Several parallelisms can be found between NMD and histone mRNA degradation (Figure 8). First, both NMD and histone mRNA degradation occur on actively translating mRNAs. Second, NMD is thought to take place on CBP80/20-associated polyadenylated transcripts (He and Jacobson, 2015). Likewise, histone mRNAs are primarily translated via a CBP80/20 mechanism, and downregulation of CBP80/20 stabilizes histone transcripts (Choe et al., 2013). Third, in eukaryotic cells NMD is enhanced when a premature stop codon (PTC) is found > 50-52 nt upstream of an Exon Junction Complex (EJC) (Lykke-Andersen and Jensen, 2015). Correspondingly, histone mRNA degradation requires a stop codon at a distance of 30-70 nt upstream of the stem-loop (Kaygun and Marzluff, 2005a). Finally, NMD and histone mRNA degradation share the main degradation-triggering protein UPF1 (Figure 8.) Despite these parallelisms, NMD and the histone pathway seem to differ downstream of UPF1 activation (Lykke-Andersen and Jensen, 2015). Furthermore, the crucial difference is that histone mRNAs are not aberrant. It should be noted, however, that even though NMD is a mechanism to get rid of aberrant, PTC-containing mRNAs, this process has been reported to occur on normal messages (Peccarelli and Kebaara, 2014).

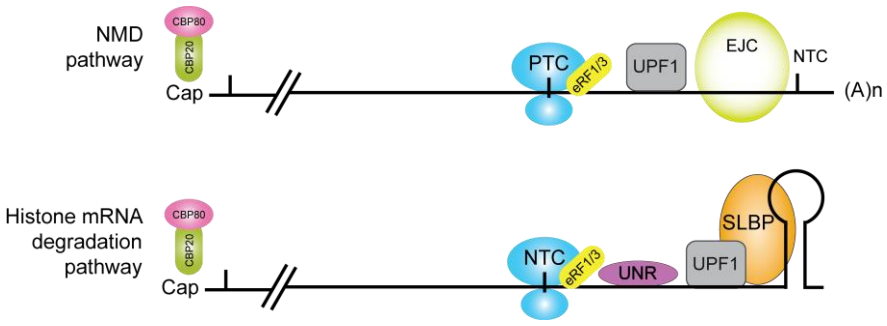


**Figure 8. Parallelism between NMD and histone mRNA degradation.** UPF1 mediated degradation is activated in both pathways when a ribosome reaches a PTC (in non-histone transcripts) and when ribosome reaches a normal termination codon (NTC) (in histone mRNAs).

## 4. Senescence

The first observation of cellular senescence was made by Hayflick and Moorehead and dates back to 1961. They described that normal human fibroblasts showed limited proliferation in culture, a process that they termed cellular senescence (Hayflick and Moorhead, 1961). Later, cellular senescence (sometimes termed replicative senescence or cellular aging) was proposed to drive organismal ageing by exhaustion of tissue repair capacity (Hayflick, 1965). While the association of replicative senescence with aging was established early on, two decades had to span before senescence was grounded as a tumour suppressor mechanism (O'Brien et al., 1986).

Senescence is induced by a variety of intrinsic and extrinsic stimuli, such as persistent telomeric and genomic damage, oncogene induction, epigenetic perturbations, reactive oxygen species (ROS) stress and tumour suppressor gene activation. Apart from aging and tumour suppression, senescence has been implicated in other biological contexts including wound healing, tissue repair and embryonic development (Demaria et al., 2014; Dimri et al., 1995; Jun and Lau, 2010; Kang et al., 2011; Muñoz-Espín et al., 2013; Storer et al., 2013)

Common features have been ascribed to senescent cells. Of these, probably the most important are grow arrest, resistance to cell death and production and secretion of the senescence-associated secretory phenotype (SASP) (Muñoz-Espín and Serrano, 2014).

Description of different cellular senescence triggers as well as main key features of senescent cells will be covered in the following sections and further detailed information will be only referred to oncogene-induced senescence (OIS).

## 4.1. Triggers of cellular senescence

Senescence can be induced by multiple triggers (Figure 9).

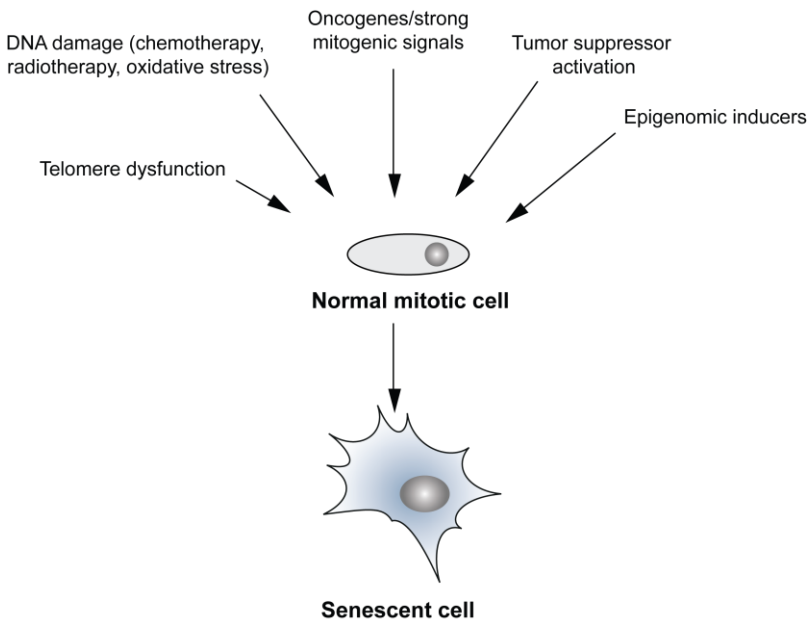


**Figure 9. Triggers of senescence.** Adapted from Campisi, 2013 and Bolden and Lowe, 2015.

*Telomere shortening and replicative stress*. Initial studies correlated irreversible cell cycle arrest with shortening of telomeres (Harley et al., 1990). Telomeres shorten at every cell division, and this process is counteracted by the reverse transcriptase telomerase, which replenishes the repetitive telomeric DNA (Bolden and Lowe, 2015). In the absence of telomerase, repeated cells divisions lead to critically short and dysfunctional telomeres. Telomeres are coated by specific proteins that inhibit DNA repair at chromosome termini to prevent chromosomal fusion and genome instability (O'Sullivan and Karlseder, 2010). However, critically short or dysfunctional telomeres lead to activation of persistent

DNA damage response (DDR) (Fumagalli et al., 2012; Takai et al., 2003), p53-dependent p21 activation and growth arrest (Choudhury et al., 2007; Fagagna et al., 2003).

*Genomic damage.* Cellular senescence is activated in response to damaged DNA independently of the affected genomic region. In addition to replicative senescence, genomic damage can be caused by oncogene overexpression, ionizing radiation, oxidative stress or cytotoxic chemotherapy. These triggers generate persistent DDR signalling leading to senescence (Childs et al., 2017).

*In vitro culture.* Deficient culture conditions can induce cellular senescence. When cells are explanted from an organism and placed in culture, they have to adapt to an artificial environment. Often, this environment is based on abnormal concentrations of growth factors and nutrients, and lacks extracellular matrix components and additional neighbouring cell types which are normal in a tissue (Sherr and DePinho, 2000). This enormous stress can cause cellular senescence.

*Mitogens and proliferation-associated signals.* Senescence can be induced by strong, chronic or unbalanced mitogenic signals (Blagosklonny, 2003). Oncogene-induced senescence (OIS) is one of the best-studied examples and will be commented in detail in the following section. Similarly, loss of tumour suppressors such as PTEN, pRB (retinoblastoma) or NF1 (Neurofibromin 1) among others can trigger senescence (Courtois-Cox et al., 2008; Shamma et al., 2009). While most activated oncogenes induce senescence in a DDR-dependent manner (one exception is BRAF V600E), tumour suppressor loss triggers permanent growth arrest in a DDR-independent manner (one exception is pRB) through $p19^{ARF}$ and $p16^{INK4a}$ activation (Bartkova et al., 2006; van Deursen, 2014).

*Tumour suppressor activation.* For establishment and/or maintenance of growth arrest, the tumour suppressive p53/p21 and $p16^{INK4a}$/pRB pathways are clearly of major importance (Sharpless and Sherr, 2015).

Depending on the stimuli, one or both pathways will be activated. Chronic activation or overexpression of these factors is generally sufficient to induce cellular senescence (Campisi, 2013). Thus, the relationship of tumour suppressors with senescence is complex, as either their overexpression or loss can induce senescence, depending on the particular tumour suppressor and the cellular context.

*Epigenomic modifiers.* Perturbations in the epigenome can elicit the senescence response, often in the absence of physical DNA damage. For example, histone deacetylase inhibitors can cause global chromatin relaxation and induce senescence by de-repressing the $p16^{INK4a}$ tumour suppressor (Munro et al., 2004).

### 4.1.1. Oncogene-Induced Senescence (OIS)

A common initial step of cancer development is the stimulation of cell proliferation due to oncogene activation. Proliferation is a necessary step for tumour promotion but it may also act as a trigger of senescence. Senescence induced by oncogenes is termed oncogene-induced senescence (OIS) and strong evidence suggest that OIS serves as the first barrier of defence against cancer development (Gorgoulis and Halazonetis, 2010).

Several examples of OIS have been described with alterations in RAS. Primary human and mouse fibroblasts harbouring oncogenic mutations in *Ras*, were irreversible cell cycle arrested and expressed high levels of the tumour suppressors p53 and $p16^{INK4a}$ accompanied with enlarged and distinct morphology (Lin and Lowe, 2001; Lin et al., 1998; Serrano et al., 1997). Accordingly, overexpression of *Ras* induced senescence *in vivo* (Sarkisian et al., 2007). Several other oncogenes have also been shown to induce senescence (*c-Myc*, *Cyclin E*, *Cdc6*, *E2F1*, *Mos*, etc).

A general feature of OIS is the de-repression the CDKN2A locus, encoding $p16^{INK4a}$ and $p19^{ARF}$ (Muñoz-Espín and Serrano, 2014) Moreover, activation of the DDR pathway was shown to have an important

role in senescence induced by several oncogenes in human and murine fibroblasts (Bartkova et al., 2006) (Figure 10). DDR can be generated by reactive oxygen species (ROS) that accumulate as a result of oncogene activation or by hyper-replication of DNA (Xu et al., 2014). Experimental inactivation of DDR can abrogate OIS and promote cell transformation, highlighting the tumour suppressive role of DDR signalling in OIS (Bartkova et al., 2006; Di Micco et al., 2006).

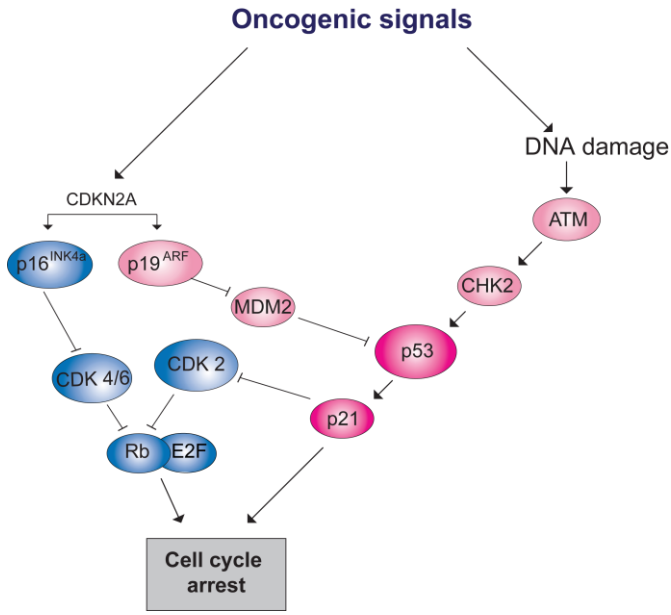


**Figure 10. Pathways involved in OIS.** Oncogenic signals activate the CDK2NA locus and (often) DNA damage response pathway, leading to increased pRb, p53 and p21 expression. Adapted from Tonnessen-Murray et al., 2017.

The relative importance of these mechanims ($p16^{INK4a}$, $p19^{ARF}$, or DDR) varies depending on the cell type and organism. For example, the crucial activator of OIS in humans seems to be the DDR-p53 axis, whereas $p19^{ARF}$-p53 has a more important role in mice. The role of $p16^{INK4a}$ is modest in promoting senescence in mice (Efeyan and Serrano, 2007; Evan and d'Adda di Fagagna, 2009; Halazonetis et al., 2008).

Other pathways such as p38/MAPK and PI3K/AKT/mTOR have been reported to mediate OIS. Several studies indicate that these pathways are important for RAS-induced senescence (Figure 11) (Liu et al., 2018; Xu et al., 2014).

In summary, OIS is elicited in cells upon oncogenic insult as a failsafe mechanism to restrict proliferation and oppose oncogenic transformation. OIS occurs in early stages of tumorigenesis, as senescent cells are abundant in premalignant lesions compared to malignant tumours, suggesting that the senescent barrier needs to be overcome in order to progress into full malignancy (Braig et al., 2005; Chen et al., 2005; Collado et al., 2005).

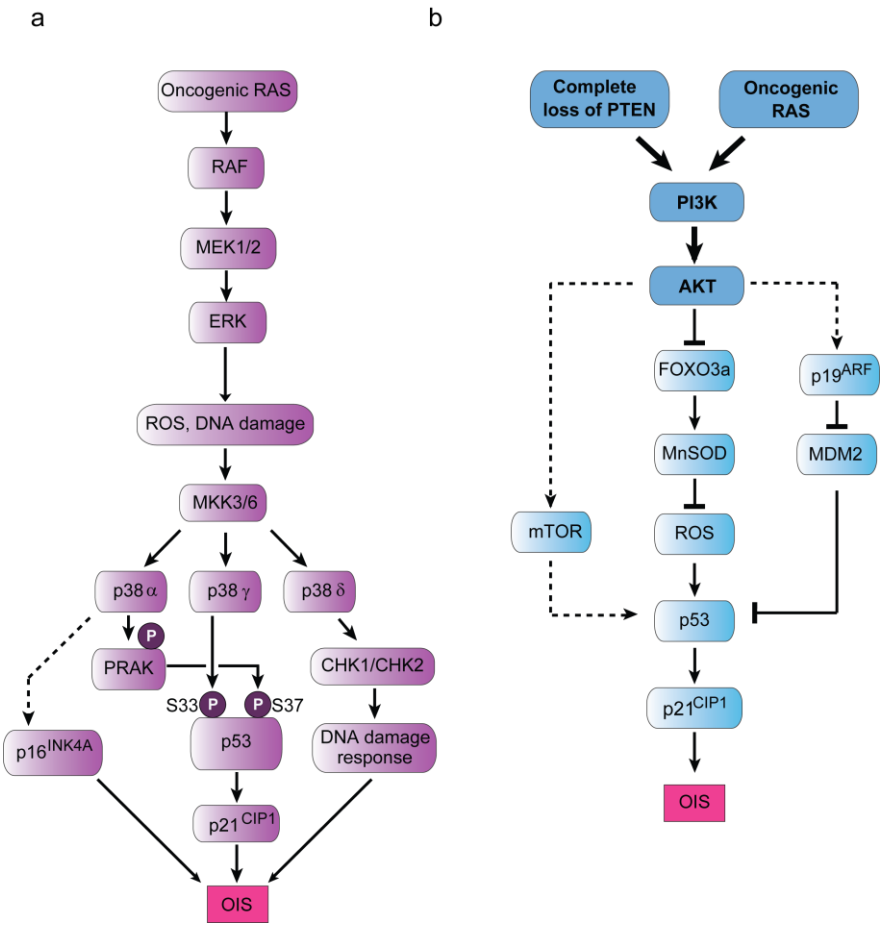


**Figure 11. Signalling pathways contributing to RAS-induced senescence. (a)** The RAF/MAPK pathway. RAS activates the RAF-MEK axis, which leads to ROS production and DNA damage. This results in activation pf p38/MAPK. The mammalian genome encodes four p38 isoforms (p38α, p38β, p38γ and p38δ) but only three isoforms play roles in OIS. p38α likely induces transcription of $p16^{INK4a}$. In addition, p38α directly activates PRAK kinase, which in turn activates p53 through Ser37 phosphorylation. p38γ directly stimulates p53 through phosphorylation of Ser33. p38δ mediates OIS through a p53- and $p16^{INK4A}$-independent mechanism, possibly by regulating the activity of the DNA-damage checkpoint kinases CHK1 and CHK2 . Dashed line represents indirect interaction. **(b)** The PI3K/mTOR pathway. Strong activation of AKT inhibits FOXO3a, which promotes the transcription of radical scavenger genes (such as manganese superoxide – MnSOD), leading to ROS production and activation of p53. AKT also activates mTOR, stimulating the translation of p53. Adapted from Xu et al., 2014.

## 4.2. Features of senescent cells

Senescent cells are diverse and defined by multiple specific features. These differences may arise from the tissue of origin, the stimuli that triggered the senescent program, or the intrinsic mechanisms activated to establish cell cycle arrest (Hernandez-Segura et al., 2017). Below, I discuss the most prevalent features among senescent cells.

*Growth arrest.* Perhaps the only universal feature of senescent cells is that they enter in a state of permanent growth arrest. Thus, the absence of proliferation markers is commonly used to detect senescent cells. Cell cycle re-entry, however, has been reported upon artificial manipulation of the levels of cell cycle inhibitors (Beausejour, 2003; Dirac and Bernards, 2003; Sage et al., 2003).

*Expression of cell cycle inhibitors.* Permanent growth arrest in senescent cells functions through two crucial pathways controlled by the cell cycle inhibitors $p16^{INK4a}$ and $p19^{ARF}$ (p14 in humans) (Figure 10). In cycling cells, E2F-mediated transcription promotes S phase entry. E2F is inhibited by pRB. $p16^{INK4a}$ inhibits CDK4/6, a kinase that hyper-phosphorylates and inhibits pRB, leading to cell cycle arrest. $p19^{ARF}$ directly inhibits the p53-negative regulator MDM2, triggering a p53-dependent transcription program that leads to either G1 phase arrest or to apoptosis. The $p16^{INK4a}$ and $p19^{ARF}$ pathways are interconnected through $p21^{CIP1}$, a downstream transcription target of p53 (van Deursen, 2014; Lowe and Sherr, 2003; Sherr, 2001).

*Senescence-associated β-galactosidase activity (SA-β-Gal).* Expression of this lysosomal enzyme is associated with senescent cells, although some other conditions (high cell confluence, treatment with hydrogen peroxide) can also stimulate β-Gal activity, and some senescent cells do not show SA-β-Gal (Lee et al., 2006). Detection of β-galactosidase activity at suboptimal pH (5,5 for mouse and 6 for human) is possible due to its overexpression and the increase of the lysosomal mass upon senescence (Dimri et al., 1995; Lee et al., 2006).

*Autophagy*. Autophagy is a protective process associated with energy homeostasis that allows the controlled degradation of cytoplasmic substrates in lysosomes, creating a way for cells to adapt to the energetic demand. In replicative senescence, autophagy is thought to be a gradual adaptive process, whereas in OIS autophagy is acute and contributes to the dramatic cell remodelling occurring at 2-3 days of oncogene overexpression. Consequently, inhibition of autophagy delayed the OIS-related phenotype (Young et al., 2009). Paradoxically, however, suppression of autophagy may induce senescence (Hoare et al., 2011).

*Enlarged cell size and vacuolization.* Senescent cells in culture clearly display a characteristic phenotype, which is obvious under the microscope. Cells increase in size, acquire a flat morphology with an enlarged nucleus, and present severe vacuolization. In addition, multinucleated senescent cells are often observed (Denoyelle et al., 2006; Hayflick, 1965; Serrano et al., 1997). Senescent cells found *in vivo* do not show such a distinct phenotype, probably because of tissue architecture constraints (Muñoz-Espín and Serrano, 2014).

*DNA damage markers.* Some senescent triggers induce DNA damage, with the consequent activation of the DDR and the generation of DNA damage foci. DNA damage markers include γH2AX or p53-binding protein 1 (53BP1) (Bartkova et al., 2006; Di Micco et al., 2006). However*, in vivo* most cells that express DNA damage markers are not senescent, so these markers have little specificity (Sharpless and Sherr, 2015).

*Resistance to apoptosis.* Senescence and apoptosis are thought to be mutually exclusive. The crucial determinants of whether a cell responds to damage by undergoing senescence or apoptosis are the cell type and the nature and intensity of the damage (reviewed in Childs et al., 2014). Differential accumulation of p53 and other apoptotic markers distinguish these two processes (Li et al., 2012; Tavana et al., 2010). With pro-senescent stress, p53 accumulates to a lesser extent compared to apoptosis, and reduced levels of pro-apoptotic PUMA (p53-upregulated modulator of apoptosis) and NOXA are found, together with higher levels

of anti-apoptotic BCL-2 family members (BCL-2, BCL-XL and BCL-W) (reviewed in Roos and Kaina, 2006; Zuckerman et al., 2009). Importantly, a small molecule inhibitor (ABT-737) targeting BCL-2, BCL-W and BCL-XL causes preferential apoptosis of senescent cells *in vitro* and *in vivo*. Elimination of these cells from tissues would decrease the deleterious long-term effects of senescent cell retention (Yosef et al., 2016).

*Lamin-associated changes.* Lamins are components of the nuclear lamina (fibrous layer on the nucleoplasmic side of the inner nuclear membrane) that interact with chromatin. Loss of LAMIN B1 is a common feature of many types of senescence (Freund et al., 2012; Shimi et al., 2011).

*Senescence-associated heterochromatin foci (SAHF).* SAHF are specialized domains that contribute to silencing of proliferation-promoting genes. They are associated with heterochromatin markers such as H3K9me3, heterochromatin protein 1 (HP1) and macroH2A (Narita et al., 2003; Zhang et al., 2005). As for SA-β-Gal, SAHF formation and senescence are not always coupled. Of note, SAHF are preferentially formed during OIS but not during replicative senescence or upon aging (Muñoz-Espín and Serrano, 2014). In addition, SAHF occur in a cell type-dependent manner (Kosar et al., 2011).

*Senescence associated secretory phenotype (SASP).* Together with growth arrest, the senescence associated secretome is perhaps de most relevant feature of senescent cells. The secreted factors exert multiple functions in a paracrine and autocrine manner.

The next section will focus on the nature and effects of SASP.

## 4.3. The senescence-associated secretory phenotype (SASP)

The SASP accompanies the senescent phenotype only if senescence is triggered by genomic or epigenomic perturbation. Thus, the simple overexpression of p21 or $p16^{INK4a}$, despite inducing a senescent phenotype, does not induce SASP (Coppé et al., 2011). SASP expression requires activated ATM, a kinase that couples replication

stress to DDR activation and metabolic reprogramming (Aird et al., 2015; Rodier et al., 2009). SASP induction by strong genotoxic stress is counteracted by p53 (Coppé et al., 2008)(Coppé et al Plos Biology 2008). Thus, p53 acts as a cell-autonomous tumour suppressor by promoting cell cycle arrest, and as a cell-nonautonomous tumour suppressor by dampening the pro-tumorigenic activities of the SASP.

The SASP composition is variable, and depends on the cell type and the stimulus that induced the senescence response, although considerable overlap exists (Campisi, 2013; Coppé et al., 2008, 2010). The SASP includes inflammatory cytokines, chemokines, growth factors, proteases and extracellular matrix (ECM) components (Childs et al., 2017). Some of the frequent SASP components are indicated in Table 1.

| **Interleukins** | **Chemokines (MCPs and MIPs)** |
|---|---|
| IL-1a | IL-8 |
| IL-1b | CXCL-1/ -2/ -3 (GRO-a/ -b/ -g) |
| IL-6/ -7 | CCL-2/ -7/ -8/ -13/ -16 |
| IL-13 | CCL-3 (MIP-1a) |
| **Growth factors** | CCL-20 (MIP-3a) |
| IGFBP-2/-3/-4/-5/-6/ -7 | CCL-26 (Eotaxin-3) |
| HGF | CXCR-2 (IL-8RB) |
| VEFG | CXCL-5 (ENA-78) |
| TGF-b family ligands | CCL-1 (I-309) |
| **Proteases and regulators** | CCL-4 (MIP-1b) |
| MMP-1/ -3/ -10/ -12/ -13/ -14 | **Other** |
| uPA/ tPA/ PAI-1 | ICAM-1/ -3 |
| TIMP-1/ -2 | TNF-receptors |
| **ECM components** | GM-CSF |
| Fibronectin | SGP130 |
| Collagen | G-CSF |
| Laminin | BLC |

**Table 1. SASP factors**. Common factors classified according to their nature. The “Other” category includes soluble/ shed receptors/ ligands and other inflammatory factors. Factors

exclusively found after OIS are highlighted in red. (Acosta et al., 2013; Coppé et al., 2008, 2010; Liu and Hornsby, 2007; Pérez-Mancera et al., 2014; Wajapeyee et al., 2008; Wang et al., 2017)

Oncogenic RAS promotes a rapid and strong SASP (2-4 days after Ras exposure) with unique factors such as ENA-78 (CXCL-5), I-309 (CCL-1), BCL, MIP-1b and G-CSF, in addition to more common factors which are nonetheless largely amplified (Coppé et al., 2008) (Table 1).

The SASP is a double-edge sword, as it can have beneficial or detrimental effects. On one hand, the SASP reinforces cell cycle arrest on an autocrine and paracrine manner (Acosta et al., 2013; Kuilman et al., 2008). Paracrine senescence results in increased clearance of potential tumorigenic cells via immune infiltration (Neves et al., 2015). These events, contribute to limit the propagation and lifespan of damaged cells. In the case of OIS, an acute SASP has tumour suppressive roles (Figure 12a). The SASP can also have beneficial effects in other contexts such as embryonic development (Muñoz-Espín et al., 2013; Storer et al., 2013), wound healing (Demaria et al., 2014) or cell regeneration (Ritschka et al., 2017).

In sharp contrast, SASP factors have been associated with a host of deleterious effects. A range of several diseases associated with age such as osteoarthritis, cardiovascular problems or diabetes are related to chronic SASP (Demaria et al., 2015; Ghosh and Capell, 2016; Greene and Loeser, 2015, 2015; Muñoz-Espín and Serrano, 2014). In the OIS context, the SASP was shown to promote tumorigenesis in neighbouring cells by inducing proliferation, survival, epithelial to mesenchymal transition (EMT), angiogenesis and metastasis (Coppé et al., 2006; Kessenbrock et al., 2010; Krtolica et al., 2001; Laberge et al., 2012; Malaquin et al., 2013; Parrinello, 2005; Rao and Jackson, 2016). In addition, the recruitment of the immune system can have undesired effects, for example, by promoting an immunosuppressive

microenvironment or by eliciting chronic inflammation that that would favour tumour progression (Rao and Jackson, 2016) (Figure 12b).

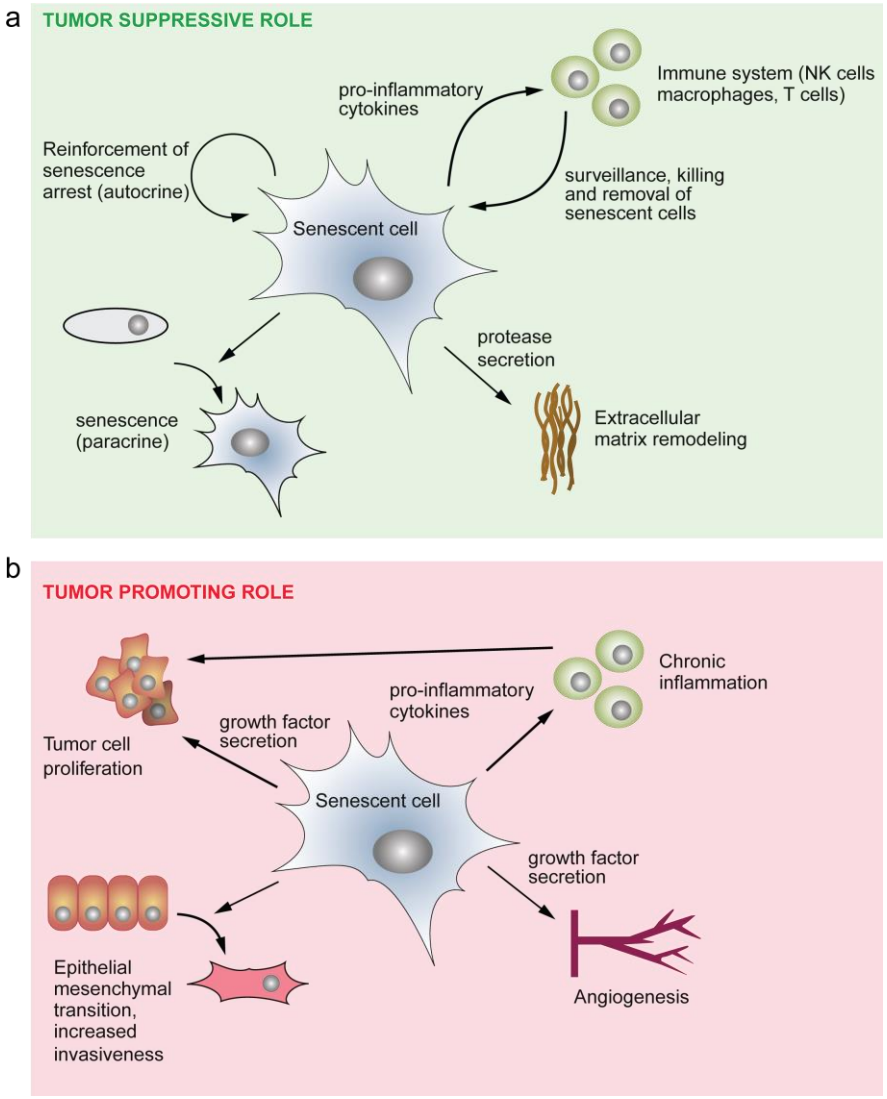


**Figure 12. Tumour suppressive and tumour promoting effects of the SASP. (a)** The SASP reinforces cell cycle arrest in senescent and neighboring cells. Secretion of proteases enables remodeling of the damaged tissue. Immune cell recruitment through pro-inflammatory cytokines clears damaged cells and restores tissue integrity. **(b)** Pro-inflammatory cytokines and growth factors can promote cell proliferation and transformation, angiogenesis and invasiveness. Adapted from Bolden and Lowe, 2015.

# Objectives

UNR is a key post-transcriptional regulator that participates in multiple biological processes by regulating mRNA translation and stability. Previous work in our laboratory identified the targets of UNR in melanoma cells. Two major group of targets were those encoding histones and SASP factors. The objective of this thesis is to unveil the role of UNR binding to these sets of targets. Towards this goal, we aim to:

1. Validate UNR binding to histone mRNAs.

2. Understand the role of UNR binding to histone transcripts.

3. Determine whether UNR has a role in oncogene-induced senescence (OIS). If so,

4. Characterize changes in steady state mRNA levels as a first approach to understand the molecular function of UNR in OIS.

# Materials and Methods

## Plasmids and constructs

### *Vectors for retroviral production*

shRNA-PIG: retroviral construct for shRNA expression included in a pLMP backbone. Gift from Bill Keyes's Laboratory (IGBMC). 97 mer purchased from Sigma with specific shRNA sequence were amplified using primers containing restriction enzymes XhoI and EcoRI (Fw-XhoI and Rev-EcoRI) in the 5' and 3' respectively. The amplified fragments and the empty vectors were incubated with these restriction enzymes and ligated overnight at 16 ºC. The restriction sites are highlighted in blue.

| Name of primer | Sequence 5'-3' |
|---|---|
| Fw-XhoI | CAGAAGGCTCGAGAAGGTATATTGCTGTTGACAGTG AGCG |
| Rev-EcoRI | CTAAAGTAGCCCCTTGAATTCCGAGGCAGTAGGCA |

Initially we used shLuc as a control shRNA, however, we later changed to a scramble sequence (shLW) identical to the one in TRIPZ shCtrl (see below), to avoid interference with luciferase activity of potential experiments with mice in the future. Experiments in Figures 23, 28, 30-34 were performed with shLuc and the rest with shLW (figures 26, 27 and 29). shUNR sequence is identical to the one found in the TRIPZ shUNR (see below). The guide strand for each shRNA is highlighted in red.

| shRNA name | Sequence 5'-3' |
|---|---|
| shLuc (shCtrl) | TGCTGTTGACAGTGAGCGCCCGCCTGAAGTCTCTGATT AATAGTGAAGCCACAGATGTATTAATCAGAGACTTCAGG CGGTTGCCTACTGCCTCGGA |
| shLW (shCtrl) | TGCTGTTGACAGTGAGCGCTTACTCTCGCCCAAGCGAG AATAGTGAAGCCACAGATGTATTCTCGCTTGGGCGAGA GTAATTGCCTACTGCCTCGGA |

| | |
|---|---|
| shUNR | TGCTGTTGACAGTGAGCGCGGAGATGATGTTGAATTTGA ATAGTGAAGCCACAGATGTATTCAAATTCAACATCATCTC CTTGCCTACTGCCTCGGA |

MSCV-Empty: vector used as infection control. Hygromycin resistance gene is under the control of a PGK promoter. Gift from Bill Keyes's Laboratory (IGBMC).

H-RAS V12: vector coding for human *H-RAS* in a pWZL backbone. A single nucleotide change (G → C) leads to the oncogenic missense variant Gly12Val. Gift from Bill Keyes's Laboratory (IGBMC). Hereafter, H-RAS V12 will be referred as H-RAS.

### *Vectors for recombinant protein expression*

pET21d-hUNR-His: plasmid containing recombinant isoform 2 of hUNR (encoded by NM_007158.5 or NM_001242893.1 NCBI reference sequences) fused to a six-histidine-tag (His-tag). Gift from Anne Willis.

### *Reporter vectors*

pLuc: plasmid for *luc* gene expression, under the control of the SV40 promoter in a pGL3-Control vector. Gift from Susana de la Luna's laboratory (CRG). Commercially available by Promega (#0747VA08_4A).

pRenilla: plasmid for *renilla* gene expression under the control of the SV40 promoter in a pSG5 vector.

### *Vectors and DNA fragments for in vitro transcription and translation*

*H*2AD-WT: plasmid for wilt type *H2AD* transcripts in a pGL3-Basic vector. The pGL3-Control vector was a gift from Susana de la Luna's Laboratory (CRG), commercially available by Promega (#0746VA08_4A). The vector

lacks any promoter and enhancer sequences. Originally containing *luc* but replaced by *H2AD* transcript (5'UTR, ORF and mature 3'UTR) with reference NM_021065.3 in NCBI. Upstream the H2AD transcript a T7 promoter and a stretch of six alternately methionine and cysteine were also inserted. The complete double stranded insert (T7-5'UTR-Met/Cys-ORF-3'UTR) flanked by restriction sites (NcoI in the 5' and BamHI in the 3') was ordered to Integrated DNA Technologies (IDT) company. The insert and the vector were incubated at 37 ºC with restriction enzymes and ligated overnight at 16 ºC.

H2AD-STOP-MUT: pGL3-Basic vector identical to the one described above with a unique substitution (T → C) mutating a stop codon to a Gln codon. Insert generated by amplification of H2AD-WT vector with a forward primer annealing in the T7 promoter (Fw-T7-5'end) and a reverse primer containing the punctual mutation in the 3'UTR (Rev-3-end-mut) (this change is highlighted in red in the sequence). Next, a second amplification was used to include restriction sites flanking the insert (Fw-NcoI-T7 and Rev-3UTR-BamHI). The product was introduced in the pGEM-T Vector (Promega #A3600) as an intermediate cloning. NcoI and BamHI were incubated at 37 ºC with the H2AD-MUT-pGEM-T and the released fragment (insert) was ligated overnight at 16 ºC with pGL3-Basic vector.

| Name of primer | Sequence 5'-3' |
|---|---|
| Fw-T7-5'end | TAATACGACTCACTATAGGGACTTTTACATTTTTGTCT TCATTGCTTAACA |
| Rev-3-end-mut | TGGCTCTGAAAAGAGCCTTTGTTAAGACTGCTTCCTT AAAAAGCCAATATAAGAGTTCTCGTTTTGCTTGCCC |
| Fw-NcoI-T7 | TGCCATGGTAATACGACTCACTATAGGG |
| Rev-3UTR-BamHI | CGGATCCTGGGTGGCTCTGAAAAGAGC |

Mini-H2AD-WT / Mini-H2AD-MUT: DNA fragment generated by PCR using specific primers (Fw-T7-CD and Rev-3-end-wt). The DNA fragment containing T7 promoter followed by the 50 last nucleotides of the ORF

and the complete mature 3'UTR (containing wild type or mutant stop), was produced using H2AD-WT-pGL3-Basic and H2AD-STOP-MUT-pGL3-Basic plasmids as template, respectively.

| Name of primer | Sequence 5'-3' |
|---|---|
| Fw-T7-CD | TAATACGACTCACTATAGGGCT GTACTGCTCCCCAAGAAGAC |
| Rev-3-end-wt | TGGGTGGCTCTGA-AAAGAGC |

Mini-H2AD-Multi-MUT: DNA fragment of 140 nucleotides containing T7 promoter, last 50 nucleotides of the ORF and a multi-mutated-pyrimidine-3'UTR construct was designed. IDT company provided the complete sequence and specific oligos (T7 and Rev-3-end) were used to amplify the construct by PCR.

| Name of primer | Sequence 5'-3' |
|---|---|
| Fw-T7 | TAATACGACTCACTATAGGG |
| Rev-3-end | TGGGTGGCTCTGA-AAAGAGC |

## Primary Mouse Keratinocytes (PMK)

PMK from newborn mice (0-48 hours) were isolated, in general terms, as described in (Lichti et al., 2008). However, some modifications have been done over years. Briefly, mice were sacrificed with an intraperitoneal injection of Duolethal (20 mg/ml, provided by the animal house). Pups were immersed in betadine, rinsed with PBS 1X, immersed with 70% ethanol, dried with paper, immersed again with PBS 1X and left at 4 ºC. Clean dissecting tools and a lid to a 100-mm dish for skin removal were used. The dissecting steps for skin removal are performed as described in (Lichti et al., 2008). The released skins were placed completely flat with dermis side down in a tissue culture dish. For proper epidermis-dermis separation from the total skin, incubation of Dispase II (Roche #04942078001; final concentration = 2.5 mg/ml) is necessary. Proper stretching of skins on the plate makes them float when Dispase II is added. Closed plates were kept in at 4 ºC overnight or 1 hour at 37 ºC.

Using a laminar-flow hood skins were taken and placed in a new 100-mm lid with the dermis up while steadying the epidermis with other forceps, gently gilding away the dermis and discarding it. Epidermis were chopped using scissors and a blade until homogenous pieces were small enough to be collected with a 10 ml pipette. Skins were stirred with media during 30-40 minutes at room temperature. Using a cell strainer of 70 µm (Corning #352350) cell suspension was filtered into a 50ml Falcon tube and centrifuged it to keep the cell pellet. Cells were resuspended in the desired volume (EMEM complete media) and plated in previously collagen treated plates. Collagen I from Rat tail (Invitrogen #A1048301) 1/60 diluted in PBS is incubated with the plates for at least 40 minutes at 37 ºC. 24 hours later, cells were washed several times with PBS 1X.

EMEM complete media contains 450 ml of Modified Eagle's Medium (EMEM, with Earle's Balanced Salt Solution, L-Glutamine, and Non-Essential Amino Acids, without Calcium. Lonza #06-174G), 8% of chelated FBS (Fetal Bovine Serum) (see below), 0,05 mM $CaCl_2$ 2M, 10 ng/ml of EGF (Sigma-Aldrich #E4127) and 1% penicillin/streptomycin (Life technologies #15070063).

For chelated FBS preparation, 500 ml of FBS (Invitrogen #10270106R) are heat inactivated for 30 minutes at 56 ºC. 150 g of Chelex 100 Resin (Bio-Rad #142-2832) are stirred slowly with 2 litres of MiliQ water overnight at room temperature. The following day pH is adjusted to 7-7,5. Resin is decanted and recovered with the help of a blotting paper filter. The Chelex resin together the heat inactivated FBS are stirred 1 hour at room temperature. Filter and aliquot under the cell culture hood.

## Retroviral infections

48 hours after seeding, PMK were infected using retroviral particles. The 293T-based cells Phoenix ecotropic packaging cell line (generated by Garry Nolan laboratory, Stanford University, Stanford) were transfected with the transfer plasmid of interest (MSCV-Empty vector, *H-RAS*, shCtrl, shUNR) together with a helper virus to increase the efficiency of viral

particles production. However, the infected cells turned out to be virus producers as well. We checked the expression of human *H-RAS* in freshly growing keratinocytes treated with conditioned media from immortal PMK (iPMK-3: *H-RAS* and shUNR infected) and compared the expression of the human gene in PMK treated with fresh EMEM complete media. Specific primers for human *H-RAS* (Fw-qhHRAS and Rev-qhHRAS) were used.

| Name of primer | Sequence 5'-3' |
|---|---|
| Fw-hHRAS | GGCATCCCCTACATCGAGA |
| Rev-hHRAS | CTCACGCACCAACGTGTAGA |

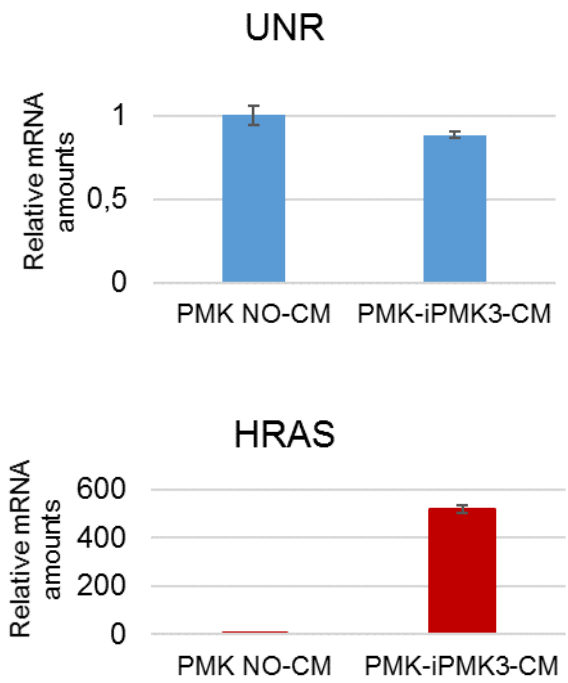


**Figure 13. RT-qPCR amplification of mouse *Unr* and human *H-RAS*.** UNR levels do not considerably change, however, *H-RAS* mRNA levels are strikingly induced in PMK cells treated with immortal PMK-conditioned media (CM).

The resulted qPCR fragment of 75 nucleotides was run in an agarose gel and the corresponding band was cut. Following the manufacture

instructions of gel band purification kit (GE Healthcare #28-9034-70) the amplified cDNA was isolated and cloned into the pGEM-T vector for further sequencing. DNA sequencing results confirmed that the identity of the fragment was human *H-RAS.*

As UNR expression is affected by lentiviral transduction *per se* (Moore KS et al Scientific Reports 2017), we decided to stop using helper plasmid for retroviral production. In Results section, I will highlight which experiments are performed with helper (■) and without helper (□).

Prior to phoenix E transfection chloroquine (Sigma-Aldrich #C6628) was added to the media to a final concentration of 25 µM. 10 µg of the transfer plasmid and 60 µl of 2.5M $CaCl_2$ were mixed with MiliQ water up to 500 µl. After 10 min, 2X concentrated HEPES Buffered Saline (281 mM NaCl, 100 mM HEPES and 1.5 mM $Na_2HPO_4$ in water; pH=7.12) was added into the DNA mix dropwise while vortexing. The mixture is incubated 15 minutes at room temperature, then added drop wise to the cells. Media was replaced after 6-8 hours. PMK were infected (48 hours after seeding) following three rounds of 2 hours with the supernatant of the phoenix-virus producing cells. In the case of double infection, both supernatants were added simultaneously to the PMK. Polybrene was used at 10 µg/ml. 24 hours after the last infection cells were split and selected with 1 µg/ml of puromycin for 48 hours and, in case of double infections, followed by 25 µl of hygromycin. Cells were maintained in EMEM complete media prior to analysis (usually from 6 to 14 dpi) (See time line in Figure 23).

## Melanoma SK-Mel-103 cell line

SK-Mel-103 human melanoma cell line was characterized previously Alonso-Curbelo et al., 2014. Provided by María Sol Soengas's Laboratory (CNIO, Madrid).

shCtrl or shUNR SK-Mel-103 used in Wurth et al. 2016 were applied to this work. To generate these cells, scramble shCtrl (Dharmacon TRIPZ #RHS4743) or shUNR (Dharmacon TRIPZ # RHS4696-200681476 clone

ID V2THS_212077) were used (Wurth et al., 2016). Cells were cultured in Dulbecco's Modified Eagle Media (DMEM) supplemented with pyruvate (Life Technologies #31966), 10% fetal bovine serum (FBS) and 1% penicillin-streptomycin.

Briefly, lentiviral particles were produced in 293T cells transfected with 4 µg of vector plasmid, 5 µg of pCMV-VSV-G and 15 µg of pCMV-dR8.91 packaging vectors following standard calcium phosphate precipitation. Media were changed after 8-12 hours. Viral particles were collected 48 hours later and Sk-Mel-103 were infected through two rounds of 4 hours using 4 µg/ml of polybrene. Cells were then selected with 1 µg/ml puromycin. By adding 0.5 µg/ml doxycycline to the medium, co-expression of shRNA and red fluorescent protein (RFP) was induced. Experiments were performed after at least 3 days of shRNA induction.

UNR knockdown was also achieved by transfecting SK-Mel-103 cells with specific siRNA pools (siPOOLS BIOTECH #7812). siRNAs pools consist in 30 individual non-overlapping siRNAs to avoid RNAi off-target effects (Hannus et al., 2014). ). The siPOOLS kit included also a siRNA designed against non-human/mouse/rat sequences, which was used as negative control (siCtrl). $3x10^5$ cells/well of a six-well-plate were reverse transfected (cells are seeded at the same time of transfection) with a final concentration of 3 nM of siPOOLs using 1.4 µl of RNAiMax and following the manufacturer's instructions. After 24 hours of transfection, cells were split 1:2 and ready for further analysis.

## Cellular transfections

DNA transfections were performed using Effectene Transfection Reagent (Qiagen #301425). $3x10^5$ cells were seeded in each well of a six-well-plate the day before transfection. 50 ng of pGL3-control plasmid and 10 ng of *renilla*-containing plasmid were transfected as specified in the manufacturer's instructions. At six hours post-transfection, cells were washed with PBS 1X and new medium was added. The following day cells were collected for expression analysis.

RNA transfections were performed using TransMessenger Transfection Reagent (Qiagen #301525). $3x10^5$ cells were seeded in each well of a six-well-plate the day before transfection. 100 ng of H2AD mRNA and 30 ng of *renilla* RNA were transfected according to manufacturer's instructions.

## Fluorescence activated cell sorting (FACS)

For cell phase sorting cells were incubated with Hoescht-33342 at a final concentration of 5 µg/ml for 1 hour at 37 ºC. Cells were trypsinised and resuspended in a maximum concentration of 10 million cells/ml in Hoescht-containing medium and phase sorted.

For GFP sorting, cells were trypsinised and resuspended in media. To discard dead cells DAPI was added to a final concentration of 1 µg/ml.

## Colony forming assay (CFA)

shCtrl and shUNR cells (7 dpi) were seeded in duplicates at three different seeding densities in six-well-plates: 500, 1000 and 2000 cells per well. Experiments were performed as described in Jensen et al., 2010. Colonies were visualized with 1% Rhodamine B.

## Conditioned media (CM)

Conditioned media from shCtrl and shUNR (7 dpi) cells were collected, filtered (0.45 µm), aliquot and stored at -20 ºC. Conditioned media were added into freshly growing keratinocytes (24-72 hours after seeding) every 24 hours for 6 days.

## BrdU incorporation

$2x10^4$ cells were seeded in previously collagen-treated special 96-well-plates (Corning falcon #353377). BrdU was added for 18 hours and the manufacturer's instructions for Cell proliferation ELISA (Roche #11-669-915-001) were followed.

## In vitro transcription

Radioactive short probes for GEMSA experiments were synthesized as follows. An initial mix of 0.5-1 µg of PCR amplified fragment, 1X Transcription Buffer, 10 mM of fresh DDT, 0.4 mM of CTP and ATP, 40 µM of UTP, 1.6 mM ApppG cap, 3 µl of 32P-αUTP and 10U of RNA pol T7 (Agilent #600123) in a total volume 24µl was incubated 5 minutes at 37 ºC to allow capping. 1 µl of 0.4 mM of GTP completed the mix. 1 hour at 37 ºC allowed transcription. For DNA digestion, 2 µl of DNase I (RQ DNase Promega #M610A) were added to the mix and incubated 15 minutes at 37 ºC. Phenol/chloroform protocol was used for RNA extraction. 1 µl was collected for subsequent cpm counting (total signal). After removal of unincorporated nucleotides, again 1 µl was collected (incorporated signal). Using the scintillation counter incorporation of 32P-αUTP determined the quantity of RNA synthesized.

For longer non-radioactive mRNA *in vitro* transcription, plasmids were linearized with single restriction enzyme digestion and manufacturer's instructions of MEGAscript kit were followed (Ambion #AM1333M). After RNA isolation with phenol-chloroform extraction, samples were passed through G-25 columns, preceding RNA precipitation.

RNA quality and quantity control were performed with urea or agarose gels.

## GEMSA

RNA was heated at 98 ºC for 5 minutes. To allow RNA folding in different native conformations, the samples were then left in the thermo block until the temperature reached 25 ºC. Reactions with 3 µg of tRNA, 40 mM KCl, 20.000 cpm (RNA), and recombinant hUNR protein (0, 50, 100, 300 and 500 nM) were incubated on ice for 30 minutes. The whole reaction was run in a 4% acrylamide gel at 250 volts.

## TNT coupled transcription/translation system

RNA or DNA constructs were used for TNT assays together with hUNR recombinant protein or buffer D (in the negative counterparts). Reaction preparation and time of incubation were done following the manufacturer's instructions (Promega #L1170). A positive control was provided with the kit. 1/50 of the transcription/translation reaction was used for gel electrophoresis. The presence of translated proteins was determined by autoradiography of SDS-PAGE dried gels.

## RNA extraction and DNA digestion

Either TRIzol reagent (Invitrogen #15596-026) or Maxwell kit (Promega #AS1280) were used to extract RNA. Following RNA extraction, samples were subjected to DNase digestion using the Turbo DNA-free kit (Invitrogen #AM1907).

## Quantitative real-time PCR (qPCR)

RNA was reverse-transcribed using 2.5 µM of oligo(dT), 2.5 ng/µl of random primers, 0.05 mM of a mix of dNTPs, 1 mM DTT, 1X first strand buffer, 1 µl of RNase OUT (Invitrogen #P10777-019), and 50U of SuperScript II (Invitrogen #100004925) (final volume = 20 µl). The resultant cDNAs were used as templates for qPCR using the Light Cycler 480 SYBR Green I Master (Roche #04707516001) following the manufacturer's instructions.

List of primer sequences used for qPCR:

| Gene | Forward | Reverse |
|---|---|---|
| **Renilla** | ACAAATATCTTACTGCATG | TATTGCTTTGATCTTATCTTGATGC |
| **H2AD** | ATGTGTTGCATGTGTATGTCCG | GACTCGCTCGGAGTAGTTGC |
| **Psmb4** | CCTCTGGCGACTACGCTGATTT | CCATCTCCCAGAAGCTCCTCATC |
| **Luc** | AACACCCAACATCTTCGAC | TTTTCCGTCATCGTCTTTCC |
| **GusB** | CAAGCATGAGGATGCGGACA | GCTGGTACGGAAAGCGTTGG |
| **hUNR** | ACACAGACTGAGTACCAAGGA | CCTTTCTGCAGGCAATCCC |
| **mUNR** | AGGGAGTGTATGCTACGAACG | TCCAGCTGAACATTCCCTTC |

| Gene | Forward | Reverse |
|---|---|---|
| **mActin** | GATCTGGCACCACACCTTCT | GGGGTGTTGAAGGTCTCAAA |
| **p16** | ACCAGCGTGCCAGGAAG | CGTACCCCGATTCAGGTG |
| **p21** | TCTTGCACTCTGGTGCTGA | CTGCGCTTGGAGTGATAGAA |
| **Ki67** | GCTGTCCTCAAGACAATCATCA | GGCGTTATCCCAGGAGACT |
| **p19** | GCCGGCAAATGATCATAGAG | CAGCAAGAGCTGGATCAGAA |

## Purification of hUNR recombinant protein

BL21 bacteria containing pET21d-hUNR plasmid were grown at 37 ºC and induced with 0.5 mM of IPTG. Bacteria were pelleted and resuspended in lysis buffer (50 mM Tris-HCl pH=7.4, 500 mM NaCl, 10% glycerol, 0.5% Triton X-100, 20 mM imidazole and freshly added 1X Protease Inhibitor cocktail, 1 mM PMSF, 2 mM DTT) and passed three times through a French press. Cell lysate was incubated 1 hour at 4 ºC under rotation with previously equilibrated Ni-NTA beads. The mix was added into a column and elutions were collected using solutions (50 mM Tris-Cl pH=7.4, 500 mM NaCl, 10% glycerol) with increased amounts of imidazole (55, 164, 260, 380, 500 mM). Elutions with higher quantity and purity of hUNR were dialyzed in buffer D (20 mM HEPES pH=8.0, 20% glycerol, 0.2 mM EDTA, 1 mM DTT and 0.01% NP-40). Protein quantification was performed using BSA standards and electrophoresis.

## Immunoprecipitation (IP)

An optimized ratio of 20 µl of beads with 4 µg of antibody and 300 µg of cell extract (UV cross-linked samples) was used for this experiment. Antibodies were cross-linked to the beads to avoid interferences with SLBP detection. IP was performed in a final volume of 500 µl of Ipp500 buffer (100 mM Hepes, 750 mM NaCl, 7,5 mM $MgCl_2$, 2,5 mM DTT and 0,25% NP-40), 1.5 hours at 4 ºC. Following IP washes, RNase I (Ambion #AM2295) digestion was indispensable for protein elution. However, none or several washes after RNase I incubation differentiate RNA dependent/ independent interactions respectively. Final samples were boiled at 98 ºC for 10 minutes in 1X SDS buffer.

| Primary antibody | Host | Source |
|---|---|---|
| UNR | Rabbit | Home-made |
| UPF1 | Goat | Bethyl Laboratories #A300-036A |
| SLBP | Rabbit | Bethyl Laboratories #A303-968A |

## Immunofluorescence (IF)

Cells were fixed using 4% paraformaldehyde (Santa Cruz #sc-281692) 15 minutes at room temperature. Fixed cells were permeabilized with PBS-0.1% triton for 15 minutes at room temperature. After washes (PBS 1X) blocking solution (PBS with 5% of normal goat serum) was added and incubated for 1 hour at room temperature. Incubation with specific primary antibody diluted in blocking solution was performed overnight at 4ºC. After washes, cells were incubated with secondary antibody in blocking solution 1 hour at room temperature. Nuclei were stained with PBS 1X and DAPI (1 µg/ml) 15 minutes at room temperature. After washes, mowiol (Sgima #81381) was added to cover the sample.

| Primary antibody | Host | Dilution | Source |
|---|---|---|---|
| UNR | Rabbit | 1/1200 | Abcam #201688 |

| Secondary antibody | Host | Dilution | Source |
|---|---|---|---|
| Alexa Fluor 488 | Goat | 1/500 | Life Technologies #A-11008 |

## Western blot

Protein extraction was performed with HNTG (histone project) or RIPA (senescence project) buffer. HNTG buffer (20 mM Hepes pH 7.9, 150 mM NaCl, 1% triton, 10% glycerol, 1 mM MgCl2, 1mM EGTA and 1X protease inhibitors) is used for cytoplasmic proteins isolation , whereas RIPA buffer (150 mM NaCl, 10 mM Tris-HCl pH 7.5, 0.1% SDS, 1% DOC, 5 mM EDTA, 1% Triton X-100 and 1X protease inhibitors) allows both nuclear and cytoplasmic protein extraction. Protein samples were run in home-made acrylamide gels (SDS-PAGE), transferred to PVDF membranes,

blocked with 5% In TBS-Tween (10 mM Tris-HCl pH=7.5, 100 mM NaCl 0.1% Tween-20 (TBS-T), and incubated with primary antibody overnight at 4ºC. Membranes were then washed with TBS-T and incubated with Horseradish Peroxidase (HRP)-coupled secondary antibody 1 hour at room temperature. Proteins were detected by ECL, using a chemiluminescent substrate (GE Healthcare #RPN2209). Primary and secondary antibodies used for western blot are specified below.

| Primary antibody | Host | Dilution | Source |
|---|---|---|---|
| Cyclin A | Rabbit | 1/500 | Santa Cruz #sc-751 |
| Cyclin B1 | Mouse | 1/500 | Santa Cruz #sc-245 |
| UPF1 | Goat | 1/1000 | Bethyl Laboratories #A300-036A |
| SLBP | Rabbit | 1/1000 | Bethyl Laboratories #A303-968A |
| UNR | Rabbit | 1/40 | Home-made |
| p53 | Rabbit | 1/1000 | Leica Microsystem #NCL-p53-CM5p |
| PCNA | Mouse | 1/3000 | Sigma-Aldrich #P8825 |
| p21 | Mouse | 1/250 | BD Pharmingen #556431 |
| p19 | Rabbit | 1/1000 | Abcam #ab80 |
| p16 | Rabbit | 1/200 | Santa Cruz #sc-1207 |
| Actin | Mouse | 1/1000 | Santa Cruz #sc-47778 |

| Secondary antibody | Host | Dilution | Source |
|---|---|---|---|
| Anti-mouse IgG HRP | Goat | 1/5000 | Bio Rad #1721011 |
| Anti-Rabbit IgG HRP | Goat | 1/5000 | Bio Rad #1706515 |
| Anti-goat | Donkey | 1/5000 | Bethyl Laboratories #A50-101P |

## Two-dimensional (2-D) gel electrophoresis

The Proteomics Unit of Vall D'Hebron Institute of Oncology (VHIO) leaded by Francesc Canals performed the 2D gels.

## Mice

Wild type C57BL/6J new born mice were used for primary keratinocytes preparation as described above.

## Bioinformatical analysis

Claudia Vivori performed analysis of Part A using raw data from Wurth et al., 2016. Raw RNA-Sequencing data from Part B was analysed by the Bioinformatics Unit of the CRG. I personally performed the rest of analysis and generated most of the plots using R.

# Results

# A. Role of UNR in histone mRNA metabolism

## 1. UNR binds to mature histone mRNAs

In a previous report from our laboratory, we identified over a thousand direct UNR mRNA targets in melanoma SK-Mel-103 cells using the iCLIP (individual-nucleotide resolution crosslinking immunoprecipitation sequencing) technology (Wurth et al., 2016). Among the transcripts showing the strongest iCLIP UNR binding peaks were the histone mRNAs, suggesting that UNR regulates these transcripts. As previously reported (Tinton et al., 2005) and in support for such regulation, UNR expression is highest in the S and G2/M phases of the cell cycle, when histone mRNAs find their peak of expression (Figure 14a). Interestingly UNR binds to almost 90% of the histone transcripts expressed in melanoma cells (Figure 14b, Supplemental table 1). Evaluation of the iCLIP profiles indicated that UNR binding was most prominent in the 3'UTR just upstream of the stem-loop structure, and frequently spread to the stop codon and the last nucleotides of the ORF (Figure 14c). Further, whereas the first nucleotides of histone-iCLIP reads (i.e. the 5' reads) are distributed throughout the end of the ORF and the 3'UTR (Figure 14d green), the last nucleotides (the 3' reads) sharply condense to the second position after the stem-loop (Figure 14d, red). Because mature histone mRNAs finish at this position, these data suggest that UNR binds to mature histone mRNAs, and not to unprocessed mRNAs or transcripts in their way to degradation which contain oligo-uridine termini.

a

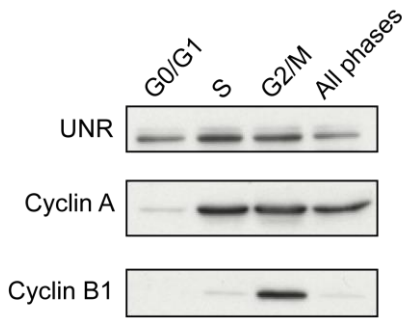

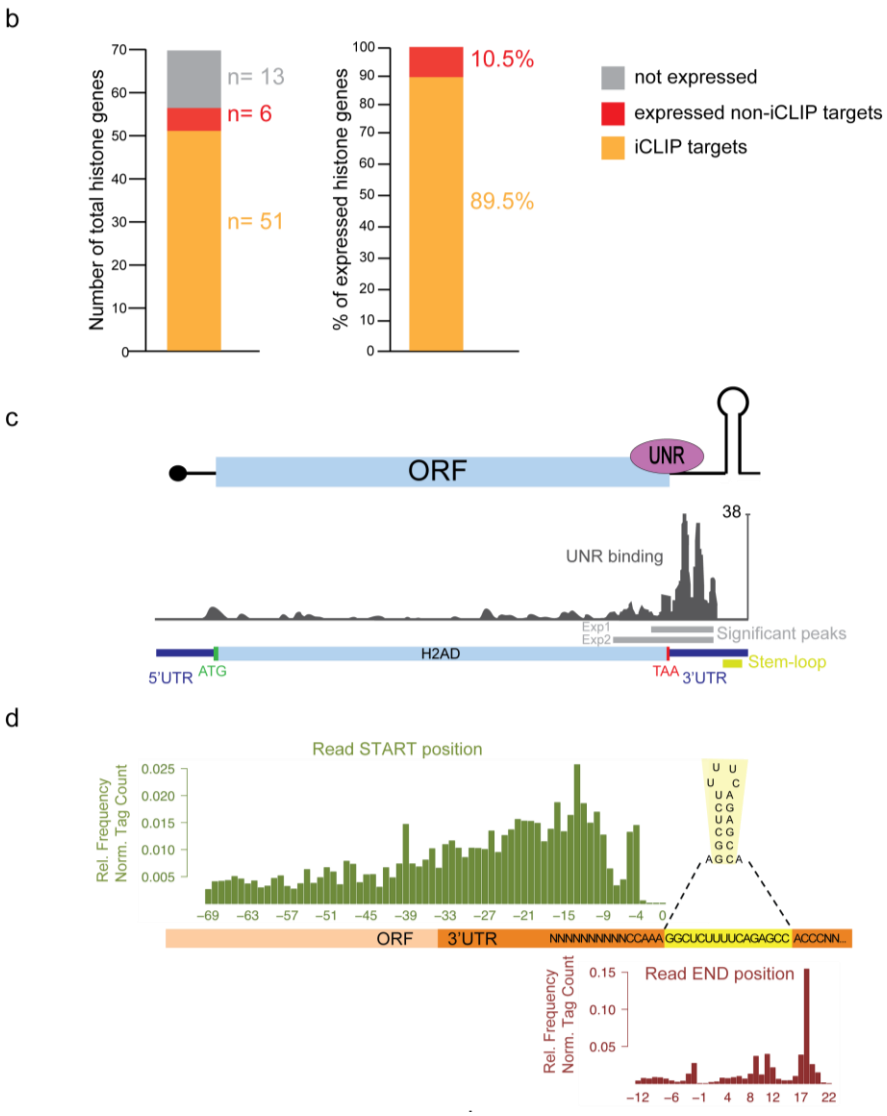


**Figure 14. UNR binds to mature histone mRNAs. (a)** Western blot to check UNR levels along the cell cycle. Cyclin A2 and B were used as controls for differential expression between phases. **(b)** Quantification of histone transcripts bound by UNR. **(c)** *Top*, schematic representation of UNR bound to a histone transcript. *Bottom*, iCLIP profiles of UNR binding to H2AD mRNA visualized with the UCSC genome browser. Exp1 and Exp2 represent independent experiments. The position of the stem-loop is depicted in yellow. **(d)** Metagene analysis of iCLIP tag frequency distribution along histone mRNAs (stem-loop highlighted in yellow). Green and red bars represent tags spanning the first and last position of the read, respectively.

## 2. Characterization of UNR binding to histone mRNAs

*In vivo* iCLIP and *in vitro* SELEX (Systematic Evolution of Ligands by EXponential selection) experiments identified a 6-nucleotide UNR consensus binding motif on UNR targets (Figure 15a) (Triqueneaux et al., 1999; Wurth et al., 2016). We assessed the presence of this motif in histone targets. For this analysis, we selected the last 50 nucleotides of the ORF together with the first 50 nucleotides of the 3'UTR, where UNR binding is most prominent. A meta-analysis of this region indicated that the motif was indeed present in the region, but was curiously located more frequently upstream of the center of UNR peaks (Figure 15b, left panel). We observed that the last 2 nucleotides of the motif potentially overlapped with the stop codon of histone mRNAs (**TA**A), and that elimination of the stop codon by deletion of the uridine drastically reduced the occurrence of the UNR binding motif, despite this position being variable in the overall UNR binding consensus (Figure 15b, right panel). This observation suggested that the uridine is invariable in UNR binding sites present in histone mRNAs, and that the stop codon might be necessary for UNR binding.

To test whether this was the case, we used electrophoretic mobility shift assays (EMSAs). Radioactively labeled histone RNA constructs containing wild type or mutated stop codons were incubated with increasing amounts of recombinant UNR, and complexes separated by non-denaturing gel electrophoresis (Figure 15c). Contrary to our expectations, mutation of the stop codon did not affect UNR binding. Further, mutation of all potential UNR binding motifs present in the histone construct did not reduce UNR binding, indicating that UNR binding to histone mRNAs is independent of the previously described UNR binding signature (Figure 15c).

Given the strong preference of UNR binding between the stop codon and the stem-loop (Figure 14c), we reasoned that factors binding to these landmarks may attract UNR to bind in such position. We thus wondered whether there was any sharp positioning of UNR relative to the stop

codon or the stem-loop. We calculated the distribution of distances for every UNR tag to these sequence elements, and expressed these frequencies along the 3' UTR length. We found that UNR tags are concentrated at 5-50% sequence length relative to the stop codon and at 20-60% sequence length relative to the stem-loop, without a particularly sharp distribution (Figure 15d), suggesting that UNR binding does not depend on these sequence elements. We conclude that UNR binds to histone mRNAs irrespective of the consensus RNA binding motif and other RNA landmarks.

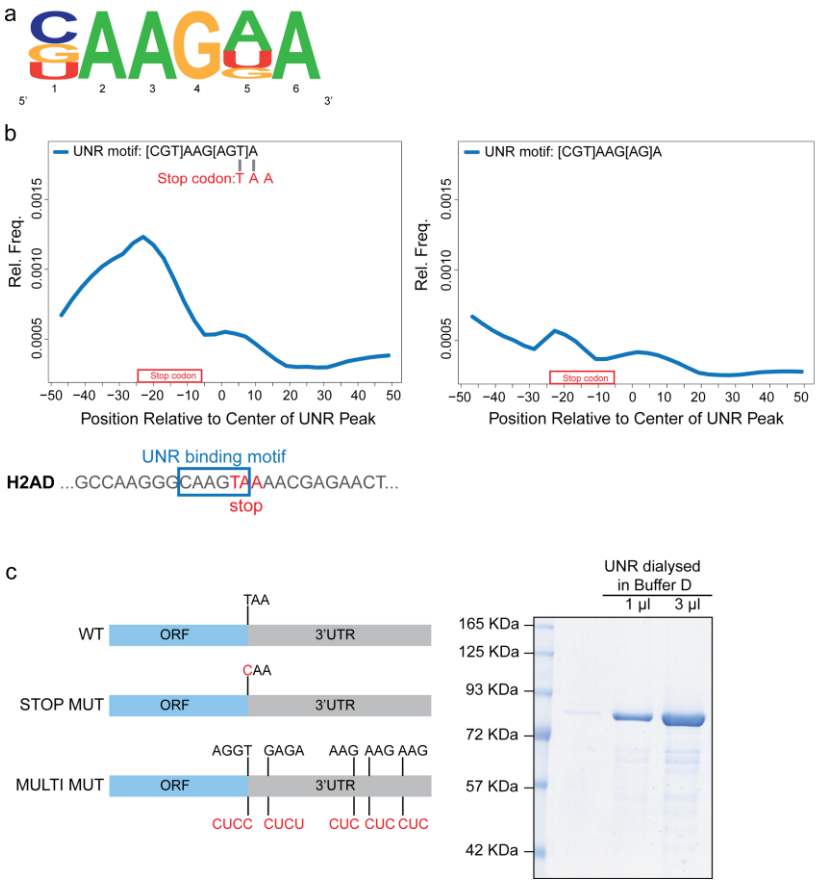

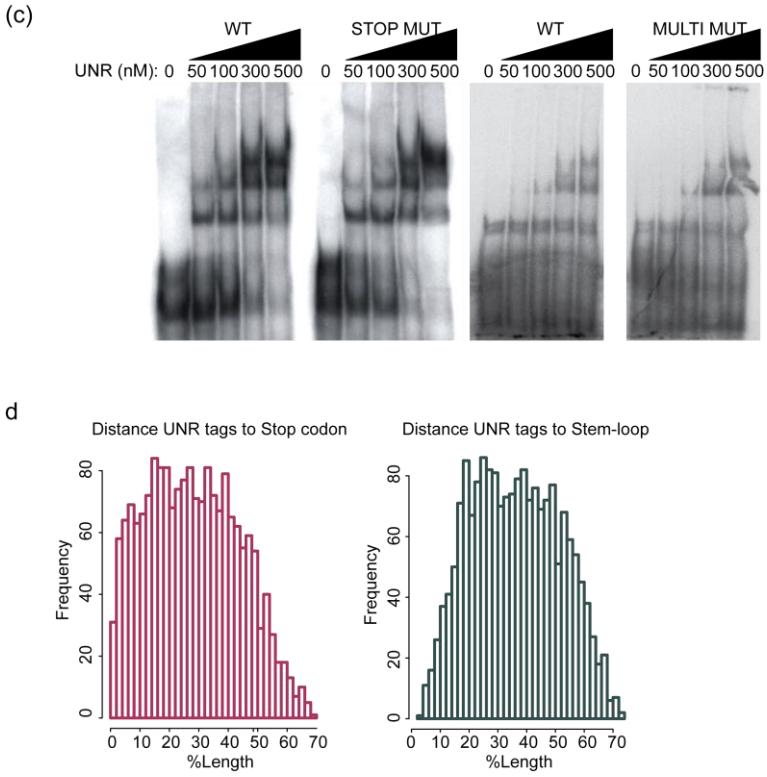


**Figure 15. UNR binds to histone mRNAs irrespective of the UNR consensus motif and other RNA landmarks. (a)** UNR binding motif, as identified with DREME (Wurth et al., 2016). **(b)** Relative frequency of wild type (left) or mutated (right) UNR binding motifs on histone mRNAs. The sequence of H2AD mRNA is shown as an example of the UNR binding motif overlapping with the stop codon. **(c)** *Top left*, schematic representation of RNA constructs used for EMSA. The RNAs consist of the last 50 nucleotides of the ORF and the full 3'UTR, either in its wild type version or containing the indicated mutations. *Top right*, acrylamide gel with purified recombinant hUNR used in the experiment. *Bottom*, EMSAs were performed with increasing amounts (0, 50, 100, 300 and 500 nM) of purified recombinant hUNR. **(d)** Distribution of UNR-tags relative to the stop codon (*left*) and the stem-loop (*right*). Zero indicate the last position of the stop codon or the first position of the stem-loop. Distances are represented as percentage of the 3' UTR.

## 3. UNR depletion decreases histone mRNA levels

As mentioned in the introduction, histone mRNAs are an unusual group of eukaryotic transcripts. They are the only mRNAs that lack a poly(A) tail and instead have a stem-loop that directs mRNA export, translation and turnover. Therefore, to assess whether UNR functions to regulate histone

mRNA levels, we used total RNA sequencing (as opposed to the more typical poly(A)-RNA-Seq) of cells where UNR had been depleted using an shRNA construct (Wurth et al., 2016).

A comparison of UNR binding (i.e. iCLIP enrichment) versus mRNA abundance upon UNR depletion indicates a poor correlation, suggesting that regulation of mRNA levels may not be the main function of UNR on its targets (Figure 16). However, histone mRNAs are generally downregulated when UNR is depleted, and represent the class of mRNAs showing the most dramatic changes (Figure 16, red dots). Indeed, almost 65% of the histone transcripts are downregulated upon UNR depletion (p value < 0.01), indicating that UNR promotes histone mRNA steady state levels (Supplemental table 1).

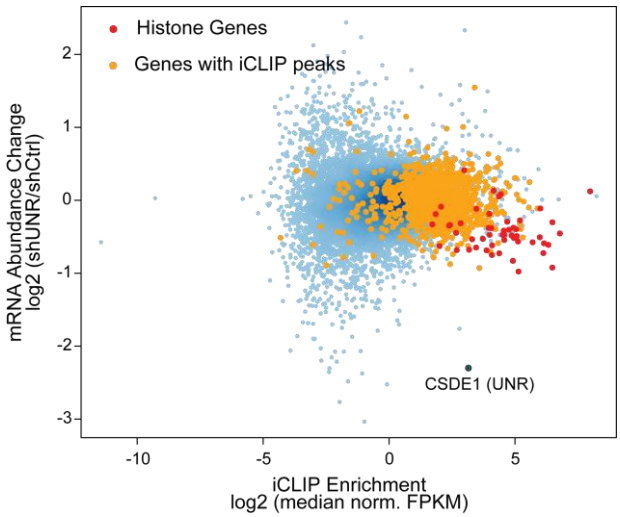


**Figure 16. UNR promotes histone mRNA levels.** Scatter plot showing the correlation between iCLIP-tag enrichment and mRNA abundance changes between shUNR and shCtrl cells. Blue dots represent non-UNR targets, orange dots denote UNR targets with the histone mRNAs highlighted in red.

## 4. Mechanisms of UNR function on histone mRNAs

Several mechanisms can be envisaged to explain the effect of UNR on histone mRNA levels. First, UNR could play a role during histone pre-mRNA transcription and processing. These processes increase about 35-fold during G1-S transition, where UNR is most highly expressed (Figure 14a). However, because UNR is primarily cytoplasmic and binds to mature histone mRNAs, we considered that UNR most likely targets cytoplasmic processes.

Mature histone transcripts are highly translated all along S phase. When DNA replication is complete, UPF1 is phosphorylated and binds immediately upstream of the stem-loop, where it contacts the stem-loop binding protein (SLBP) triggering activation of histone mRNA degradation (Brooks et al., 2015). Interestingly, this degradation is thought to occur under active translation, as translation inhibition or downregulation of CTIF (a Cap Translation Initiation Factor operating on histone mRNAs) stabilize histone mRNAs (Choe et al., 2013; Kaygun and Marzluff, 2005a). Degradation coupled to translation shows similarities to the non-sense mediated decay (NMD) pathway. Both histone mRNA degradation and NMD depend on UPF1 (Choe et al., 2014; Popp and Maquat, 2016), and in both cases degradation occurs on CBC-associated mRNAs rather than on eIF4E-associated mRNAs (Choe et al., 2013). Furthermore, NMD is activated when a stop codon is present at a certain distance from an exon junction complex (EJC) that attracts UPF1. Although most histone mRNAs are not spliced and do not contain EJCs, the stem-loop could serve as the landmark that attracts UPF1 to these transcripts. The presence of alternative in-frame stop codons in histone 3'UTRs (see below) strengthens the idea of parallel mechanisms acting on NMD and histone mRNA degradation (Figure 8). Taken together, we speculate that UNR could: 1) inhibit UPF1 function in histone mRNA degradation until end of S phase, 2) inhibit stop codon recognition by promoting readthrough, thereby avoiding histone mRNA degradation, and 3) inhibit translation,

consequently stabilizing histone mRNAs (Figure 17). In the following sections, I will describe my efforts to address these possibilities.

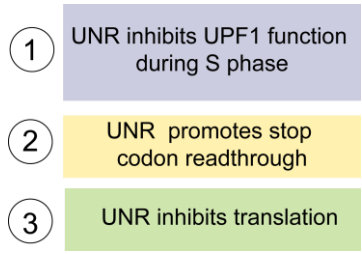


**Figure 17. Potential mechanisms to explain the effect of UNR on histone mRNA levels.** Three hypothesis to explain UNR function are indicated.

## 5. Does UNR interfere with UPF1 function during S phase?

To address this possibility, we tested whether UNR interacts with UPF1 and/or SLPB by co-immunoprecipitation. Experiments using total cell extracts showed a weak interaction between these components, which improved when we used UV-crosslinking to stabilize RNA-protein interactions (data not shown). The interaction further improved when we used extracts from cells staged at the end of S phase (Figure 18b) following double thymidine block (Figure 18a), where the interaction of UPF1-SLBP is thought to take place. We found that UNR interacted with both UPF1 and SLBP in an RNA-dependent fashion, as treatment with RNase dramatically reduced the signal (Figure 18c). The interaction with UPF1 is stronger. However, the RNA-dependency of this interaction suggested that UNR-UPF1 contacts are not direct. Coupled with the difficulties of producing these proteins in recombinant versions, we did not pursue this line of research further.

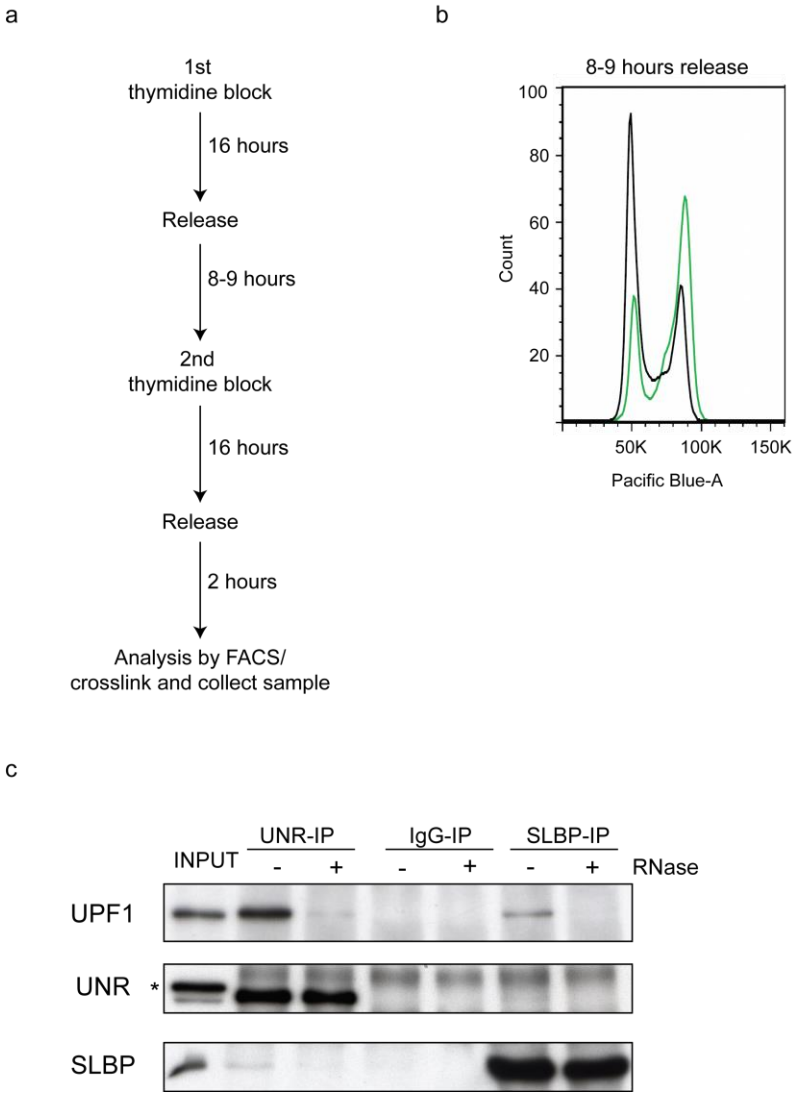


**Figure 18. UNR interacts with UPF1 and SLBP during S phase. (a)** Protocol used to obtain cells at the end of S phase. Thymidine addition blocks cells during S phase as the excess of thymidine compared with the other nucleotides results in the blockage of the RNA polymerase. Standard double thymidine block for 16 hours is interspersed by a release step whose length can be adapted to the duration of the S phase of the cell of interest. **(b)** In melanoma SK-Mel-103 cells, which divide approximately every 24 hours, and 8-9 hour release showed a high accumulation of cells in late S phase after the second thymidine block (measured by FACS). **(c)** Immunoprecipitation of UNR with SLBP and UPF1. Non-specific IgG was used as negative control. A step of treatment with RNase ONE (+) or buffer (-) was included during immunoprecipitation.

## 6. UNR does not promote stop codon read-through

To investigate the relationship between UNR and potential stop codon read-through, we first analysed the occurrence of stop codons in the 3' UTRs of histone transcripts and their position relative to UNR binding. In Figure 19a, a meta-analysis is shown where normalized UNR tags (red), the beginning of the stem-loop (black), and in-frame stop TAA, TGA and TAG codons (blue, green and yellow, respectively) are represented relative to the 3' UTR start. For the three possible stop codons, the sharpest peak is present at the canonical stop (mainly TAA), as expected. However, several in-frame stop codons which concentrate before the beginning of the stem-loop can be observed. Strikingly, we found that about 45% of UNR-histone targets contain two or more in-frame stop codons at or near UNR binding sites (Figure 19b). Thus, UNR could promote recognition of these sites by the translation machinery, preventing recognition of the canonical stop codon by the UPF1-NMD machinery.

Stop-codon read-through is a phenomenon that plays important physiological roles (reviewed in Dabrowski et al., 2015). For example, this mechanism operates on VEGF mRNA to produce an extended VEFG isoform that has opposite properties compared to canonical VEGF. In this case, the RBP hnRNPA2B1 binds downstream of the stop codon and prevents its recognition by translation termination factors. UNR could have similar roles as hnRNPA2B1, leading to the production of histones with elongated carboxyl-ends which could bear novel capacities. To test whether UNR promotes stop-codon read-through, we explored the ribosome profiling data available in the laboratory for SK-Mel-103 cells containing (shCtrl) and lacking (shUNR) UNR (Wurth et al., 2016). We checked whether the number of Ribosome Protected Fragments (RPFs) in the 3' UTRs of histone transcripts was different in shCtrl and shUNR cells, after normalization with RPFs detected in the ORF. This analysis was performed with three independent biological replicates (Figure 19c,

RPF1-3), and yielded a negative result as differences were not significant, suggesting that UNR does not promote stop-codon read-through.

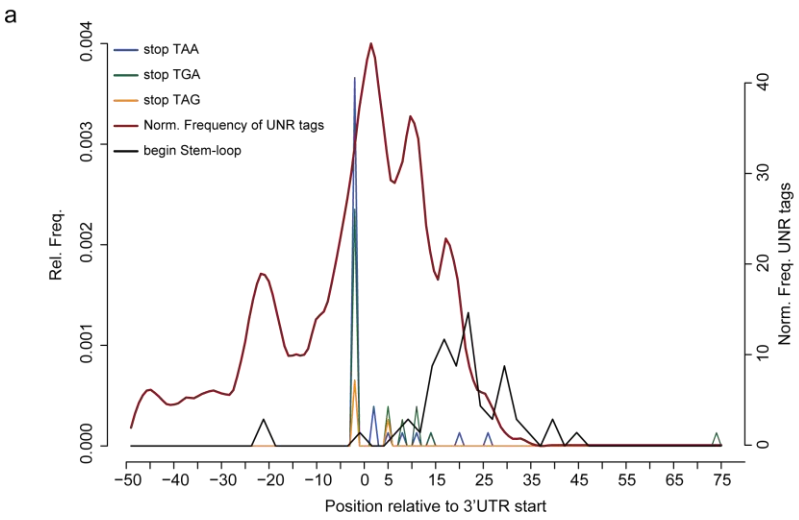


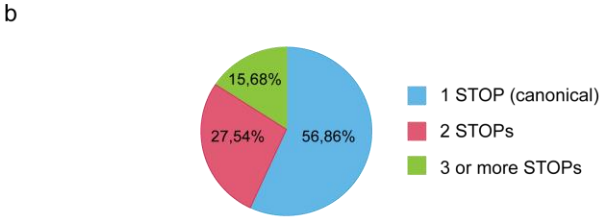


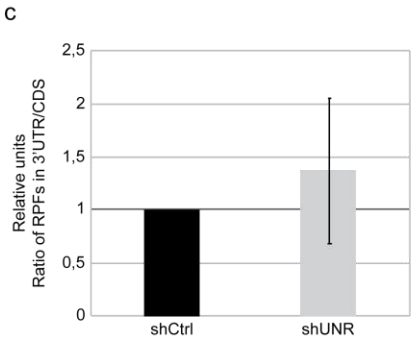


| | | 50nt End of CDS | 50nt beginning of 3UTR | 3'UTR/CDS |
|---|---|---|---|---|
| RPF1 | shCtrl | 121835 | 229 | 0,00188 |
| | shUNR | 84822 | 340 | 0,00401 |
| RPF2 | shCtrl | 29733 | 142 | 0,00478 |
| | shUNR | 25214 | 142 | 0,00563 |
| RPF3 | shCtrl | 105374 | 376 | 0,00357 |
| | shUNR | 66979 | 193 | 0,00288 |

**Figure 19. *In silico* analysis to address stop codon read-through by UNR. (a)** Normalized frequency of UNR tags (red) was calculated considering the total number of tags for each HIST gene. In-frame stop codons (TAA blue; TGA green; TAG yellow), and the beginning of the stem-loop (black) in histone 3' UTRs. Zero in the X-axis represents the start

of the 3' UTR. **(b)** Quantification of histone UNR targets that contain one (canonical) (blue), two (red) and three or more (green) in-frame stop codons. **(c)** Analysis of ribosome profiling data. The chart summarizes the ratio of RPFs found in the first 50 nt of histone 3'UTRs compared with those found in the last 50 nt of the ORFs, in shCtrl versus shUNR cells.

However, because of the observed variability between replicates we decided to undergo experimental validation of this conclusion. We selected a histone mRNA containing an in-frame alternative stop codon far enough from the canonical one such that the potential incorporation of extra amino acids could be distinguished by a change in the size of the protein after PAGE separation. *H2AD* mRNA was a good candidate, as it allowed an extension of 13 amino acids, increasing the size of the protein about 1.6 kDa (Figure 20a). We therefore cloned the whole *H2AD* mRNA sequence (including the 5', ORF and 3' UTRs) under the T7 promoter, and added a stretch of six alternate methionine and cysteine (MCCMCM) at the beginning of the ORF to allow for efficient labeling with $^{35}$S-Met/Cys, as the original transcript does not contain any (Figure 20b). A version with a mutated canonical stop codon was also included. Both RNA and DNA from these constructs were used as templates in a TNT transcription-translation system, with and without addition of recombinant UNR, and translated histone products were separated in a 15% acrylamide gel (Figure 20c). No stop codon readthrough was detected after addition of UNR (compare – with + lanes). Curiously, a reduction in histone levels is observed when DNA –but not RNA- is used as template, irrespective of the construct used. This result suggests that UNR does not repress histone mRNA translation directly, and that the effect on histone levels depends on transcription.

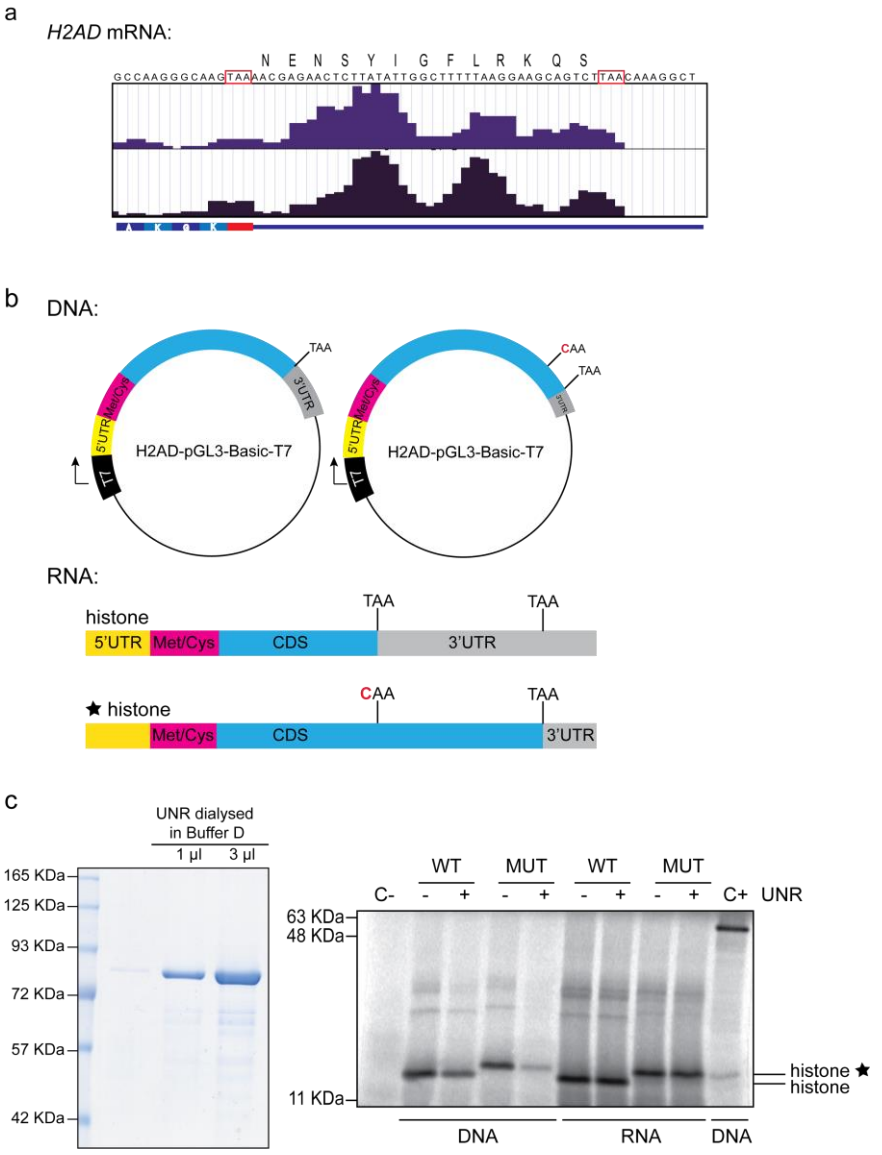


**Figure 20. UNR does not promote stop codon read-through. (a)** *H2AD* mRNA contains an in-frame stop codon in the 3' UTR, allowing an extension of 13 amino acids after potential stop codon readthrough. The stop codons are indicated with a red square, and the amino acids that would be incorporated should stop codon readthrough take place are indicated. **(b)** Schematic representation of the constructs used in this experiment. Met/Cys (pink) indicates a stretch of MCCMCM amino acids that was included at the amino-terminal for labeling purposes. Mutation of the canonical stop codon in the control histone construct (star) is indicated. **(c)** *Left*, acrylamide gel with purified recombinant hUNR used in the experiment. *Right, in vitro* translation after adding 1 µg of DNA or RNA to TNT coupled transcription-translation extracts. 4.2 µg of UNR (+) or buffer D (-) were also added. C- (no

construct added) and C+ (construct from Figure 21a *luc*) indicate negative and positive controls respectively.

## 7. UNR promotes mRNA levels in a transcription-dependent manner

To evaluate a transcription-dependent role of UNR, we first used the TNT system as described above, using plasmid DNA as template and including a Firefly luciferase (*luc*) construct as control (Figure 21a). Recombinant UNR addition resulted in reduction of both histone and luc levels when the plasmid were tested separately (Figure 21b, lanes 2-5). However, when both plasmids were included together in the same reaction, reduction of luc but not of histone was observed (lanes 6-7). Further, RT-qPCR of the RNA remaining in the TNT reactions showed a direct correlation between protein and RNA levels, indicating that UNR does not promote translation inhibition *in vitro*, but rather affects mRNA levels, most likely at the level of transcription and in a non-specific manner (Figure 21c). As we are using recombinant UNR, these non-specific effects could be due to a contaminant in the UNR preparation present at sub-stoichiometric amounts (Figure 21a*)*.

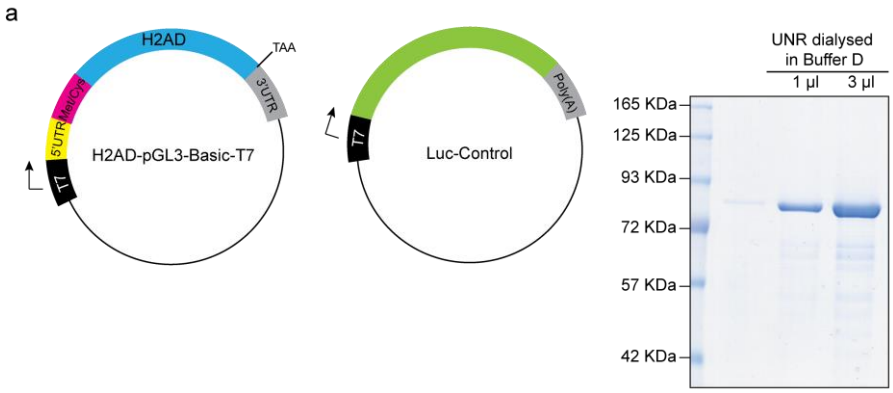

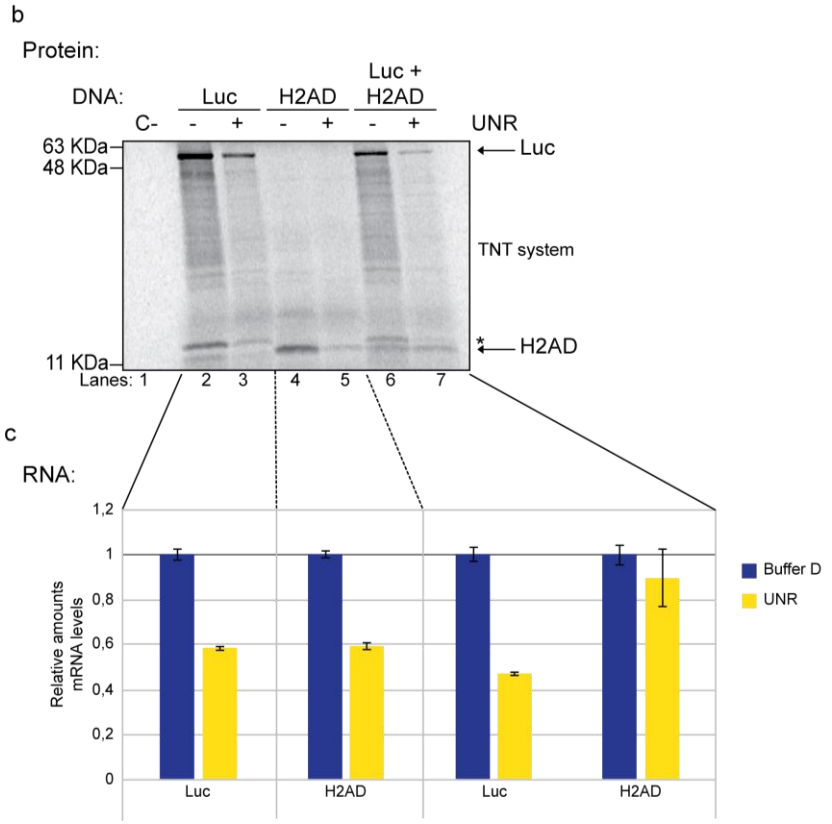


**Figure 21. Analysis of the effect of UNR in an *in vitro* TNT system. (a)** *Left*, representation of the plasmids used as templates. *Right*, acrylamide gel with purified recombinant hUNR used in the experiment. **(b)** 25 ng of plasmids were added separated (lanes 2-5) or together (lanes 6-7) to TNT extracts in the presence of 1.4 µg of recombinant UNR (+) or buffer D (-), and products were separated in a 15% acrylamide gel. The first lane (C-) indicates no construct added. The asterisk indicates a degradation product of luc. **(c)** Analysis of *luc* and *H2AD* mRNA levels after completion of the TNT reaction by RT-qPCR. Error bars represent the standard deviation between qPCR technical replicates.

To assess whether UNR affects transcription in a more physiological setting, we turned to melanoma SK-Mel-103 cells. UNR was depleted from these cells using either a shRNA hairpin (shUNR) or siRNA pools (siUNR), the latter allowing more acute and highly specific depletion. We then transfected H2AD histone constructs, either in the form of DNA to test for nuclear effects, or RNA to test for cytoplasmic effects. In addition, we included co-transfected Renilla as an internal control. RNA

transfection experiments showed that *H2AD* RNA levels were not affected by UNR depletion, indicating that UNR does not regulate the stability of *H2AD* mRNA in the cytoplasm (Figure 22a). However, depletion of UNR resulted in reduced RNA levels when DNA transfection was used (Figure 22b). There was no distinction on whether a Renilla or a Luc construct were transfected, indicating a non-specific effect of UNR on transcription. This raises the possibility that UNR affects transcription elongation or termination. Alternatively, UNR may affect the nuclear history of mRNAs in some other way with further consequences in the cytoplasm (see Discussion).

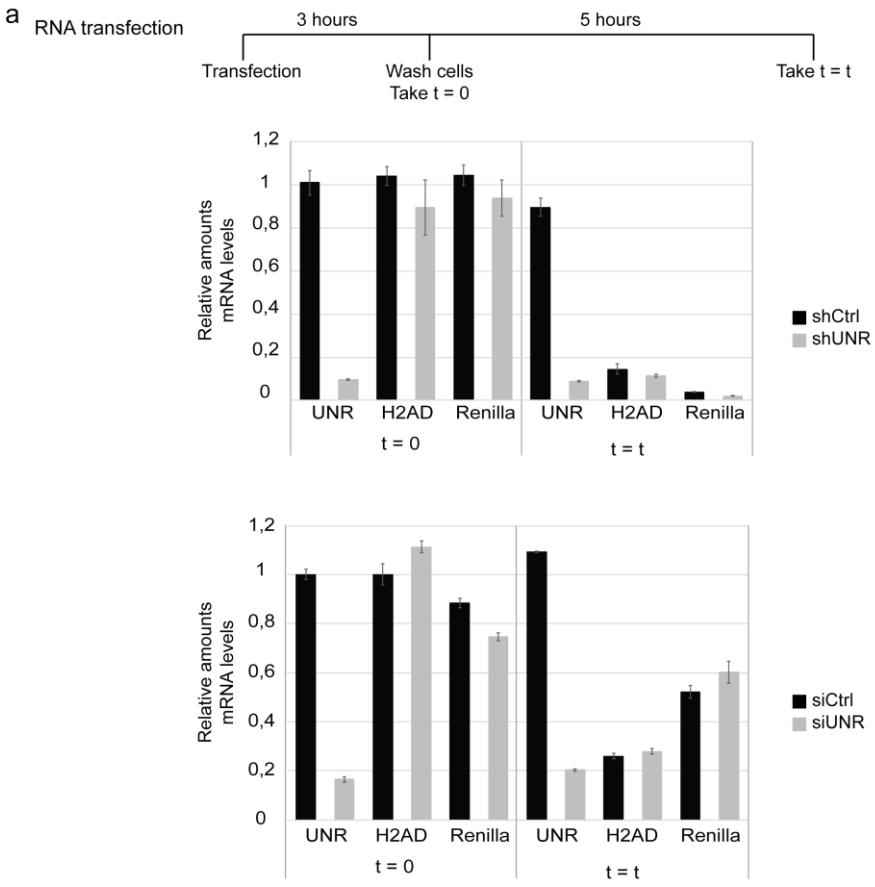

b

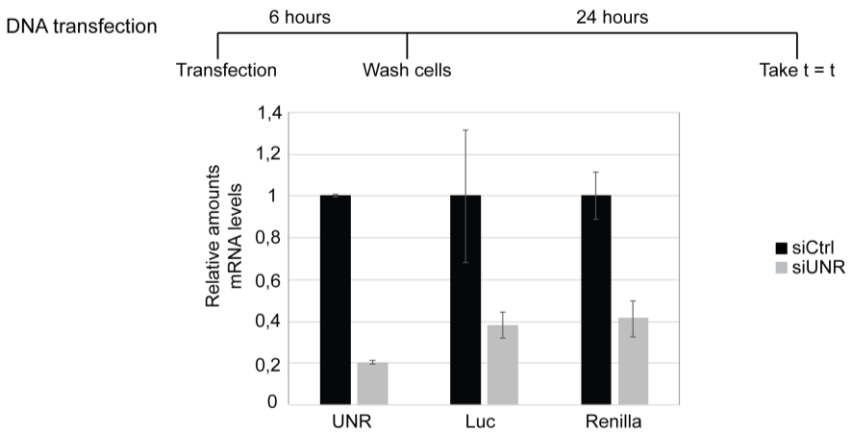


**Figure 22. UNR promotes mRNA levels in a transcription-dependent manner. (a)** RNA transfections. Histone *H2AD* and *renilla* mRNAs were co-transfected into Sk-Mel-103 cells that contained (shCtrl, siCtrl) or lacked (shUNR, siUNR) UNR. RNA was extracted after 3h (t=0) or 8h (t=t) of transfection, and transcripts were quantified by RT-qPCR. *UNR* mRNA levels are shown in the graph. *GusB* and *PSMB4* mRNAs were used as normalizers, respectively. Error bars represent the standard deviation of technical triplicates. **(b)** DNA transfections. Renilla and histone H2AD plasmids were co-transfected into cells containing (siCtrl) or lacking (siUNR) UNR. Samples were after 30 h (t=t) after transfection and RNA levels measured by RT-qPCR. *PSMB4* mRNA was used as normalizer. Error bars represent the standard deviation of technical triplicates.

Given the constant negative results, and the difficulties in assessing specific effects of UNR on histone transcripts, we decided to re-direct our efforts towards the analysis of UNR in senescence.

## B. Role of UNR in oncogene-induced senescence

### 1. UNR expression is necessary for oncogene-induced senescence in primary mouse keratinocytes (PMK)

In addition to histone mRNAs, UNR binds to a sizeable number of transcripts encoding SASP factors, including such well known as CCL2, IL-1B, IL-8, MIF, MMPs or SERPINE1 among others. This observation prompted us to test for a possible role of UNR in cellular senescence. We tested this possibility using an oncogene-induced senescence (OIS) model established by expressing oncogenic H-RAS in primary mouse keratinocytes (PMK) (Ritschka et al., 2017). We extracted PMKs from newborn (0-48 hours) mice, and infected them with a retrovirus expressing human oncogenic *H-RAS V12* in order to induce senescence, or with the empty retroviral vector as control (Figure 23a). To test for an effect of UNR in senescence, retroviruses expressing either shCtrl or shUNR were co-infected together with *H-RAS V12* (Figure 23a). After selection with puromycin and hygromycin (the selectable markers contained in the viral vectors), we monitored for the appearance of senescent cells by microscopy (see a schematic representation of the protocol in Figure 23b). Senescent cells are clearly distinguished from their non-senescent counterparts by their enlarged appearance ("fried-egg"-like). We observed that cells infected with the empty vector were small and died before one month in culture (Figure 23c, left). H-RAS V12 expressing cells (either alone or in the presence of shCtrl) underwent a phase of rapid proliferation followed by a decline leading to a complete loss of division potential. Cessation of proliferation was concomitant with the appearance of greatly enlarged and flattened cells containing stress-related vacuoles in the cytoplasm, typical of senescence (Figure 23c, middle). These cells detached from the plate and finally died at around 20 days post infection (dpi). Strikingly, although H-RAS cells co-infected with shUNR underwent comparable early events, they seemed to bypass senescence. This was visible by a greatly reduced number of senescent

cells and increased number of small proliferating cells already at 6 dpi (Figure 23c, right) which, in many cases, preceded cell immortalization. We conclude that UNR is necessary for oncogene-induced senescence.

Hereafter, H-RAS+shCtrl and H-RAS+shUNR cells will be referred to as shCtrl and shUNR cells, respectively.

a


b

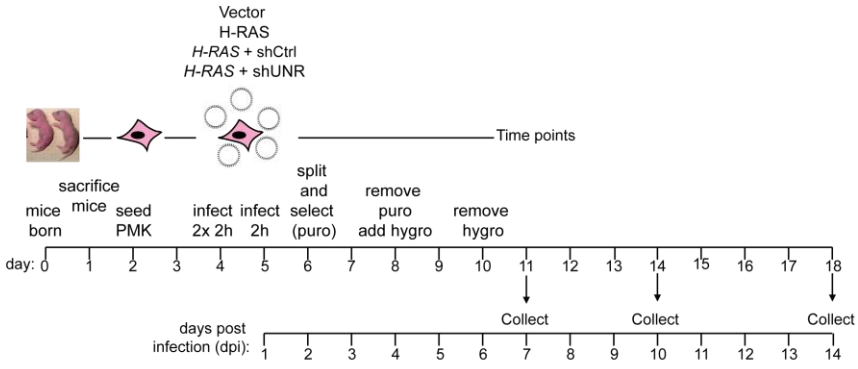


c

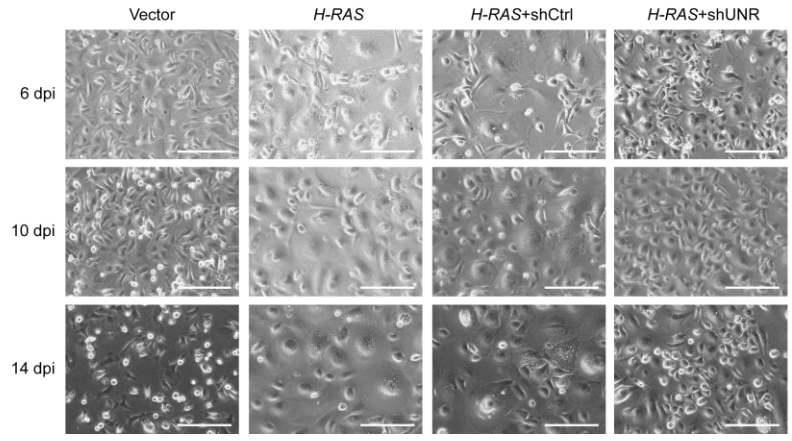

**Figure 23. UNR expression is necessary for oncogene-induced senescence (OIS) in primary mouse keratinocytes PMK. (a)** Viral vectors used in this study. **(b)** Schematic representation of the protocol followed to study the role of UNR in OIS. PMKs were infected either with the empty retroviral vector (MSCV), or with vectors expressing a constitutively active form of *H-RAS* (H-RAS V12) together with shCtrl or shUNR. After infection, cells were split and selected consecutively with puromycin and hygromycin. Cells were collected at increasing time points, typically 6-7, 10 and 14 dpi. **(c)** Depletion of UNR blocks senescence. Images of infected cells at 6, 10 and 14 dpi (see text for details). Scale bar: 200 µm. These images correspond to an experiment using helper plasmid (■) however, it is perfectly reproducible without helper (□).

## 2. UNR expression along OIS

Given the relevance of UNR for the establishment or maintenance of the senescent program, we characterized its expression along OIS using Western blot and RT-qPCR. We also used microscopy to characterize the localization of UNR in PMK cells. First, as previously reported for other cells, UNR is primarily cytoplasmic in PMK (Figure 24a). The distribution of UNR appears to be asymmetric, consistent with potential co-localization with the endoplasmic reticulum, as observed for melanoma cells (unpublished data from our laboratory). In Western blot, UNR was detected as a doublet using an affinity-purified polyclonal antibody (Figure 24b). Quantification using Ponceau S as loading reference indicated that UNR levels increase by viral infection, and they are maintained along senescence (Figure 24b). The levels of *UNR* mRNA remained constant at all conditions and time-points tested, suggesting that changes in UNR protein levels upon viral infection are due to post-transcriptional regulation (Figure 24c).

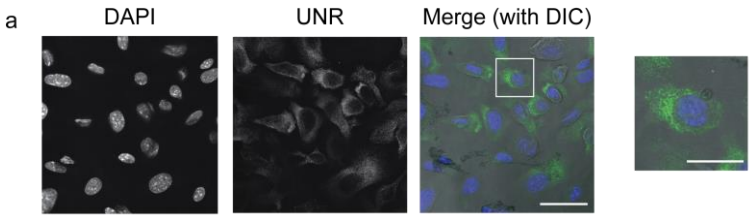

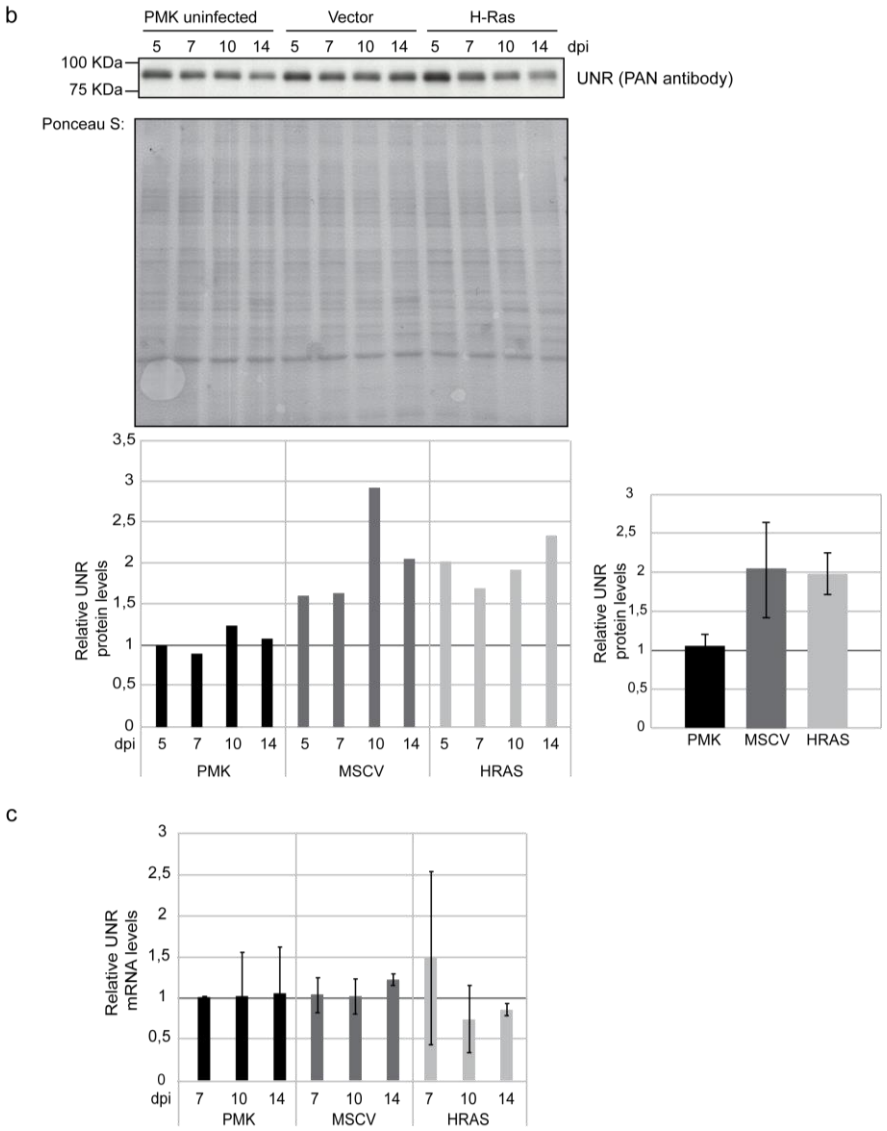


**Figure 24. UNR expression along OIS. (a)** UNR is a cytoplasmic protein. Immunofluorescence of proliferating PMKs, performed with a monoclonal anti-UNR antibody (Abcam #ab201688, green) together with DAPI (blue), and including a bright field view. Left scale bar = 4 µm. Right scale bar = 2 µm**. (b)** Expression of UNR protein along senescence. *Top*, Western blot of uninfected, vector-infected and H-RAS-infected PMKs with an affinity-purified polyclonal anti-UNR (PAN) antibody (home-made). *Middle*, Ponceau S staining of the Western blot membrane, used as loading control. *Bottom*, quantification of the Western blot. The amount of UNR in uninfected PMK at day 5 was used as reference. The quantification on the *right* shows the average level of UNR protein at each condition. (n = 1)

(□) **(c)** Expression of UNR mRNA along senescence. UNR mRNA levels were assessed by RT-qPCR, and expressed relative to the amount in uninfected PMK at day 7. (n = 2) (□)

## 3. UNR isoforms in PMK

Different isoforms and post-translational modifications have been described for UNR in databases. To analyse whether different UNR isoforms could be detected in PMK, we used two-dimensional (2-D) gel electrophoresis. Here, proteins are first separated according to their isoelectric point, and then resolved according to their size. Using a polyclonal affinity-purified antibody generated in the lab (PAN antibody) we compared the isoforms detected in SK-Mel-103, HeLa and PMK cell extracts. We indeed observed a variety of dots, each representing a UNR variant. As previously observed (A. Nogales, Master thesis) five variants were identified at the expected size of ~90 KDa in SK-Mel-103 cells, suggesting extensive post-translational modifications (Figure 25a, nº 1-5). Four of these were also identified in HeLa, a cell line showing an additional variant (Figure 25b, nº 6). Comparatively, PMK showed striking differences (Figure 25c). Variants detected in SK-Mel-103 and Hela cells were weak, while the major signal corresponded to two prominent new variants. Altogether, at least six additional variants were detected in PMK. Incubation with a monoclonal commercial antibody (Abcam #ab201688) showed the same pattern, and UNR depletion resulted in decreased signal intensity indicating specificity (data not shown). These results indicate that a variety of UNR isoforms are expressed in cells, and open new questions as to their function and oncogenic relevance.

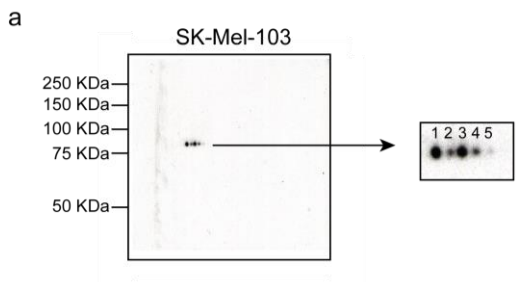

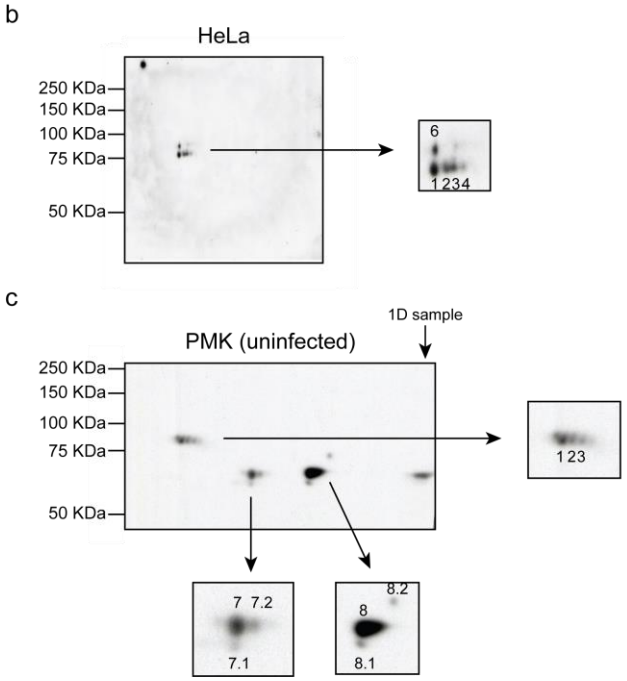


**Figure 25. UNR isoforms. (a, b)** Extracts from melanoma SK-Mel-103 and HeLA cells respectively. **(c)** Uninfected PMK shows striking differences in UNR variants. Additional dots (7, 7.1, 7.2, 8, 8.1 and 8.2) are identified in these cells. These additional blots ran according to one dimension (1D) sample separation, suggesting that correspond to UNR protein. (n = 1)

## 4. UNR depletion leads to senescence bypass

We next decided to confirm that UNR is required for OIS using quantitative assays. Senescent cells undergo distinctive morphological alterations, which are not always easy to quantify. Especially for adherent cells, morphological changes (size, shape) are easy to detect by microcopy but they might be lost upon detachment from the tissue culture plate. As striking differences were observed in cells attached to culture plates, we first decided to check their size upon suspension by flow cytometry. Indeed, a change in cell size distribution is observed upon UNR depletion, with an increased proportion of cells in smaller and intermediate sizes (Figure 26a). This indicates a reduction in cell size

upon UNR depletion that correlates with the observations under the microscope.

As senescent cells undergo irreversible growth arrest, we next assessed the proliferative capacity of cells using a variety of assays. Colony-forming assays indicated that the number and size of colonies increased upon UNR depletion, consistent with a higher proliferation capacity (Figure 26b). BrdU incorporation tests followed the same tendency (Figure 26c). Reassuringly, the dynamics of BrdU incorporation along infection follows the expected pattern: while BrdU incorporation decreases over time in shCtrl cells, it slightly increases in shUNR cells. These observations correlate with the observed changes in the senescent behavior.

Finally, shCtrl (senescent) cells did not survive a protocol of repeated passages, while shUNR cells often survived to passage and kept proliferating to finally become immortal. We have already derived three independent PMK cell lines and have been able to pass these cells so far indefinitely (see two examples in Figure 26d). Altogether, these data indicate that UNR is required for OIS, and suggest that UNR may have tumor suppressive properties in this context.

a

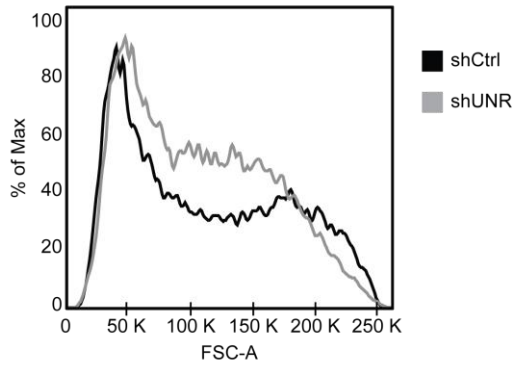

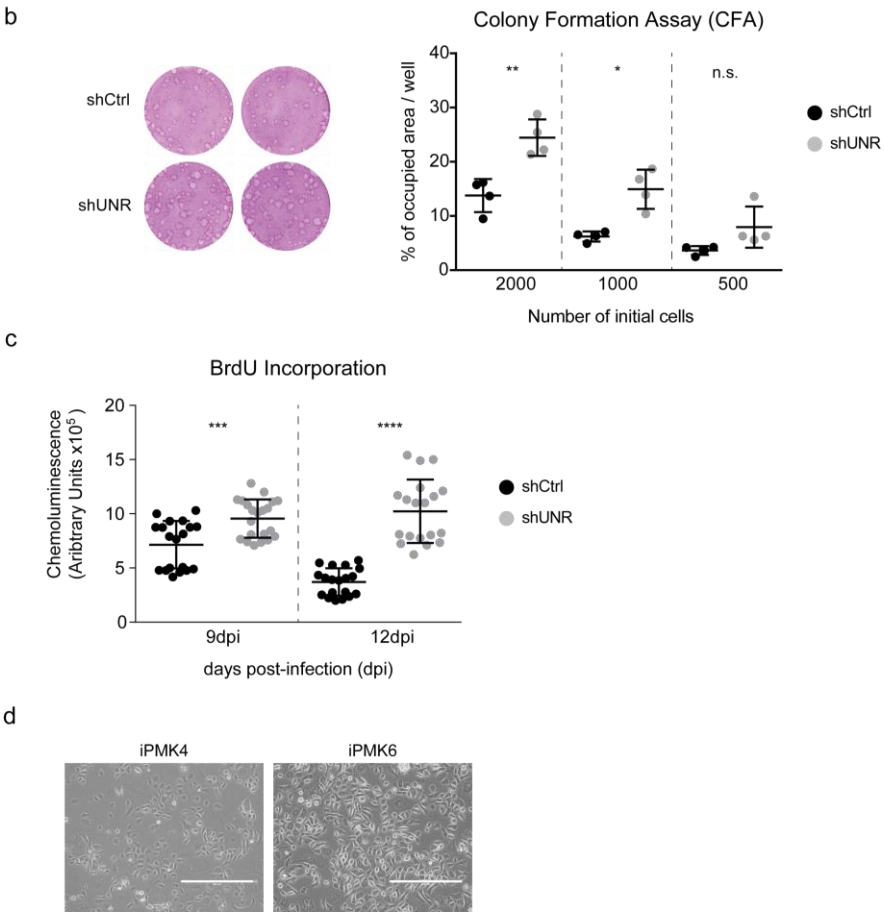


**Figure 26. UNR depletion leads to senescence bypass. (a)** UNR depletion leads to smaller cells. Distribution of cell sizes was measured by FACS. FSC-A: Forward Side Scatter Area. (□) **(b)** UNR depletion results in higher colony forming capacity. shCtrl and shUNR PMKs were seeded on a layer of mitotically inactivated feeder cells (see Materials and Methods for details). *Left,* typical images obtained after seeding 1000 PMK cells. *Right*, quantification of results (area occupied by cells) upon 2000, 1000 and 500 PMK cells. (n = 2, technical replicates = 2). Statistical unpaired t-test was used. p-value < 0.01 (**); p-value < 0.05 (*). (□) **(c)** BrdU incorporation is higher in shUNR PMKs. This assay measures DNA synthesis, which is increased in proliferating cells. BrdU incorporation was measured at 9 and 12 dpi using a kit (Roche #11-669-915-001). (n = 2, technical replicates = 11). Statistical unpaired t-test was used. p-value < 0.001 (***); p-value < 0.0001 (****). (□) **(d)** Images of two immortalized PMK-shUNR cell lines. Scale bar = 400 µm. (□)

## 5. UNR reinforces the SASP-associated tumour suppressor response

The senescence-associated secretory phenotype (SASP) is responsible for the activities of senescent cells through the secretion of multiple biomolecules. SASP comprises cell-autonomous functions such as the growth arrest observed in senescent cells and mediates paracrine interactions with the adjacent microenvironment.

To assess the effect of UNR in the SASP response, we investigated the role of UNR in secretion of SASP factors. We collected medium from shCtrl and shUNR cells at early time points after infection (7 dpi) and incubated fresh PMKs with these media following the protocol indicated in Figure 27a. A control with normal media (NO CM) was included. Differences were monitored by microscopy every 24 hours, and were already obvious after 3 days of CM treatment (Figure 27b). As previously described (Ritschka et al., 2017), the recipient shCtrl-CM cells exhibited features of paracrine senescence and detached after 6 days (notice that the only cells remaining in the plate are melanocytes, which are naturally resistant to senescence) (Figure 27b). Strikingly, this effect was completely lost in recipient shUNR-CM cells. Far from becoming senescent, these cells seemed to acquire proliferative capacity and/or resistance to cell death, as judged by a more crowded plate compared to the NO-CM control.

To confirm these results we measured BrdU incorporation in recipient cells after 5 days of CM-treatment. These assays revealed that recipient shCtrl-CM cells showed a strong decrease in proliferation compared with NO-CM or shUNR-CM recipient cells, as expected (Figure 27c). However, no striking differences were observed between NO-CM and shUNR-CM cells when pooling two independent biological experiments. These data reinforce our conclusion that UNR plays a critical role in senescence, and show that UNR contributes to modulation of the microenvironment.

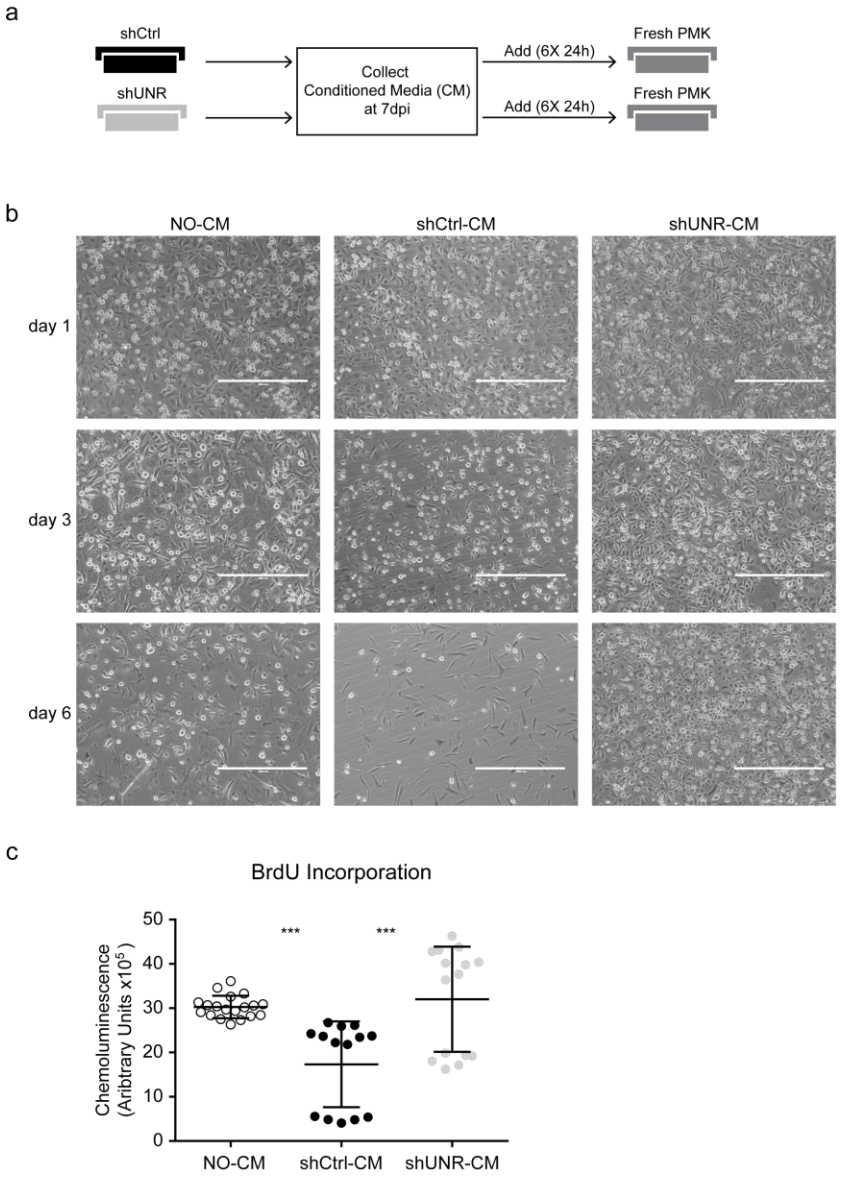


**Figure 27. UNR reinforces the SASP-associated tumour suppressor response. (a)** Schematic representation of the protocol used to test the effect of UNR in the SASP response. Conditioned medium (CM) from 7 dpi shCtrl and shUNR cells were added to fresh PMKs and renewed every 24 hours for a total of 6 days. **(b)** Images of recipient cells at days 1, 3 and 6 after CM addition. Scale bar = 400 µm. **(c)** BrdU incorporation assay of recipient cells after 5 days of CM treatment. (n = 2, technical replicates = 10). Statistical unpaired t-test was used. p-value < 0.001 (***); p-value < 0.01 (**). (□)

## 6. Molecular characterization of PMK cells that bypass senescence

Senescent cells are characterized by a set of molecular properties that define the senescent phenotype. These include a specific secretion program (SASP), a distinct reorganization of chromatin (SAHF), increased DNA damage (senescence-associated DNA damage foci or SDF), increased lysosomal activity (SA-β-gal), and cell cycle arrest marked by increased levels of CDK inhibitors ($p16^{INK4a}$, $p19^{ARF}$, $p21^{Cip1}$, p53 –the first three hereafter will be referred as p16, p19 and p21) (Campisi and d'Adda di Fagagna, 2007; Matjusaitis et al., 2016). Not all senescent cells display these arrays of properties, however, and perhaps the only universal characteristic of senescence is that cells cease to proliferate and become permanently arrested.

To understand at the molecular level how UNR depleted cells bypass senescence, we analysed some of these senescence biomarkers. We first checked for β-galactosidase activity by comparing proliferating PMK, shCtrl and shUNR cells (at 14 dpi), and immortalized keratinocytes (iPMK at passage 26). As expected, proliferating PMK stained negative for the marker while shCtrl cells stained positive (Figure 28a). Unexpectedly, however, both shUNR cells and immortal keratinocytes showed high levels of β-galactosidase activity. Therefore, SA-β-gal is not useful in our model. We conclude that shUNR senescence bypass is independent of changes in lysosomal activity.

We next assessed the levels of the cell cycle inhibitors p53, p21, p19 and p16 as well as the proliferation marker PCNA, along senescence by Western blot (Figure 28b). p19 and p21showed differential behavior in shUNR compared to shCtrl cells. p21 followed the expected dynamics in shUNR cells while p19 changed unexpectedly in the opposite direction (Figure 28b, c). However, variability between experiments was high, and in general, no consistent differences could be observed between shCtrl and shUNR cells.

In the next section, we aimed to understand the source of this variability.

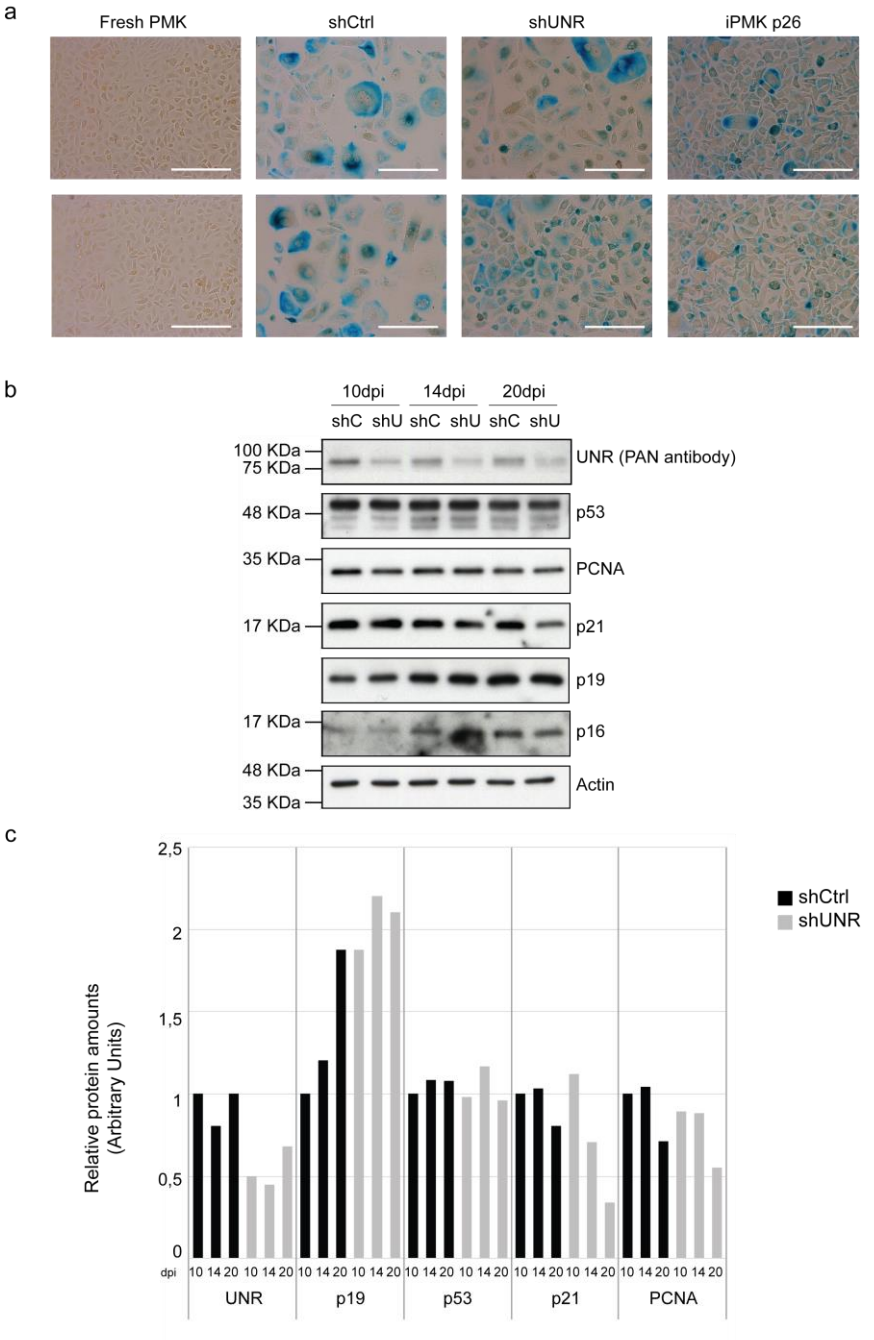


**Figure 28. Molecular characterization of shUNR senescence bypass. (a)** β-galactosidase staining. Scale bar = 200 µm. (n = 1) (■) **(b)** Levels of proliferation and senescence markers. UNR was detected using a polyclonal affinity-purified antibody (PAN antibody). **(c)** Quantification of the above Western blot. (n = 1) (■)

## 7. Dissecting the heterogeneity of PMK cell populations

Lack of reliable conclusions regarding the analysis of senescence molecular markers suggested that the heterogeneity of shCtrl and shUNR cell populations, readily observed by microscopy (e.g. Figures 23c and 28a), might underlie this effect. To dissect this heterogeneity, we used FACS analysis.

Cells were sorted at 15 dpi based on expression of GFP, which is carried in the viral vectors expressing shRNA (Figure 23a), and cell size, as senescent cells are larger. We observed that, despite the addition of selectable drugs during cell culture, cell populations were highly heterogeneous, because approximately only 50% of the cells were GFP-positive (Figure 29a, left panel). Both GFP-positive and -negative cells are heterogeneous in size (Figure 29a, middle and right panels). We selected the biggest and the smallest cells from each GFP population, and extracted RNA to assess the levels of senescence markers by RT-qPCR.

In general, no significant differences were observed between small and big cells, except for a tendency of small cells to express lower levels of cell cycle inhibitors and higher levels of the proliferation marker Ki67, alluding to a more proliferative character (Figure 29b). Clearly, UNR was depleted only in the GFP-positive shUNR cells. The level of Ki67 was elevated in these cells, consistent with their higher proliferation rate. Strikingly, however, the levels of cell cycle inhibitors remained high (Figure 29b). Not only a decrease was not observed, but rather increased expression of p16 and p19 was detected. These results are interesting, as they suggest that depletion of UNR leads to senescence bypass in conditions of elevated levels of cell cycle inhibitors. How can cells proliferate in this context and what is the mechanism of senescence bypass?

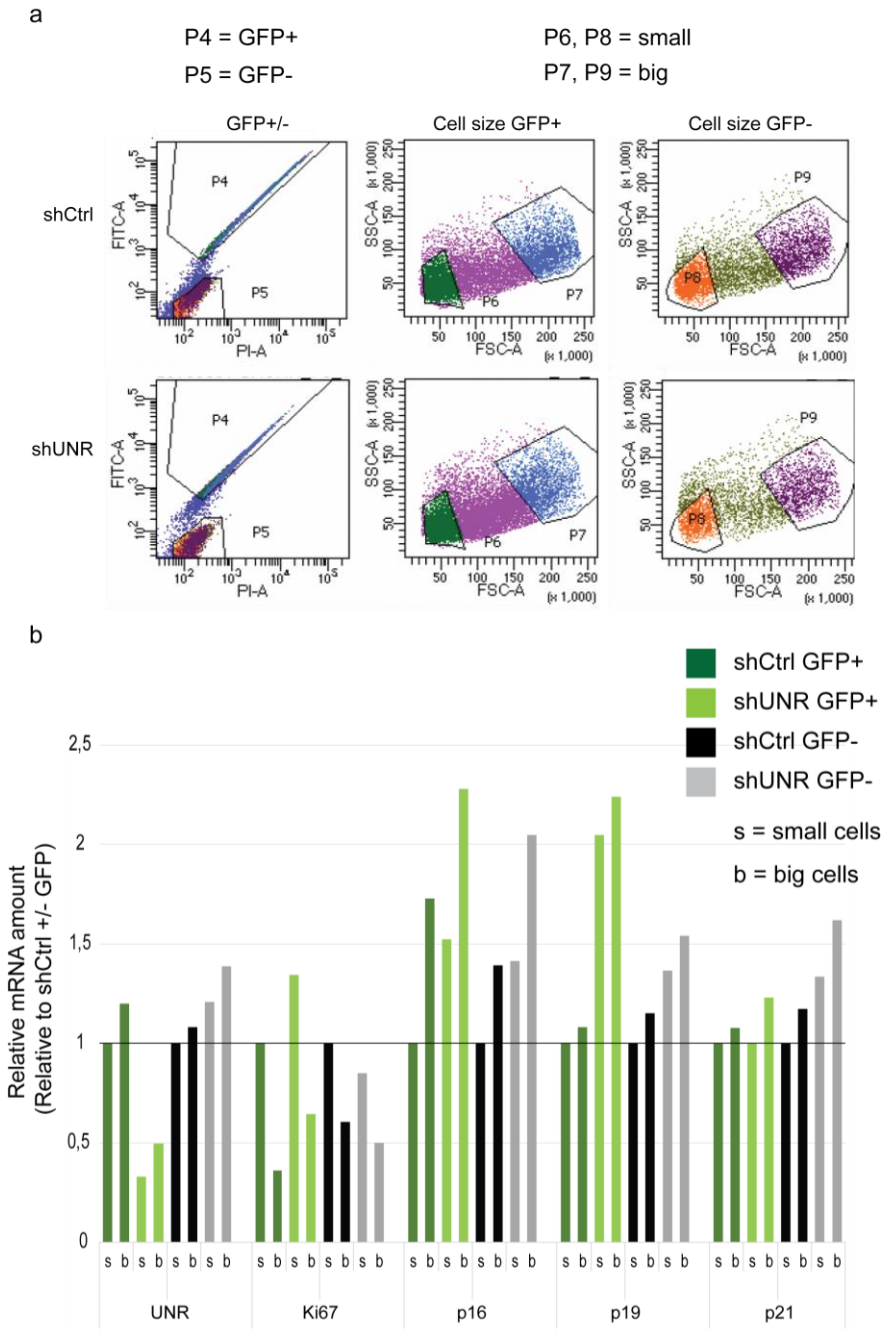


**Figure 29. Dissecting shUNR and shCtrl cell populations. (a)** FACS profiles. *Left*, separation of GFP-positive and GFP-negative cells. Combination of FITC-A and PI-A lasers is used to discriminate between auto-florescence (cells in the diagonal, P5) and real GFP signal (cells diverted from the diagonal, P4). GFP-positive (*Middle*) and -negative (*Right*) cells were further separated by size (FSC-A) and complexity (SSC-A). **(b)** Levels of UNR,

Ki67, p16, p19 and p21 transcripts for the different sorted populations analysed by RT-qPCR and normalized for actin. Values are shown relative to that obtained for shCtrl small cells in each GFP population. (n = 1) (□)

## 8. Genome-wide analysis of mRNA levels confirms that cell cycle inhibitors do not decrease upon UNR depletion

UNR has been shown to regulate the translation and/or stability of its mRNA targets (reviewed in Ray et al., 2015). To gain insight into how UNR promotes senescence, and how senescence is bypassed upon UNR depletion, we performed RNA-Seq of poly(A)+ RNA at different times of senescence induction (6 and 10 dpi). We also carried vector-infected cells to monitor for changes simply due to viral infection, and immortalized PMK to assess for permanent changes. We collected three independent biological replicates for each sample, except for immortalized PMK (as we lacked three independent cell lines at the time of performing this experiment).

Principal component (PC) analysis indicated large differences likely due to cell adaptation to grow in culture (Figure 30a, notice that cells collected at 6 dpi segregate from cells collected at 10 dpi and from immortalized cells). Cells infected with vector alone are distinguished as a different group. PC analysis also shows variability between biological replicates, which is expected due to the fact that PMK are primary cells obtained from different mice and each infection process has intrinsic variability. However, small but consistent differences can be observed between shCtrl and shUNR cells within each replicate, especially at 10 dpi.

We further analysed the differences between shUNR and shCtrl cells, and represented them as volcano plots in Figure 30b. As expected, larger differences were observed at 10 dpi.

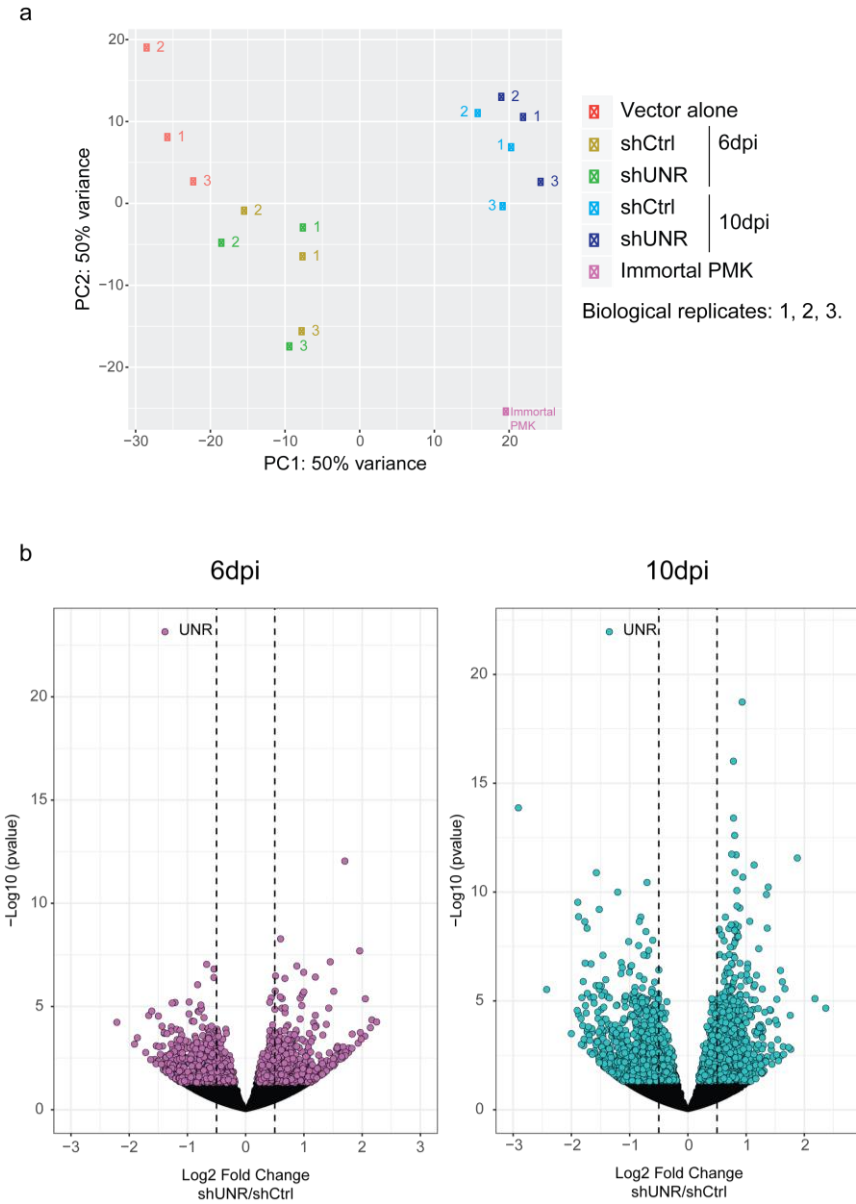


**Figure 30. Overview of RNA-Seq data. (a)** Principal Component Analysis (PCA). RNA-Seq was performed on poly(A)+ RNA extracted from cells infected with vector alone, shUNR or shControl at 6 and 10 dpi. Immortalized PMK (passage 26) were also included. **(b)** Volcano plots comparing the degree (log2 fold change) and significance (-log10 p-value) of gene expression differences between shCtrl and shUNR cells at 6 (*Left*) and 10 (*Right*) dpi. Dashed lines indicate the thresholds for amplitude (±0.5), and colored dots represent genes with significant changes (p-value < 0.05). The dot corresponding to UNR is indicated. (n = 3) (■)

To identify genes that change at both time-points in shUNR versus shCtrl cells, we used a scatter plot (Figure 31a). Three different colors -purple, blue and yellow- were used to represent genes changing significantly (p-value < 0.05) at 6 dpi, 10 dpi and both (6 and 10) dpi, respectively. (Supplemental table 2). KEGG pathway enrichment analysis using *Enrichr* indicated that cancer-related pathways were upregulated in shUNR cells (Figure 31b). Additionally, cell cycle and DNA replication appeared in the top three categories at 6 dpi, suggesting that cells try to evade the senescence program already at early time points (Figure 31b, first panel). Downregulated genes, in contrast, did not show highly significantly enriched pathways (data not shown). These analyses suggest that UNR inhibits cancer-related genes in cells undergoing senescence.

a

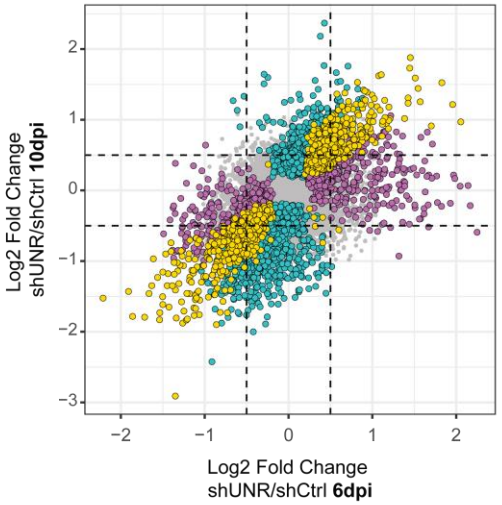


b

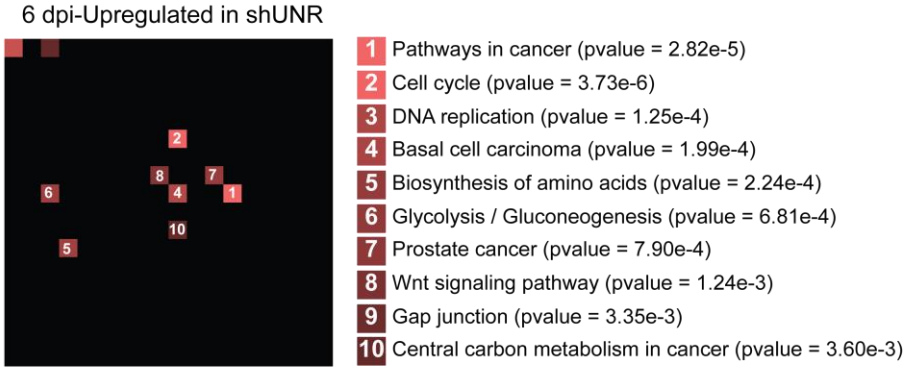

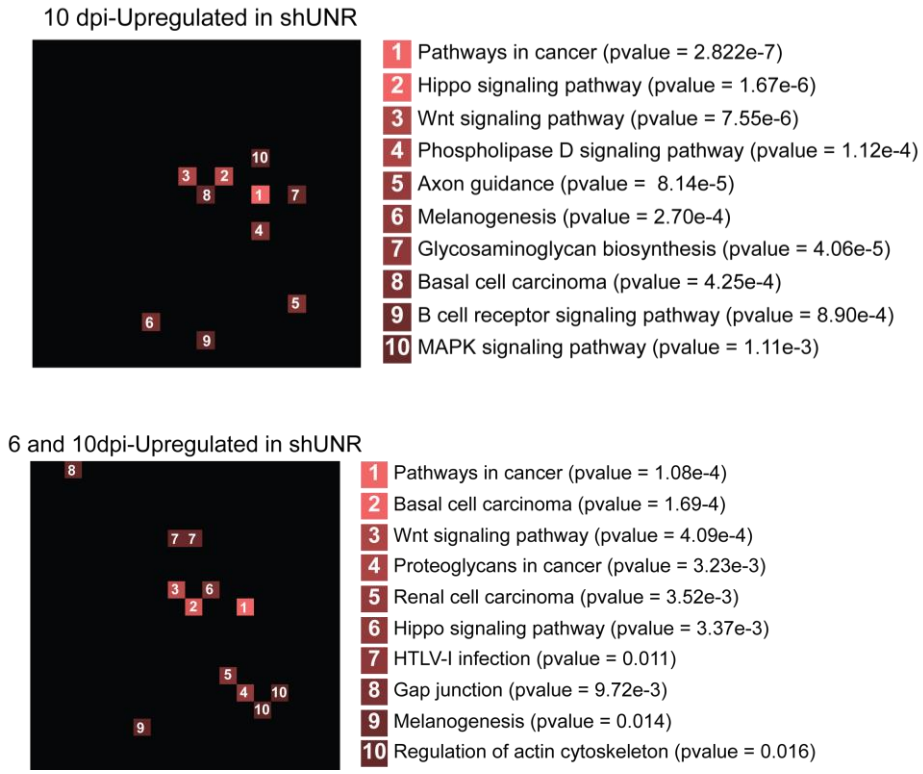


**Figure 31. Cancer related pathways are upregulated in shUNR cells. (a)** Scatter plot to visualize changes in gene expression dynamics between shUNR and shCtrl cells. Only significant genes (p-value < 0.05) are colored. Pink, genes changing only at 6 dpi; Blue, genes changing only at 10 dpi; Yellow, genes changing at both 6 and 10 dpi. **(b)** KEGG pathway enrichment analysis of significant upregulated genes upon UNR depletion for each time point. (■)

We next checked for transcripts differentially expressed upon senescence using the RNA-Seq dataset. Consistent with our previous RT-qPCR analysis (Figure 29b), mRNA levels encoding the cell cycle inhibitors p16/p19 and p21 did not decrease upon UNR depletion (Figure 32). Surprisingly, contrary to expectations *p16/p19* mRNAs were significantly upregulated in shUNR cells. Moreover, levels of the cell cycle inhibitor *p15* and the tumor suppressor *Pten* were also upregulated. At 6 dpi, shUNR cells expressed higher levels of *Lmnb1*, *Vim* and the proliferation markers *Pcna* or *Mcm3* as well as reduced levels of the cell cycle inhibitor *p57*.

However, these changes were not maintained at 10 dpi. The levels of *p53* were not significantly altered. However, levels of other mRNAs encoding senescent markers, such as *Stx4* or *Ntal* (Althubiti et al., 2014) were significantly downregulated in shUNR cells. Finally, the autophagy-related gene *Ulk3* showed a steady downregulation along time. Importantly, UNR depletion did not affect the levels of endogenous *H-Ras*, excluding indirect effects simply due to modulation of the OIS trigger.

In summary, analysis of typical senescence markers did not reveal striking differences that could explain the proliferative phenotype upon UNR depletion, at least at the mRNA level.

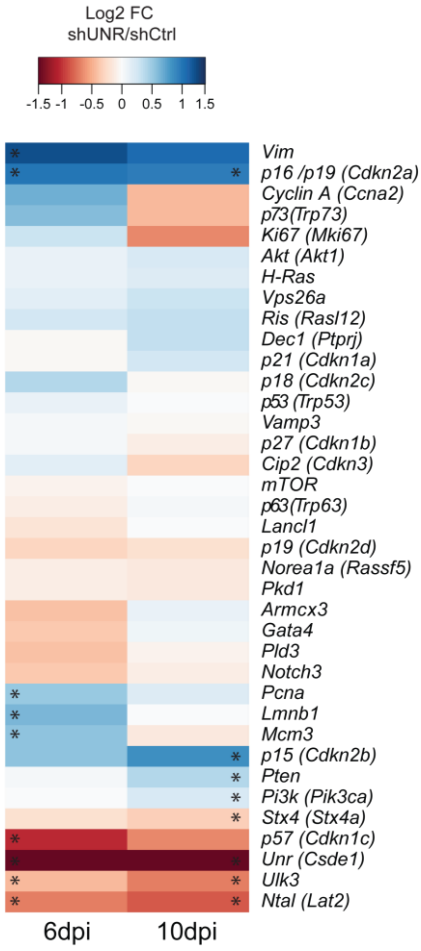

**Figure 32. Cell cycle inhibitors do not decrease upon UNR depletion.** Heat map of log 2 fold changes upon UNR depletion for typical genes affected in senescence. Significant changes are highlighted with a star (*) (p-value = < 0.05). (■)

## 9. UNR modulates the levels of some transcripts encoding SASP factors

Coppé and colleagues suggest that the SASP might be controlled transcriptionally, because many SASP factors were upregulated at the mRNA level in senescent cells (Coppé et al., 2008). We checked the levels of mRNAs encoding SASP factors in our dataset at 6 and 10 dpi. Most of them were not affected in a significant manner. Out of 59 SASP factors analysed, only 16 (~ 27%) were significantly regulated, and mostly at 10 dpi. Transcripts encoding *Gdnf* and *Il6st* (sgp130) (soluble factors), *Serpine1* and *Timp2* (proteases and regulators) and the growth factor *Fgf2* were upregulated in shUNR cells. Conversely, mRNAs for the growth factors *Mst1*, *Igfbp3*, *Fgf7*; for cytokines *Csf2ra* and *Csf3*; or for chemokines such as *Ccl2*, *Ccl20*, *Cxcl1* and other factors (*Il1a*, *Axl* or *Thpo*) were downregulated upon UNR depletion (Figure 33). That is, 11 out of 16 SASP-encoding transcripts decrease upon UNR depletion, consistent with the observed loss of paracrine SASP (Figure 27b, c).

In conclusion, our results suggest that UNR functions in OIS primarily by downregulating proliferation and cancer-related transcripts, rather than by activating cell cycle inhibitors. In addition, UNR promotes the expression of SASP factors to help modulate the microenvironment.

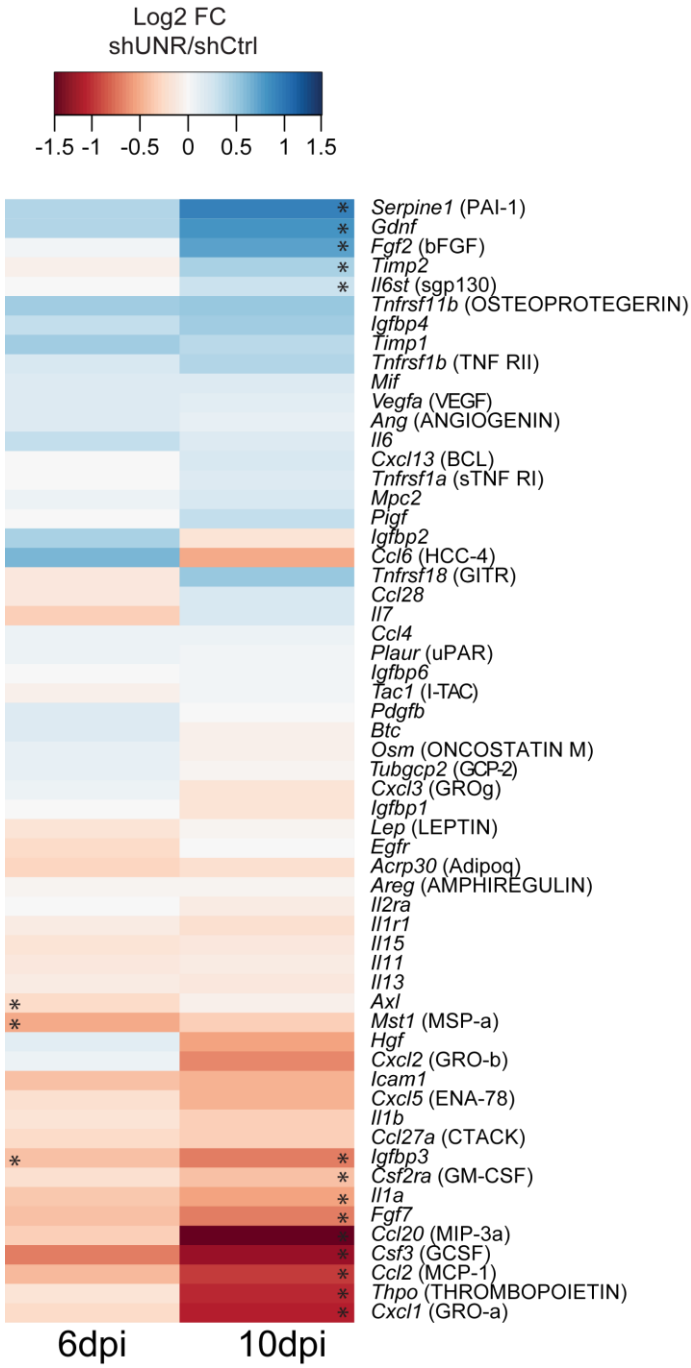


**Figure 33. UNR modulates the levels of some transcripts encoding SASP factors.** Heat map representing log2 fold changes upon UNR depletion for mRNAs encoding SASP factors. Other names or aliases of the encoded proteins are specified in brackets. Significant changes are highlighted with a star (*). (p-value = < 0.05) (■)

## 10. Cancer-related pathway enrichment is maintained in iPMK cells

When evaluating transcriptomic data, it might be difficult to distinguish whether the observed changes are the cause or the consequence of the phenotype. In the case of UNR depletion, for example, late changes might be secondary to the establishment of a proliferative phenotype. For this reason, we focused on early changes upon shUNR addition, that is, changes already present at 6 dpi. We reasoned that, for the maintenance of the phenotype, these changes should continue at 10 dpi and even remain in immortalized PMK. To identify these changes, we selected the group of genes with significant changes at 6 and 10 dpi (yellow genes in Figure 31a) and compared their levels with those in immortal PMK. Especially interesting were those genes differentially expressed (log 2 fold change > 0.5 or < -0.5) in shUNR versus shCtrl, but similarly expressed (log 2 fold change between -0.5 and 0.5) when comparing immortal PMK versus shUNR 6 dpi. A group of 325 genes was identified, of which 157 genes were upregulated (Figure 34a blue shadow) and 168 were downregulated (Figure 34a red shadow) (Supplemental table 3). As for the analysis of shUNR/shCtrl (see Figure 31), genes that remained upregulated in immortal PMK showed high enrichment in pathways related to cancer such as *Wnt* or *Hippo signaling*. Moreover, terms such as *basal cell*, *renal or colorectal carcinoma* were also highly represented (Figure 34b). The downregulated genes displayed less significant pathways with apparently less related functions (Figure 34c).

These results indicate that UNR-depleted cells overexpress a network of proliferative and cancer-related genes early after infection that might be necessary for the eventual immortalization and transformation of cells, highlighting the role of UNR as a tumor suppressor.

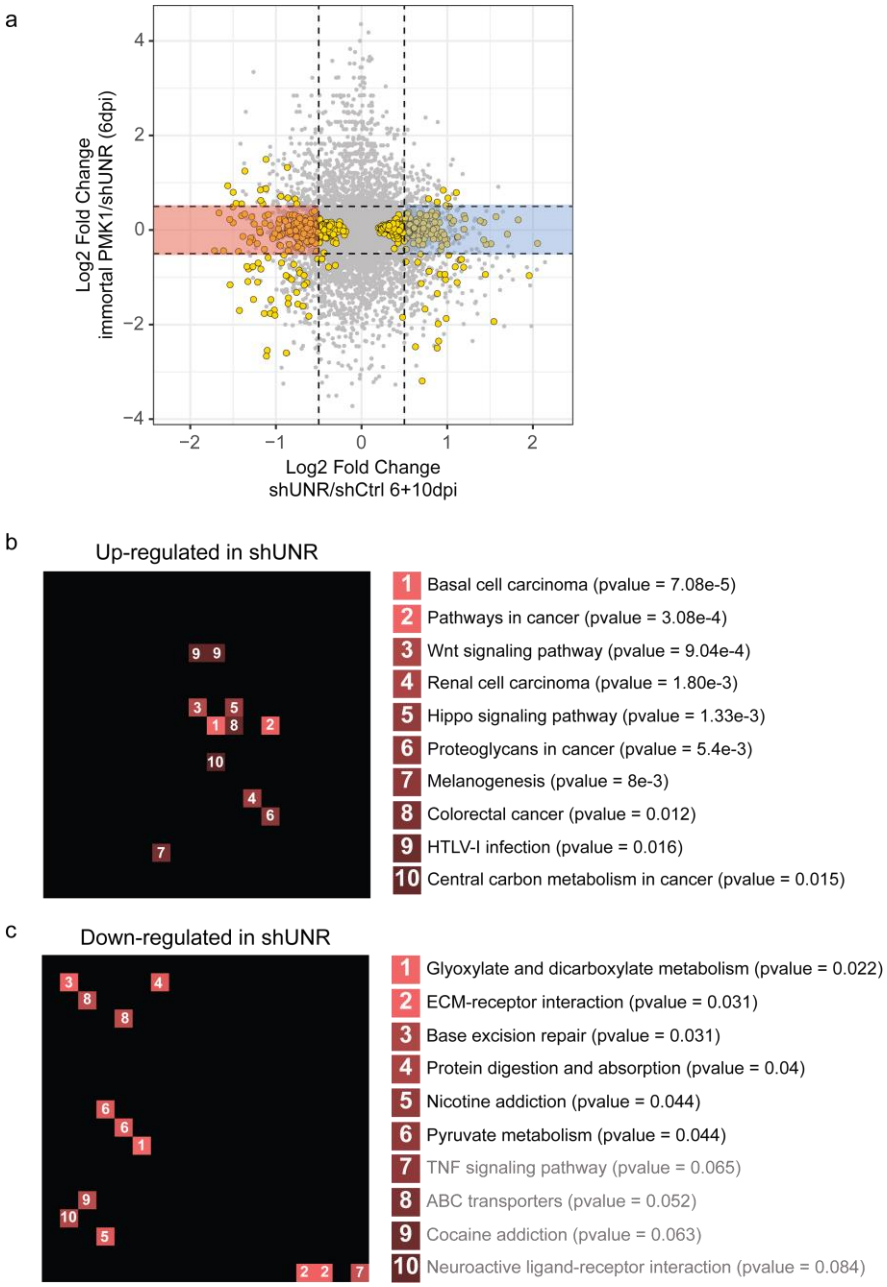


**Figure 34. Cancer-related pathway enrichment is maintained in iPMK cells. (a)** Scatterplot of significant genes (p-value < 0.05) that change at 6 and 10 dpi (yellow genes). Colored areas (blue and red) represent genes differentially expressed in shUNR versus shCtrl (6 dpi) but similarly expressed in shUNR versus immortal PMK (iPMK). **(b, c)** KEGG pathway enrichment analysis of genes subtracted from the colored areas (blue and red respectively). (■)

# Discussion

## A. Role of UNR in histone mRNA metabolism

Histone mRNAs constitute one of the most enriched iCLIP-target groups of UNR (Figure 16). UNR binds sharply to the 3' UTR of these transcripts. UNR-bound histone transcripts terminate precisely two nucleotides after the stem-loop, which is indicative of mature histone mRNAs. This feature and the preferential location of UNR in the cytoplasm strongly suggested UNR regulation at the post-transcriptional level in this compartment.

To understand the possible role of UNR in this context, we aimed to investigate what governs UNR binding to histone mRNAs. The UNR binding motif was found at increased frequency in the intersection of the ORF and the 3'UTR, often overlapping with the stop codon (Figure 15b). Further, multiple potential motifs could be found on a single mRNA. Mutational analysis, however, indicated that neither the stop codon nor other potential UNR-binding motifs influenced UNR binding *in vitro,* suggesting that -similar to UNR recognition of *roX2* mRNA- a simple purine-rich context may be sufficient for binding (Militti et al., 2014). Interestingly, UNR formed multimers on the RNA (Figure 15c). In the case of other RBPs that bind RNA with low specificity and form multimers such as FUS, multimerization is important to bind relevant co-factors (Schwartz et al., 2013). Therefore, UNR might recognize histone mRNAs in a rather relaxed fashion, where binding specificity is aided by multimerization or by additional RBPs. Indeed, in the well-studied case of UNR binding to *msl-2* mRNA, interactions with SXL are essential for high-affinity binding (Hennig et al., 2014).

Regarding regulation of histone transcripts, our original hypothesis was that UNR promotes the stabilization of histone mRNAs because, when UNR was depleted, histone mRNAs were downregulated *in mass* according to our RNA-Seq data (Figure 16). Efforts to validate this hypothesis on endogenous histone transcripts using alternative methods (e.g. RT-qPCR) were hampered by the strong similarities between histone mRNAs, which made the design of transcript-specific primers challenging.

We thereby chose to validate this hypothesis using histone reporters that were tested *in vitro* and *in cellulo*. None of our experiments could demonstrate a direct role of UNR in histone mRNA stability or translation. First, UNR did not affect translation when mRNA reporters were used in *in vitro* translation assays (Figure 20c). Effects were only observed when DNA was added, indicating roles at the levels of transcription or mRNA stability (Figure 21b, c). Second, mRNA transfection in melanoma cells did not reveal differential regulation of H2AD upon UNR depletion (Figure 22a). Again, differences were only observed when DNA was transfected, and they seemed non-specific because control reporters lacking histone sequences were equally affected (Figure 22b). Furthermore, UNR altered the expression of constructs independently of the promoter used to direct transcription, as mRNA expression was affected both when the prokaryotic T7 promoter was used *in vitro*, or when the eukaryotic SV40 promoter was used *in cellulo*. Therefore, at this point we do not know how UNR controls histone mRNA levels, and what purpose serves this control.

An alternative scenario is that UNR does not really regulate histone mRNA levels, but rather that histone mRNAs regulate UNR activity and the effect we observe on histone levels upon UNR depletion is a residual effect with no functional relevance. In this scenario, histone mRNAs could act as a sponge to limit the availability of functional UNR molecules during the cell cycle. Indeed, appropriate UNR levels are important for mitotic progression of KEH293T cells (Schepens et al., 2007) as well as embryonic development (Patalano et al., 2009), and just a 2-fold overexpression of UNR can convert a non-metastatic cell into a malignant one (Wurth et al., 2016).

In conclusion, despite the fact that histone mRNAs are one of the most prominent UNR target groups, the functional relationship between UNR and this set of transcripts remains an open question.

## B. Role of UNR in oncogene-induced senescence

Senescence is one of the most complex and variable cellular processes and can be initiated by many intrinsic and extrinsic stimuli. One of the typical inducers of senescence is the activation of oncogenes, which is, in many cases, the initial step of tumor development. If cells properly sense oncogenic insults, activation of the senescence program (OIS) will take place to ensure cell-autonomous and non-autonomous cell cycle arrest. Thus, OIS acts, at first instance, as a fail-safe mechanism of damaged cells.

Previous work in our lab found many transcripts encoding SASP factors as iCLIP-targets of human UNR in melanoma cells (Wurth et al., 2016). This prompted us to investigate the role of UNR in oncogene-induced senescence in this thesis. To do so, we overexpressed a constitutively activated variant of H-RAS (H-RAS V12) in PMK cells from newborn mice. Under these conditions, cells undergo senescence; however, when UNR is simultaneously depleted, cells bypass this program as judged by i) loss of the typical enlarged cell appearance under the microscope (Figure 23c right panel), ii) greater colony formation capacity (Figure 26b), and iii) increased BrdU incorporation and higher proliferation (Figure 26c). Furthermore, contrary to shCtrl cells, conditioned media from shUNR cells shows a defective SASP (Figure 27b, c).

An important open question is whether UNR is necessary for the establishment and/or the maintenance of the senescent phenotype upon oncogene induction. With the experiments performed to date, we are unable to distinguish between these two possibilities. Future experiments with sequential -instead of simultaneous- overexpression of H-RAS and subsequent depletion of UNR (e.g. after establishment of the hyper-replicative phase) will be useful to better understand the role of UNR in this context. In addition, experiments to test whether UNR overexpression alone suffices to induce senescence should be performed.

To gain insight into the function of UNR in senescence, a complete characterization of the protein during OIS is important. In PMK, UNR is localized primarily to the cytoplasm (Figure 24a) and is present in multiple isoforms (Figure 25c). Interestingly, PMK contains isoforms not present in cancerous cells, raising the possibility that these contribute to the senescent phenotype. Different UNR isoforms, arising by post-translational modification or alternative processing of the UNR-encoding transcripts, could explain the different behaviors of UNR in melanoma, where it functions as an oncogene, and in PMK, where UNR seems to function as a tumor suppressor. Untangling the complexity of UNR isoforms by mass spectrometry, their intracellular localization, and their differentially associated factors may contribute to understand these apparently contradictory functions of UNR.

The levels of UNR seem constant during the establishment (5 or 7 dpi) and maintenance (10 and 14 dpi) of OIS (Figure 24b). Although this result is somewhat variable among independent experiments and needs to be confirmed. What appears very reproducible is the increase in UNR expression upon retroviral infection irrespective of the virus-containing construct (5 dpi of Figure 24b). This observation is in agreement with the claim that lentiviral transduction *per se* strongly induced UNR expression (Moore et al., 2018). Upon virus infection, cells rapidly arrest bulk protein synthesis and elicit the formation of stress granules (McCormick and Khaperskyy, 2017). UNR has been recently associated to stress granules (Youn et al., 2018), an observation that is also true for melanoma cells (unpublished data from our laboratory). Thus, stress granule formation may underlie stabilization of UNR upon viral infection.

We have derived immortal cells from shUNR-treated PMK and called them iPMK (for immortalized PMK). Immortalization is a required, but not sufficient, step for cellular transformation. To date we have three immortal cell lines, two of which are featured in Figure 26d. Usually, the proliferative phenotype of shUNR cells is already evident at 6 dpi, where the number of small round cells is higher than in shCtrl counterparts

(Figure 23c). At around 10-14 dpi, a relatively large number of cells remain attached to the plate and, in some cases, clumps of proliferative cells can be distinguished. A good strategy to select for immortal cells is to split them at 15-20 dpi, a procedure that senescent cells rarely survive.

Although rare, shCtrl cells can also form spontaneous clumps and become immortalized if kept in culture at low densities for extended times, indicating that spontaneous cell transformation occurs at low frequency. Either intrinsic gene regulation differences or unfortunate insertions of the viral constructs in critical genome regions (such as interfering with crucial tumor suppressor genes) could direct spontaneous cell immortalization and clonal expansion. However, neither the frequency nor the number or the time to formation of transformed clumps are comparable with shUNR-PMK.

Because immortalization does not necessarily mean transformation, we have initiated experiments to inject several of our iPMK lines into nude mice and follow tumor formation. If that was the case, cell transformation would be confirmed. In addition, we have injected shCtrl and shUNR cells at early time points (7 dpi) to monitor for early transformation in an experiment carrying an appropriate negative control. We expect that, if any, only shUNR cells can give rise to subcutaneous tumours in immunocompromised mice.

Altogether, our results indicate that UNR is important for the cell-autonomous effects of senescence. Our next step was to evaluate the non-autonomous senescent functions exerted through the SASP. To do so, we collected conditioned media (CM) shCtrl and shUNR cells at 7 dpi and added it to freshly growing PMK. As expected, shCtrl-CM induced senescence and detachment of recipient PMK. However, shUNR-CM did not induce detachment. Further, in one of the two independent experiments performed, shUNR-CM led to better survival (or higher proliferation) of recipient cells compared to fresh medium (NO-CM condition, Figure 27b). Additional experiments will determine if UNR depletion promotes proliferation or resistance to cell death in a non-

autonomous manner. In general, these results suggest that UNR is an important inductor of non-autonomous senescence.

Phenotypic differences are accompanied by molecular changes. Typical markers of senescence such as the SA-β-Gal marker did not decrease in shUNR cells and was present even in iPMK. Western blot analysis of critical cell cycle inhibitors (p53, p21, p19, p16) or proliferation markers (PCNA) also did not reveal major changes between shUNR and shCtrl cells (Figure 28b). However, the variability of these experiments was high, and we started to suspect of cell heterogeneity. FACS analysis of our PMK populations indeed showed a large heterogeneity. Despite selection of infected cells using antibiotics (the shRNA-PIG vectors also contain antibiotic resistance markers), many cells do not express GFP. Each shUNR or shCtrl population consist of a pool of GFP-positive and –negative cells, in which only shUNR GFP-positive cells show depleted UNR mRNA levels (Figure 29b). Thus, cell sorting will become indispensable in future experiments. Yet, surprisingly, in sorted cells neither p16, p19 nor p21 mRNA levels decrease in shUNR cells, which bypass senescence and are actively dividing.

To test which mRNAs change after UNR depletion, we performed RNA-Seq. Samples at 6 and 10 dpi were sequenced in three independent biological replicates, and log 2 fold differences of transcript levels in shUNR/shCtrl cells were calculated (Figure 31a). Transcripts significantly upregulated in shUNR cells showed functional classifications in pathways related to cancer, including metabolic processes known to be hyper-activated in cancerous cells such as glycolysis or amino acid biosynthesis (Fadaka et al., 2017) (Figure 31b). Additional categories included *Wnt signaling* and the *Hippo pathway*, which controls multiple cellular functions including proliferation and cell growth (Harvey et al., 2013; Zhan et al., 2017) (Figure 31b). Downregulated genes in shUNR cells did not classify into any major category. Again, major cell cycle inhibitors were not downregulated upon UNR depletion (Figure 32).

A detailed analysis of the expression of genes related to senescence, proliferation or malignancy is shown in Figure 32. Out of 36 genes analysed, only 12 were significantly regulated (represented by stars in the heatmap), and only 3 showed significant changes at both time points: *Cdkn2a*, *Ulk3* and *Ntal*.

The *Cdkn2a* locus, encoding p16 and p19, is significantly upregulated, in agreement with the RT-qPCR results (see Figure 29b). Although expression of p16 functions to limit cell cycle progression and promote cellular senescence, MEFs exiting senescence by p53 knockdown maintain high levels of p16 (Dirac and Bernards, 2003). p16 is overexpressed in several tumours, and it has been suggested that p16 activation is a characteristic of all emerging cancers *in vivo* (Burd et al., 2013; Romagosa et al., 2011). Thus, the fact that shUNR cells express high p16 levels is not necessarily at odds with the proliferative phenotype of these cells.

*Ulk3* is an autophagy-related gene that is upregulated during senescence, attesting to the described increased in the autophagy program upon OIS (Young et al., 2009). Autophagy contributes to cell cycle arrest and production of senescence-associated interleukins (Kuilman et al., 2010). In shUNR cells *Ulk3* is downregulated, an effect that correlates with decreased senescence.

NTAL, STX4, VPS26A, PDL3, ARMCX3 or VAMP3 were recently characterized as novel markers of senescence with prognostic potential in cancer (Althubiti et al., 2014). Of these, *Ntal* and *Stx4* mRNAs are downregulated in shUNR cells, although only *Ntal* shows significant downregulation at both time points.

Among genes showing significant changes in one time-point we find *Vim*. VIM is an intermediate filament protein responsible for maintaining cell shape and integrity of the cytoplasm, and it is a marker of epithelial-to-mesenchymal transition (EMT). Interestingly, *VIM* mRNA is also a target of UNR in melanoma, where it is upregulated at the level of translation

elongation by UNR (Wurth et al., 2016). Thus, although *VIM* is regulated in opposite ways in these two contexts, the function of UNR is also opposed, suggesting that UNR regulates VIM in accordance to its function as a metastasis promoter (melanoma) or tumor suppressor (OIS).

Finally, and in discordance with expectations, *p15* and *Pten* transcripts are upregulated in shUNR cells, although only significantly at 10 dpi. p15 was described to oppose cell transformation by RAS *in vitro* (Malumbres et al., 2000). Thus, we would expect downregulation of this gene in shUNR cells, which are potentially undergoing transformation. Regarding the tumour suppressor PTEN, it should not be upregulated in cancerous cells, although it cannot be ruled out that it is the N-terminally extended form of PTEN that is overexpressed. This PTEN isoform functions in mitochondrial metabolism and promotes energy production (Liang et al., 2014).

We also checked the levels of transcripts encoding SASP factors in shUNR/shCtrl cells (Figure 33). Coppé and colleagues determined that proteins comprising the SASP were, in general, upregulated at the level of mRNA abundance (Coppé et al., 2008). Thus, in this case, mRNA levels seem to be reliable to infer protein expression. According to our RNA-Seq data, SASP factor levels do not substantially change upon UNR depletion. However, we do observe a decrease of specific SASP factors, which could have a dominant role in the SASP effects in our system (Figure 33). This could explain our observed suppression of paracrine SASP effects upon UNR depletion (Figure 27b, c).

Is important to note that RNA-Seq samples were not obtained from GFP-sorted cells. RNA-Seq using exclusively GFP-positive cells might yield more reliable data, providing robust hints on the molecular consequences of UNR depletion, including a more sensitive detection of changes in the SASP.

One way to further dissect the list of relevant genes important for senescence bypass upon UNR depletion is to compare those changing in

shUNR cells at both time points with those changing in iPMK. We reasoned that relevant genes should be those that change significantly in shUNR versus shCtrl and maintained in iPMK. This comparison is shown in Figure 34a (red and blue shadows). Upregulated genes continue showing a high representation of pathways in cancer, suggesting that these pathways are activated early upon UNR depletion and are necessary for cell immortalization/transformation (Figure 34b). Downregulated pathways (Figure 34c) are also comparable to those showing down in the shUNR/shCtrl alone comparison (data not shown). Intriguingly, two of the top categories in this group are *ECM-receptor interaction* and *base excision repair* pathways. Downregulation of ECM-receptor interaction might confer an advantage to malignant cells and may promote the acquisition of a migratory phenotype. In the same line, base excision repair pathways are important for senescence as part of the activation of DDR. It seems reasonable, thus, that these pathways are less represented in the shUNR condition.

In summary, our results are consistent with the interpretation that UNR functions as a tumour suppressor in PMK, coordinating the inhibition of proliferation and cancer related regulons upon OIS in a cell autonomous manner. Future experiments with exclusively UNR-depleted sorted cells will narrow down the specific molecular function of UNR in this system.

# Conclusions

## Part A

1. UNR binds to mature histone mRNAs in melanoma cells.
2. The binding site is located upstream of the stem-loop in the 3' UTR. UNR binds in a motif independent manner, and forms multimers on the RNA.
3. UNR does not affect histone mRNA translation or stability *in vitro*.
4. UNR does not promote ribosome readthrough *in vitro*.
5. UNR does not affect histone mRNA stability *in cellulo.*
6. UNR affects mRNA levels in a transcription-dependent manner.

## Part B

1. UNR is required for oncogene-induced senescence (OIS), as its depletion leads to higher proliferation and increased colony forming capacity of primary mouse keratinocytes induced to senesce by H-RAS V12 overexpression.
2. UNR is localized mainly in the cytoplasm. Several isoforms, not present in cancerous cells, can be detected in PMK.
3. UNR is required for an effective SASP.
4. UNR blocks cancer-related pathways without major effects in the levels of cell cycle inhibitors.

# References

Abaza, I. (2006). Drosophila UNR is required for translational repression of male-specific lethal 2 mRNA during regulation of X-chromosome dosage compensation. Genes Dev. *20*, 380–389.

Achsel, T., and Bagni, C. (2016). Cooperativity in RNA–protein interactions: the complex is more than the sum of its partners. Curr. Opin. Neurobiol. *39*, 146–151.

Acosta, J.C., Banito, A., Wuestefeld, T., Georgilis, A., Janich, P., Morton, J.P., Athineos, D., Kang, T.-W., Lasitschka, F., Andrulis, M., et al. (2013). A complex secretory program orchestrated by the inflammasome controls paracrine senescence. Nat. Cell Biol. *15*, 978–990.

Aird, K.M., Worth, A.J., Snyder, N.W., Lee, J.V., Sivanand, S., Liu, Q., Blair, I.A., Wellen, K.E., and Zhang, R. (2015). ATM Couples Replication Stress and Metabolic Reprogramming during Cellular Senescence. Cell Rep. *11*, 893–901.

Albihlal, W.S., and Gerber, A.P. (2018). Unconventional RNA-binding proteins: an uncharted zone in RNA biology. FEBS Lett. *592*, 2917–2931.

Alonso-Curbelo, D., Riveiro-Falkenbach, E., Pérez-Guijarro, E., Cifdaloz, M., Karras, P., Osterloh, L., Megías, D., Cañón, E., Calvo, T.G., Olmeda, D., et al. (2014). RAB7 Controls Melanoma Progression by Exploiting a Lineage-Specific Wiring of the Endolysosomal Pathway. Cancer Cell *26*, 61–76.

Althubiti, M., Lezina, L., Carrera, S., Jukes-Jones, R., Giblett, S.M., Antonov, A., Barlev, N., Saldanha, G.S., Pritchard, C.A., Cain, K., et al. (2014). Characterization of novel markers of senescence and their prognostic potential in cancer. Cell Death Dis. *5*, e1528–e1528.

Baltz, A.G., Munschauer, M., Schwanhäusser, B., Vasile, A., Murakawa, Y., Schueler, M., Youngs, N., Penfold-Brown, D., Drew, K., Milek, M., et al. (2012). The mRNA-Bound Proteome and Its Global Occupancy Profile on Protein-Coding Transcripts. Mol. Cell *46*, 674–690.

Barcaroli, D., Dinsdale, D., Neale, M.H., Bongiorno-Borbone, L., Ranalli, M., Munarriz, E., Sayan, A.E., McWilliam, J.M., Smith, T.M., Fava, E., et al. (2006a). FLASH is an essential component of Cajal bodies. Proc. Natl. Acad. Sci. *103*, 14802–14807.

Barcaroli, D., Bongiorno-Borbone, L., Terrinoni, A., Hofmann, T.G., Rossi, M., Knight, R.A., Matera, A.G., Melino, G., and De Laurenzi, V. (2006b). FLASH is required for histone transcription and S-phase progression. Proc. Natl. Acad. Sci. *103*, 14808–14812.

Bartkova, J., Rezaei, N., Liontos, M., Karakaidos, P., Kletsas, D., Issaeva, N., Vassiliou, L.-V.F., Kolettas, E., Niforou, K., Zoumpourlis, V.C., et al. (2006). Oncogene-induced senescence is part of the tumorigenesis barrier imposed by DNA damage checkpoints. Nature *444*, 633–637.

Beausejour, C.M. (2003). Reversal of human cellular senescence: roles of the p53 and p16 pathways. EMBO J. *22*, 4212–4222.

Beckmann, B.M., Castello, A., and Medenbach, J. (2016). The expanding universe of ribonucleoproteins: of novel RNA-binding proteins and unconventional interactions. Pflüg. Arch. - Eur. J. Physiol. *468*, 1029–1040.

Blagosklonny, M.V. (2003). Cell senescence and hypermitogenic arrest. EMBO Rep. *4*, 358–362.

Bolden, J.E., and Lowe, S.W. (2015). 15 - Cellular Senescence. In The Molecular Basis of Cancer (Fourth Edition), J. Mendelsohn, J.W. Gray, P.M. Howley, M.A. Israel, and C.B. Thompson, eds. (Philadelphia: Content Repository Only!), pp. 229-238.e2.

Boussadia, O., Amiot, F., Cases, S., Triqueneaux, G., and Jacquemin-Sablon, H. (1997). Transcription of unr (upstream of N-ras) down-modulates N-ras expression in vivo. FEBS Lett. 5.

Boussadia, O., Niepmann, M., Creancier, L., Prats, A.-C., Dautry, F., and Jacquemin-Sablon, H. (2003). Unr Is Required In Vivo for Efficient Initiation of Translation from the Internal Ribosome Entry Sites of both Rhinovirus and Poliovirus. J. Virol. *77*, 3353–3359.

Braig, M., Lee, S., Loddenkemper, C., Rudolph, C., Peters, A.H.F.M., Schlegelberger, B., Stein, H., Dörken, B., Jenuwein, T., and Schmitt, C.A. (2005). Oncogene-induced senescence as an initial barrier in lymphoma development. Nature *436*, 660–665.

Brooks, L., Lyons, S.M., Mahoney, J.M., Welch, J.D., Liu, Z., Marzluff, W.F., and Whitfield, M.L. (2015). A multiprotein occupancy map of the mRNP on the 3′ end of histone mRNAs. RNA *21*, 1943–1965.

Brown, E.C. (2004). All five cold-shock domains of unr (upstream of N-ras) are required for stimulation of human rhinovirus RNA translation. J. Gen. Virol. *85*, 2279–2287.

Burd, C.E., Sorrentino, J.A., Clark, K.S., Darr, D.B., Krishnamurthy, J., Deal, A.M., Bardeesy, N., Castrillon, D.H., Beach, D.H., and Sharpless, N.E. (2013). Monitoring Tumorigenesis and Senescence In Vivo with a p16INK4a-Luciferase Model. Cell *152*, 340–351.

Cakmakci, N.G., Lerner, R.S., Wagner, E.J., Zheng, L., and Marzluff, W.F. (2008). SLIP1, a Factor Required for Activation of Histone mRNA Translation by the Stem-Loop Binding Protein. Mol. Cell. Biol. *28*, 1182–1194.

Campisi, J. (2013). Aging, Cellular Senescence, and Cancer. Annu. Rev. Physiol. *75*, 685–705.

Campisi, J., and d'Adda di Fagagna, F. (2007). Cellular senescence: when bad things happen to good cells. Nat. Rev. Mol. Cell Biol. *8*, 729–740.

Castello, A., Fischer, B., Eichelbaum, K., Horos, R., Beckmann, B.M., Strein, C., Davey, N.E., Humphreys, D.T., Preiss, T., Steinmetz, L.M., et al. (2012). Insights into RNA Biology from an Atlas of Mammalian mRNA-Binding Proteins. Cell *149*, 1393–1406.

Castello, A., Fischer, B., Hentze, M.W., and Preiss, T. (2013). RNA-binding proteins in Mendelian disease. Trends Genet. *29*, 318–327.

Castello, A., Fischer, B., Frese, C.K., Horos, R., Alleaume, A.-M., Foehr, S., Curk, T., Krijgsveld, J., and Hentze, M.W. (2016). Comprehensive Identification of RNA-Binding Domains in Human Cells. Mol. Cell *63*, 696–710.

Chang, T.-C. (2004). UNR, a new partner of poly(A)-binding protein, plays a key role in translationally coupled mRNA turnover mediated by the c-fos major coding-region determinant. Genes Dev. *18*, 2010–2023.

Chen, Z., Trotman, L.C., Shaffer, D., Lin, H.-K., Dotan, Z.A., Niki, M., Koutcher, J.A., Scher, H.I., Ludwig, T., Gerald, W., et al. (2005). Crucial role of p53-dependent cellular senescence in suppression of Pten-deficient tumorigenesis. Nature *436*, 725–730.

Childs, B.G., Baker, D.J., Kirkland, J.L., Campisi, J., and van Deursen, J.M. (2014). Senescence and apoptosis: dueling or complementary cell fates? EMBO Rep. *15*, 1139–1153.

Childs, B.G., Gluscevic, M., Baker, D.J., Laberge, R.-M., Marquess, D., Dananberg, J., and van Deursen, J.M. (2017). Senescent cells: an emerging target for diseases of ageing. Nat. Rev. Drug Discov. *16*, 718–735.

Choe, J., Kim, K.M., Park, S., Lee, Y.K., Song, O.-K., Kim, M.K., Lee, B.-G., Song, H.K., and Kim, Y.K. (2013). Rapid degradation of replication-dependent histone mRNAs largely occurs on mRNAs bound by nuclear cap-binding proteins 80 and 20. Nucleic Acids Res. *41*, 1307–1318.

Choe, J., Ahn, S.H., and Kim, Y.K. (2014). The mRNP remodeling mediated by UPF1 promotes rapid degradation of replication-dependent histone mRNA. Nucleic Acids Res. *42*, 9334–9349.

Choudhury, A.R., Ju, Z., Djojosubroto, M.W., Schienke, A., Lechel, A., Schaetzlein, S., Jiang, H., Stepczynska, A., Wang, C., Buer, J., et al. (2007). Cdkn1a deletion improves stem cell function and lifespan of mice with dysfunctional telomeres without accelerating cancer formation. Nat. Genet. *39*, 99–105.

Collado, M., Gil, J., Efeyan, A., Guerra, C., Schuhmacher, A.J., Barradas, M., Benguría, A., Zaballos, A., Flores, J.M., Barbacid, M., et al. (2005). Senescence in premalignant tumours. Nature *436*, 642–642.

Cooper, T.A., Wan, L., and Dreyfuss, G. (2009). RNA and Disease. Cell *136*, 777–793.

Coppé, J.-P., Kauser, K., Campisi, J., and Beauséjour, C.M. (2006). Secretion of Vascular Endothelial Growth Factor by Primary Human Fibroblasts at Senescence. J. Biol. Chem. *281*, 29568–29574.

Coppé, J.-P., Patil, C.K., Rodier, F., Sun, Y., Muñoz, D.P., Goldstein, J., Nelson, P.S., Desprez, P.-Y., and Campisi, J. (2008). Senescence-Associated Secretory Phenotypes Reveal Cell-Nonautonomous Functions of Oncogenic RAS and the p53 Tumor Suppressor. PLoS Biol. *6*, e301.

Coppé, J.-P., Desprez, P.-Y., Krtolica, A., and Campisi, J. (2010). The Senescence-Associated Secretory Phenotype: The Dark Side of Tumor Suppression. Annu. Rev. Pathol. Mech. Dis. *5*, 99–118.

Coppé, J.-P., Rodier, F., Patil, C.K., Freund, A., Desprez, P.-Y., and Campisi, J. (2011). Tumor Suppressor and Aging Biomarker p16INK4a Induces Cellular Senescence without the Associated Inflammatory Secretory Phenotype. J. Biol. Chem. *286*, 36396–36403.

Cornelis, S. (2005). UNR translation can be driven by an IRES element that is negatively regulated by polypyrimidine tract binding protein. Nucleic Acids Res. *33*, 3095–3108.

Courtois-Cox, S., Jones, S.L., and Cichowski, K. (2008). Many roads lead to oncogene-induced senescence. Oncogene *27*, 2801–2809.

Dabrowski, M., Bukowy-Bieryllo, Z., and Zietkiewicz, E. (2015). Translational readthrough potential of natural termination codons in eucaryotes – The impact of RNA sequence. RNA Biol. *12*, 950–958.

Darnell, R.B. (2010). RNA Regulation in Neurologic Disease and Cancer. Cancer Res. Treat. *42*, 125.

Demaria, M., Ohtani, N., Youssef, S.A., Rodier, F., Toussaint, W., Mitchell, J.R., Laberge, R.-M., Vijg, J., Van Steeg, H., Dollé, M.E.T., et al. (2014). An Essential Role for Senescent Cells in Optimal Wound Healing through Secretion of PDGF-AA. Dev. Cell *31*, 722–733.

Demaria, M., Desprez, P.Y., Campisi, J., and Velarde, M.C. (2015). Cell Autonomous and Non-Autonomous Effects of Senescent Cells in the Skin. J. Invest. Dermatol. *135*, 1722–1726.

Denoyelle, C., Abou-Rjaily, G., Bezrookove, V., Verhaegen, M., Johnson, T.M., Fullen, D.R., Pointer, J.N., Gruber, S.B., Su, L.D., Nikiforov, M.A., et al. (2006). Anti-oncogenic role of the endoplasmic reticulum differentially activated by mutations in the MAPK pathway. Nat. Cell Biol. *8*, 1053–1063.

van Deursen, J.M. (2014). The role of senescent cells in ageing. Nature *509*, 439–446.

Di Micco, R., Fumagalli, M., Cicalese, A., Piccinin, S., Gasparini, P., Luise, C., Schurra, C., Garre', M., Giovanni Nuciforo, P., Bensimon, A., et al. (2006). Oncogene-induced senescence is a DNA damage response triggered by DNA hyper-replication. Nature *444*, 638–642.

Dimri, G.P., Lee, X., Basile, G., Acosta, M., Scott, G., Roskelley, C., Medrano, E.E., Linskens, M., Rubelj, I., and Pereira-Smith, O. (1995). A biomarker that identifies senescent human cells in culture and in aging skin in vivo. Proc. Natl. Acad. Sci. *92*, 9363–9367.

Dinur, M., Kilav, R., Sela-Brown, A., Jacquemin-Sablon, H., and Naveh-Many, T. (2006). *In Vitro* Evidence that Upstream of N- *ras* Participates in the Regulation of Parathyroid Hormone Messenger Ribonucleic Acid Stability. Mol. Endocrinol. *20*, 1652–1660.

Dirac, A.M.G., and Bernards, R. (2003). Reversal of Senescence in Mouse Fibroblasts through Lentiviral Suppression of p53. J. Biol. Chem. *278*, 11731–11734.

Dominski, Z., and Marzluff, W.F. (2007). Formation of the 3' end of histone mRNA: getting closer to the end. Gene *396*, 373–390.

Dominski, Z., Sumerel, J., Hanson, R.J., and Marzluff, W.F. (1995). The polyribosomal protein bound to the 3' end of histone mRNA can function in histone pre-mRNA processing. RNA N. Y. N *1*, 915–923.

Dominski, Z., Yang, X., and Marzluff, W.F. (2005). The Polyadenylation Factor CPSF-73 Is Involved in Histone-Pre-mRNA Processing. Cell *123*, 37–48.

Dormoy-Raclet, V., Markovits, J., Jacquemin-Sablon, A., and Jacquemin-Sablon, H. (2005). Regulation of Unr Expression by 5'- and 3'-Untranslated Regions of its mRNA through Modulation of Stability and IRES Mediated Translation. RNA Biol. *2*, 112–120.

Dormoy-Raclet, V., Markovits, J., Malato, Y., Huet, S., Lagarde, P., Montaudon, D., Jacquemin-Sablon, A., and Jacquemin-Sablon, H. (2007). Unr, a cytoplasmic RNA-binding protein with cold-shock domains, is involved in control of apoptosis in ES and HuH7 cells. Oncogene *26*, 2595–2605.

Duncan, K. (2006). Sex-lethal imparts a sex-specific function to UNR by recruiting it to the msl-2 mRNA 3' UTR: translational repression for dosage compensation. Genes Dev. *20*, 368–379.

Duncan, K.E., Strein, C., and Hentze, M.W. (2009). The SXL-UNR Corepressor Complex Uses a PABP-Mediated Mechanism to Inhibit Ribosome Recruitment to msl-2 mRNA. Mol. Cell *36*, 571–582.

Duval, M., Korepanov, A., Fuchsbauer, O., Fechter, P., Haller, A., Fabbretti, A., Choulier, L., Micura, R., Klaholz, B.P., Romby, P., et al. (2013). Escherichia coli Ribosomal Protein S1 Unfolds Structured mRNAs Onto the Ribosome for Active Translation Initiation. PLoS Biol. *11*, e1001731.

Efeyan, A., and Serrano, M. (2007). p53: Guardian of the Genome and Policeman of the Oncogenes. Cell Cycle *6*, 1006–1010.

Elatmani, H., Dormoy-Raclet, V., Dubus, P., Dautry, F., Chazaud, C., and Jacquemin-Sablon, H. (2011). The RNA-Binding Protein Unr Prevents Mouse Embryonic Stem Cells Differentiation Toward the Primitive Endoderm Lineage. STEM CELLS *29*, 1504–1516.

Evan, G.I., and d'Adda di Fagagna, F. (2009). Cellular senescence: hot or what? Curr. Opin. Genet. Dev. *19*, 25–31.

Fabian, M.R., Sonenberg, N., and Filipowicz, W. (2010). Regulation of mRNA Translation and Stability by microRNAs. Annu. Rev. Biochem. *79*, 351–379.

Fadaka, A., Ajiboye, B., Ojo, O., Adewale, O., Olayide, I., and Emuowhochere, R. (2017). Biology of glucose metabolization in cancer cells. J. Oncol. Sci. *3*, 45–51.

Fagagna, F. d'Adda di, Reaper, P.M., Clay-Farrace, L., Fiegler, H., Carr, P., von Zglinicki, T., Saretzki, G., Carter, N.P., and Jackson, S.P. (2003). A DNA damage checkpoint response in telomere-initiated senescence. Nature *426*, 194–198.

Ferrer, N., Garcia-Espana, A., Jeffers, M., and Pellicer, A. (1999). The unr Gene: Evolutionary Considerations and Nucleic Acid-Binding Properties of Its Long Isoform Product. DNA Cell Biol. *18*, 209–218.

Freund, A., Laberge, R.-M., Demaria, M., and Campisi, J. (2012). Lamin B1 loss is a senescence-associated biomarker. Mol. Biol. Cell *23*, 2066–2075.

Frey, M.R., and Matera, A.G. (1995). Coiled bodies contain U7 small nuclear RNA and associate with specific DNA sequences in interphase human cells. Proc. Natl. Acad. Sci. *92*, 5915–5919.

Fumagalli, M., Rossiello, F., Clerici, M., Barozzi, S., Cittaro, D., Kaplunov, J.M., Bucci, G., Dobreva, M., Matti, V., Beausejour, C.M., et al. (2012). Telomeric DNA damage is irreparable and causes persistent DNA-damage-response activation. Nat. Cell Biol. *14*, 355–365.

Gebauer, F., Grskovic, M., and Hentze, M.W. (2003). Drosophila Sex-Lethal Inhibits the Stable Association of the 40S Ribosomal Subunit with msl-2 mRNA. Mol. Cell *11*, 1397–1404.

Gebauer, F., Preiss, T., and Hentze, M.W. (2012). From Cis-Regulatory Elements to Complex RNPs and Back. Cold Spring Harb. Perspect. Biol. *4*, a012245–a012245.

Gerstberger, S., Hafner, M., and Tuschl, T. (2014a). A census of human RNA-binding proteins. Nat. Rev. Genet. *15*, 829–845.

Gerstberger, S., Hafner, M., Ascano, M., and Tuschl, T. (2014b). Evolutionary Conservation and Expression of Human RNA-Binding Proteins and Their Role in Human Genetic Disease. In Systems Biology of RNA Binding Proteins, G.W. Yeo, ed. (New York, NY: Springer New York), pp. 1–55.

Ghosh, K., and Capell, B.C. (2016). The Senescence-Associated Secretory Phenotype: Critical Effector in Skin Cancer and Aging. J. Invest. Dermatol. *136*, 2133–2139.

Glisovic, T., Bachorik, J.L., Yong, J., and Dreyfuss, G. (2008). RNA-binding proteins and post-transcriptional gene regulation. FEBS Lett. *582*, 1977–1986.

Gorgoulis, V.G., and Halazonetis, T.D. (2010). Oncogene-induced senescence: the bright and dark side of the response. Curr. Opin. Cell Biol. *22*, 816–827.

Graindorge, A., Militti, C., and Gebauer, F. (2011). Posttranscriptional control of X-chromosome dosage compensation: RNA regulation in dosage compensation. Wiley Interdiscip. Rev. RNA *2*, 534–545.

Graumann, P.L., and Marahiel, M.A. (1998). A superfamily of proteins that contain the cold-shock domain. Trends Biochem. Sci. *23*, 286–290.

Graves, R. (1987). Translation is required for regulation of histone mRNA degradation. Cell *48*, 615–626.

Greene, M.A., and Loeser, R.F. (2015). Aging-related inflammation in osteoarthritis. Osteoarthritis Cartilage *23*, 1966–1971.

Grosset, C., Chen, C.-Y.A., Xu, N., Sonenberg, N., Jacquemin-Sablon, H., and Shyu, A.-B. (2000). A Mechanism for Translationally Coupled mRNA Turnover: Interaction between the Poly(A) Tail and a c-fos RNA Coding Determinant via a Protein Complex. Cell *103*, 29–40.

Halazonetis, T.D., Gorgoulis, V.G., and Bartek, J. (2008). An Oncogene-Induced DNA Damage Model for Cancer Development. Science *319*, 1352–1355.

Hannus, M., Beitzinger, M., Engelmann, J.C., Weickert, M.-T., Spang, R., Hannus, S., and Meister, G. (2014). siPools: highly complex but accurately defined siRNA pools eliminate off-target effects. Nucleic Acids Res. *42*, 8049–8061.

Harley, C.B., Futcher, A.B., and Greider, C.W. (1990). Telomeres shorten during ageing of human fibroblasts. Nature *345*, 458–460.

Harvey, R.F., and Willis, A.E. (2018). Post-transcriptional control of stress responses in cancer. Curr. Opin. Genet. Dev. *48*, 30–35.

Harvey, K.F., Zhang, X., and Thomas, D.M. (2013). The Hippo pathway and human cancer. Nat. Rev. Cancer *13*, 246–257.

Hayflick, L. (1965). The limited in vitro lifetime of human diploid cell strains. Exp. Cell Res. *37*, 614–636.

Hayflick, L., and Moorhead, P.S. (1961). The serial cultivation of human diploid cell strains. Exp. Cell Res. *25*, 585–621.

He, F., and Jacobson, A. (2015). Nonsense-Mediated mRNA Decay: Degradation of Defective Transcripts Is Only Part of the Story. Annu. Rev. Genet. *49*, 339–366.

Hennig, J., Militti, C., Popowicz, G.M., Wang, I., Sonntag, M., Geerlof, A., Gabel, F., Gebauer, F., and Sattler, M. (2014). Structural basis for the

assembly of the Sxl–Unr translation regulatory complex. Nature *515*, 287–290.

Hentze, M.W., Castello, A., Schwarzl, T., and Preiss, T. (2018). A brave new world of RNA-binding proteins. Nat. Rev. Mol. Cell Biol. *19*, 327–341.

Hernandez-Segura, A., de Jong, T.V., Melov, S., Guryev, V., Campisi, J., and Demaria, M. (2017). Unmasking Transcriptional Heterogeneity in Senescent Cells. Curr. Biol. *27*, 2652-2660.e4.

Hoare, M., Young, A.R.J., and Narita, M. (2011). Autophagy in cancer: Having your cake and eating it. Semin. Cancer Biol.

Hoefig, K.P., Rath, N., Heinz, G.A., Wolf, C., Dameris, J., Schepers, A., Kremmer, E., Ansel, K.M., and Heissmeyer, V. (2013). Eri1 degrades the stem-loop of oligouridylated histone mRNAs to induce replication-dependent decay. Nat. Struct. Mol. Biol. *20*, 73–81.

Horos, R., IJspeert, H., Pospisilova, D., Sendtner, R., Andrieu-Soler, C., Taskesen, E., Nieradka, A., Cmejla, R., Sendtner, M., Touw, I.P., et al. (2012). Ribosomal deficiencies in Diamond-Blackfan anemia impair translation of transcripts essential for differentiation of murine and human erythroblasts. Blood *119*, 262–272.

Hunt, S.L., and Jackson, R.J. (1999). Polypyrimidine-tract binding protein (PTB) is necessary, but not sufficient, for efficient internal initiation of translation of human rhinovirus-2 RNA. RNA *5*, 344–359.

Hunt, S.L., Hsuan, J.J., Totty, N., and Jackson, R.J. (1999). unr, a cellular cytoplasmic RNA-binding protein with five cold-shock domains, is required for internal initiation of translation of human rhinovirus RNA. Genes Dev. *13*, 437–448.

Iadevaia, V., and Gerber, A. (2015). Combinatorial Control of mRNA Fates by RNA-Binding Proteins and Non-Coding RNAs. Biomolecules *5*, 2207–2222.

Imig, J., Kanitz, A., and Gerber, A.P. (2012). RNA regulons and the RNA-protein interaction network. Biomol. Concepts *3*.

Jacquemin-Sablon, H., and Dautry, F. (1992). Organization of the unr/N-ras locus: characterization of the promoter region of the human unr gene. Nucleic Acids Res. *20*, 6355–6361.

Jeffers, M., Paciucci, R., and Pellicer, A. (1990). Characterization of unr; a gene closely linked to N-ras. Nucleic Acids Res. *18*, 4891–4899.

Jensen, K.B., Driskell, R.R., and Watt, F.M. (2010). Assaying proliferation and differentiation capacity of stem cells using disaggregated adult mouse epidermis. Nat. Protoc. *5*, 898–911.

Jun, J.-I., and Lau, L.F. (2010). The matricellular protein CCN1 induces fibroblast senescence and restricts fibrosis in cutaneous wound healing. Nat. Cell Biol. *12*, 676–685.

Kamakaka, R.T. (2005). Histone variants: deviants? Genes Dev. *19*, 295–316.

Kamenska, A., Simpson, C., Vindry, C., Broomhead, H., Bénard, M., Ernoult-Lange, M., Lee, B.P., Harries, L.W., Weil, D., and Standart, N. (2016). The DDX6–4E-T interaction mediates translational repression and P-body assembly. Nucleic Acids Res. *44*, 6318–6334.

Kang, T.-W., Yevsa, T., Woller, N., Hoenicke, L., Wuestefeld, T., Dauch, D., Hohmeyer, A., Gereke, M., Rudalska, R., Potapova, A., et al. (2011). Senescence surveillance of pre-malignant hepatocytes limits liver cancer development. Nature *479*, 547–551.

Kaygun, H., and Marzluff, W.F. (2005a). Translation Termination Is Involved in Histone mRNA Degradation when DNA Replication Is Inhibited. Mol. Cell. Biol. *25*, 6879–6888.

Kaygun, H., and Marzluff, W.F. (2005b). Regulated degradation of replication-dependent histone mRNAs requires both ATR and Upf1. Nat. Struct. Mol. Biol. *12*, 794–800.

Keene, J.D. (2001). Ribonucleoprotein infrastructure regulating the flow of genetic information between the genome and the proteome. Proc. Natl. Acad. Sci. *98*, 7018–7024.

Keene, J.D. (2007). RNA regulons: coordination of post-transcriptional events. Nat. Rev. Genet. *8*, 533–543.

Kessenbrock, K., Plaks, V., and Werb, Z. (2010). Matrix Metalloproteinases: Regulators of the Tumor Microenvironment. Cell *141*, 52–67.

Kosar, M., Bartkova, J., Hubackova, S., Hodny, Z., Lukas, J., and Bartek, J. (2011). Senescence-associated heterochromatin foci are dispensable for cellular senescence, occur in a cell type- and insult-dependent manner and follow expression of p16 $^{ink4a}$. Cell Cycle *10*, 457–468.

Kouzarides, T. (2007). Chromatin Modifications and Their Function. Cell *128*, 693–705.

Krtolica, A., Parrinello, S., Lockett, S., Desprez, P.-Y., and Campisi, J. (2001). Senescent fibroblasts promote epithelial cell growth and tumorigenesis: A link between cancer and aging. Proc. Natl. Acad. Sci. *98*, 12072–12077.

Kuilman, T., Michaloglou, C., Vredeveld, L.C.W., Douma, S., van Doorn, R., Desmet, C.J., Aarden, L.A., Mooi, W.J., and Peeper, D.S. (2008). Oncogene-Induced Senescence Relayed by an Interleukin-Dependent Inflammatory Network. Cell *133*, 1019–1031.

Kuilman, T., Michaloglou, C., Mooi, W.J., and Peeper, D.S. (2010). The essence of senescence. Genes Dev. *24*, 2463–2479.

Laberge, R.-M., Awad, P., Campisi, J., and Desprez, P.-Y. (2012). Epithelial-Mesenchymal Transition Induced by Senescent Fibroblasts. Cancer Microenviron. *5*, 39–44.

Lackey, P.E., Welch, J.D., and Marzluff, W.F. (2016). TUT7 catalyzes the uridylation of the 3′ end for rapid degradation of histone mRNA. RNA *22*, 1673–1688.

Lee, B.Y., Han, J.A., Im, J.S., Morrone, A., Johung, K., Goodwin, E.C., Kleijer, W.J., DiMaio, D., and Hwang, E.S. (2006). Senescence-associated β-galactosidase is lysosomal β-galactosidase. Aging Cell *5*, 187–195.

Lee, H.J., Bartsch, D., Xiao, C., Guerrero, S., Ahuja, G., Schindler, C., Moresco, J.J., Yates, J.R., Gebauer, F., Bazzi, H., et al. (2017). A post-transcriptional program coordinated by CSDE1 prevents intrinsic neural differentiation of human embryonic stem cells. Nat. Commun. *8*, 1456.

Li, G., and Reinberg, D. (2011). Chromatin higher-order structures and gene regulation. Curr. Opin. Genet. Dev. *21*, 175–186.

Li, T., Kon, N., Jiang, L., Tan, M., Ludwig, T., Zhao, Y., Baer, R., and Gu, W. (2012). Tumor suppression in the absence of p53-mediated cell cycle arrest, apoptosis, and senescence. Cell *149*, 1269–1283.

Liang, H., He, S., Yang, J., Jia, X., Wang, P., Chen, X., Zhang, Z., Zou, X., McNutt, M.A., Shen, W.H., et al. (2014). PTENα, a PTEN Isoform Translated through Alternative Initiation, Regulates Mitochondrial Function and Energy Metabolism. Cell Metab. *19*, 836–848.

Lichti, U., Anders, J., and Yuspa, S.H. (2008). Isolation and short-term culture of primary keratinocytes, hair follicle populations and dermal cells from newborn mice and keratinocytes from adult mice for in vitro analysis and for grafting to immunodeficient mice. Nat. Protoc. *3*, 799–810.

Lin, A.W., and Lowe, S.W. (2001). Oncogenic ras activates the ARF-p53 pathway to suppress epithelial cell transformation. Proc. Natl. Acad. Sci. *98*, 5025–5030.

Lin, A.W., Barradas, M., Stone, J.C., van Aelst, L., Serrano, M., and Lowe, S.W. (1998). Premature senescence involving p53 and p16 is activated in response to constitutive MEK/MAPK mitogenic signaling. Genes Dev. *12*, 3008–3019.

Liu, D., and Hornsby, P.J. (2007). Senescent Human Fibroblasts Increase the Early Growth of Xenograft Tumors via Matrix Metalloproteinase Secretion. Cancer Res. *67*, 3117–3126.

Liu, X., Ding, J., and Meng, L. (2018). Oncogene-induced senescence: a double edged sword in cancer. Acta Pharmacol. Sin.

Lowe, S.W., and Sherr, C.J. (2003). Tumor suppression by Ink4a–Arf: progress and puzzles. Curr. Opin. Genet. Dev. *13*, 77–83.

Lukong, K.E., Chang, K., Khandjian, E.W., and Richard, S. (2008). RNA-binding proteins in human genetic disease. Trends Genet. *24*, 416–425.

Lykke-Andersen, S., and Jensen, T.H. (2015). Nonsense-mediated mRNA decay: an intricate machinery that shapes transcriptomes. Nat. Rev. Mol. Cell Biol. *16*, 665–677.

Malaquin, N., Vercamer, C., Bouali, F., Martien, S., Deruy, E., Wernert, N., Chwastyniak, M., Pinet, F., Abbadie, C., and Pourtier, A. (2013). Senescent Fibroblasts Enhance Early Skin Carcinogenic Events via a Paracrine MMP-PAR-1 Axis. PLoS ONE *8*, e63607.

Malumbres, M., Perez De Castro, I., Hernandez, M.I., Jimenez, M., Corral, T., and Pellicer, A. (2000). Cellular Response to Oncogenic Ras Involves Induction of the Cdk4 and Cdk6 Inhibitor p15INK4b. Mol. Cell. Biol. *20*, 2915–2925.

Martin, F., Barends, S., Jaeger, S., Schaeffer, L., Prongidi-Fix, L., and Eriani, G. (2011). Cap-Assisted Internal Initiation of Translation of Histone H4. Mol. Cell *41*, 197–209.

Martinez-Useros, J., Georgiev-Hristov, T., Fernández-Aceñero, M.J., Borrero-Palacios, A., Indacochea, A., Guerrero, S., Li, W., Cebrián, A., Gómez del Pulgar, T., Puime-Otin, A., et al. (2017). UNR/CDSE1 expression as prognosis biomarker in resectable pancreatic ductal adenocarcinoma patients: A proof-of-concept. PLOS ONE *12*, e0182044.

Marzluff, W.F., and Duronio, R.J. (2002). Histone mRNA expression: multiple levels of cell cycle regulation and important developmental consequences. Curr. Opin. Cell Biol. *14*, 692–699.

Marzluff, W.F., and Koreski, K.P. (2017). Birth and Death of Histone mRNAs. Trends Genet. *33*, 745–759.

Marzluff, W.F., Gongidi, P., Woods, K.R., Jin, J., and Maltais, L.J. (2002). The Human and Mouse Replication-Dependent Histone Genes. Genomics *80*, 487–498.

Matjusaitis, M., Chin, G., Sarnoski, E.A., and Stolzing, A. (2016). Biomarkers to identify and isolate senescent cells. Ageing Res. Rev. *29*, 1–12.

Mayr, C. (2017). Regulation by 3′-Untranslated Regions. Annu. Rev. Genet. *51*, 171–194.

Maze, I., Noh, K.-M., Soshnev, A.A., and Allis, C.D. (2014). Every amino acid matters: essential contributions of histone variants to mammalian development and disease. Nat. Rev. Genet. *15*, 259–271.

McCormick, C., and Khaperskyy, D.A. (2017). Translation inhibition and stress granules in the antiviral immune response. Nat. Rev. Immunol. *17*, 647–660.

Merrick, W.C., and Pavitt, G.D. (2018). Protein Synthesis Initiation in Eukaryotic Cells. Cold Spring Harb. Perspect. Biol. a033092.

Mihailovich, M., Militti, C., Gabaldón, T., and Gebauer, F. (2010). Eukaryotic cold shock domain proteins: highly versatile regulators of gene expression. BioEssays *32*, 109–118.

Militti, C., Maenner, S., Becker, P.B., and Gebauer, F. (2014). UNR facilitates the interaction of MLE with the lncRNA *roX2* during *Drosophila* dosage compensation. Nat. Commun. *5*, 4762.

Mitchell, S.F., and Parker, R. (2014). Principles and Properties of Eukaryotic mRNPs. Mol. Cell *54*, 547–558.

Mitchell, S.A., Spriggs, K.A., Coldwell, M.J., Jackson, R.J., and Willis, A.E. (2003). The Apaf-1 Internal Ribosome Entry Segment Attains the Correct Structural Conformation for Function via Interactions with PTB and unr. Mol. Cell *11*, 757–771.

Moore, K.S., Yagci, N., van Alphen, F., Paolini, N.A., Horos, R., Held, N.M., Houtkooper, R.H., van den Akker, E., Meijer, A.B., ‘t Hoen, P.A.C.,

et al. (2018). Csde1 binds transcripts involved in protein homeostasis and controls their expression in an erythroid cell line. Sci. Rep. *8*.

Mullen, T.E., and Marzluff, W.F. (2008). Degradation of histone mRNA requires oligouridylation followed by decapping and simultaneous degradation of the mRNA both 5' to 3' and 3' to 5'. Genes Dev. *22*, 50–65.

Muñoz-Espín, D., and Serrano, M. (2014). Cellular senescence: from physiology to pathology. Nat. Rev. Mol. Cell Biol. *15*, 482–496.

Muñoz-Espín, D., Cañamero, M., Maraver, A., Gómez-López, G., Contreras, J., Murillo-Cuesta, S., Rodríguez-Baeza, A., Varela-Nieto, I., Ruberte, J., Collado, M., et al. (2013). Programmed Cell Senescence during Mammalian Embryonic Development. Cell *155*, 1104–1118.

Munro, J., Barr, N.I., Ireland, H., Morrison, V., and Parkinson, E.K. (2004). Histone deacetylase inhibitors induce a senescence-like state in human cells by a p16-dependent mechanism that is independent of a mitotic clock. Exp. Cell Res. *295*, 525–538.

Narita, M., Nuñez, S., Heard, E., Narita, M., Lin, A.W., Hearn, S.A., Spector, D.L., Hannon, G.J., and Lowe, S.W. (2003). Rb-Mediated Heterochromatin Formation and Silencing of E2F Target Genes during Cellular Senescence. Cell *113*, 703–716.

Neusiedler, J., Mocquet, V., Limousin, T., Ohlmann, T., Morris, C., and Jalinot, P. (2012). INT6 interacts with MIF4GD/SLIP1 and is necessary for efficient histone mRNA translation. RNA *18*, 1163–1177.

Neves, J., Demaria, M., Campisi, J., and Jasper, H. (2015). Of Flies, Mice, and Men: Evolutionarily Conserved Tissue Damage Responses and Aging. Dev. Cell *32*, 9–18.

Newkirk, K., Feng, W., Jiang, W., Tejero, R., Emerson, S.D., Inouye, M., and Montelione, G.T. (1994). Solution NMR structure of the major cold shock protein (CspA) from Escherichia coli: identification of a binding epitope for DNA. Proc. Natl. Acad. Sci. *91*, 5114–5118.

O'Brien, W., Stenman, G., and Sager, R. (1986). Suppression of tumor growth by senescence in virally transformed human fibroblasts. Proc. Natl. Acad. Sci. *83*, 8659–8663.

O'Sullivan, R.J., and Karlseder, J. (2010). Telomeres: protecting chromosomes against genome instability. Nat. Rev. Mol. Cell Biol. *11*, 171–181.

Parrinello, S. (2005). Stromal-epithelial interactions in aging and cancer: senescent fibroblasts alter epithelial cell differentiation. J. Cell Sci. *118*, 485–496.

Patalano, S., Mihailovich, M., Belacortu, Y., Paricio, N., and Gebauer, F. (2009). Dual sex-specific functions of Drosophila Upstream of N-ras in the control of X chromosome dosage compensation. Development *136*, 689–698.

Patel, G.P., Ma, S., and Bag, J. (2005). The autoregulatory translational control element of poly(A)-binding protein mRNA forms a heteromeric ribonucleoprotein complex. Nucleic Acids Res. *33*, 7074–7089.

Peccarelli, M., and Kebaara, B.W. (2014). Regulation of Natural mRNAs by the Nonsense-Mediated mRNA Decay Pathway. Eukaryot. Cell *13*, 1126–1135.

Pereira, B., Billaud, M., and Almeida, R. (2017). RNA-Binding Proteins in Cancer: Old Players and New Actors. Trends Cancer *3*, 506–528.

Pérez-Mancera, P.A., Young, A.R.J., and Narita, M. (2014). Inside and out: the activities of senescence in cancer. Nat. Rev. Cancer *14*, 547–558.

Pillai, R.S. (2001). Purified U7 snRNPs lack the Sm proteins D1 and D2 but contain Lsm10, a new 14 kDa Sm D1-like protein. EMBO J. *20*, 5470–5479.

Pillai, R.S. (2003). Unique Sm core structure of U7 snRNPs: assembly by a specialized SMN complex and the role of a new component, Lsm11, in histone RNA processing. Genes Dev. *17*, 2321–2333.

Popp, M.W., and Maquat, L.E. (2016). Leveraging Rules of Nonsense-Mediated mRNA Decay for Genome Engineering and Personalized Medicine. Cell *165*, 1319–1322.

Rao, S.G., and Jackson, J.G. (2016). SASP: Tumor Suppressor or Promoter? Yes! Trends Cancer *2*, 676–687.

Ray, S., and Anderson, E.C. (2016). Stimulation of translation by human Unr requires cold shock domains 2 and 4, and correlates with poly(A) binding protein interaction. Sci. Rep. *6*.

Ray, S., Catnaigh, P.Ó., and Anderson, E.C. (2015). Post-transcriptional regulation of gene expression by Unr. Biochem. Soc. Trans. *43*, 323–327.

Ritschka, B., Storer, M., Mas, A., Heinzmann, F., Ortells, M.C., Morton, J.P., Sansom, O.J., Zender, L., and Keyes, W.M. (2017). The

senescence-associated secretory phenotype induces cellular plasticity and tissue regeneration. Genes Dev. *31*, 172–183.

Rodier, F., Coppé, J.-P., Patil, C.K., Hoeijmakers, W.A.M., Muñoz, D.P., Raza, S.R., Freund, A., Campeau, E., Davalos, A.R., and Campisi, J. (2009). Persistent DNA damage signalling triggers senescence-associated inflammatory cytokine secretion. Nat. Cell Biol. *11*, 973–979.

Romagosa, C., Simonetti, S., López-Vicente, L., Mazo, A., Lleonart, M.E., Castellvi, J., and Ramon y Cajal, S. (2011). p16Ink4a overexpression in cancer: a tumor suppressor gene associated with senescence and high-grade tumors. Oncogene *30*, 2087–2097.

Roos, W.P., and Kaina, B. (2006). DNA damage-induced cell death by apoptosis. Trends Mol. Med. *12*, 440–450.

Sabath, I., Skrajna, A., Yang, X. -c., Dadlez, M., Marzluff, W.F., and Dominski, Z. (2013). 3'-End processing of histone pre-mRNAs in Drosophila: U7 snRNP is associated with FLASH and polyadenylation factors. RNA *19*, 1726–1744.

Sage, J., Miller, A.L., Pérez-Mancera, P.A., Wysocki, J.M., and Jacks, T. (2003). Acute mutation of retinoblastoma gene function is sufficient for cell cycle re-entry. Nature *424*, 223–228.

Saldi, T., Fong, N., and Bentley, D.L. (2018). Transcription elongation rate affects nascent histone pre-mRNA folding and 3′ end processing. Genes Dev. *32*, 297–308.

Saltel, F., Giese, A., Azzi, L., Elatmani, H., Costet, P., Ezzoukhry, Z., Dugot-Senant, N., Miquerol, L., Boussadia, O., Wodrich, H., et al. (2017). Unr defines a novel class of nucleoplasmic reticulum involved in mRNA translation. J. Cell Sci. *130*, 1796–1808.

Sanchez, R., and Marzluff, W.F. (2002). The Stem-Loop Binding Protein Is Required for Efficient Translation of Histone mRNA In Vivo and In Vitro. Mol. Cell. Biol. *22*, 7093–7104.

Sarkisian, C.J., Keister, B.A., Stairs, D.B., Boxer, R.B., Moody, S.E., and Chodosh, L.A. (2007). Dose-dependent oncogene-induced senescence in vivo and its evasion during mammary tumorigenesis. Nat. Cell Biol. *9*, 493–505.

Schepens, B., Tinton, S.A., Bruynooghe, Y., Parthoens, E., Haegman, M., Beyaert, R., and Cornelis, S. (2007). A role for hnRNP C1/C2 and Unr in internal initiation of translation during mitosis. EMBO J. *26*, 158–169.

Schwartz, J.C., Wang, X., Podell, E.R., and Cech, T.R. (2013). RNA Seeds Higher-Order Assembly of FUS Protein. Cell Rep. *5*, 918–925.

Serrano, M., Lin, A.W., McCurrach, M.E., Beach, D., and Lowe, S.W. (1997). Oncogenic ras Provokes Premature Cell Senescence Associated with Accumulation of p53 and p16INK4a. Cell *88*, 593–602.

Shamma, A., Takegami, Y., Miki, T., Kitajima, S., Noda, M., Obara, T., Okamoto, T., and Takahashi, C. (2009). Rb Regulates DNA Damage Response and Cellular Senescence through E2F-Dependent Suppression of N-Ras Isoprenylation. Cancer Cell *15*, 255–269.

Sharpless, N.E., and Sherr, C.J. (2015). Forging a signature of in vivo senescence. Nat. Rev. Cancer *15*, 397–408.

Sherr, C.J. (2001). The INK4a/ARF network in tumour suppression. Nat. Rev. Mol. Cell Biol. *2*, 731–737.

Sherr, C.J., and DePinho, R.A. (2000). Cellular Senescence: Minireview Mitotic Clock or Culture Shock? Cell *102*, 407–410.

Shimi, T., Butin-Israeli, V., Adam, S.A., Hamanaka, R.B., Goldman, A.E., Lucas, C.A., Shumaker, D.K., Kosak, S.T., Chandel, N.S., and Goldman, R.D. (2011). The role of nuclear lamin B1 in cell proliferation and senescence. Genes Dev. *25*, 2579–2593.

Skrajna, A., Yang, X., Bucholc, K., Zhang, J., Hall, T.M.T., Dadlez, M., Marzluff, W.F., and Dominski, Z. (2017). U7 snRNP is recruited to histone pre-mRNA in a FLASH-dependent manner by two separate regions of the stem–loop binding protein. RNA *23*, 938–951.

Slevin, M.K., Meaux, S., Welch, J.D., Bigler, R., Miliani de Marval, P.L., Su, W., Rhoads, R.E., Prins, J.F., and Marzluff, W.F. (2014). Deep Sequencing Shows Multiple Oligouridylations Are Required for 3′ to 5′ Degradation of Histone mRNAs on Polyribosomes. Mol. Cell *53*, 1020–1030.

Sriram, A., Bohlen, J., and Teleman, A.A. (2018). Translation acrobatics: how cancer cells exploit alternate modes of translational initiation. EMBO Rep. e45947.

Storer, M., Mas, A., Robert-Moreno, A., Pecoraro, M., Ortells, M.C., Di Giacomo, V., Yosef, R., Pilpel, N., Krizhanovsky, V., Sharpe, J., et al. (2013). Senescence Is a Developmental Mechanism that Contributes to Embryonic Growth and Patterning. Cell *155*, 1119–1130.

Sullivan, K.D., Steiniger, M., and Marzluff, W.F. (2009). A Core Complex of CPSF73, CPSF100, and Symplekin May Form Two Different Cleavage

Factors for Processing of Poly(A) and Histone mRNAs. Mol. Cell *34*, 322–332.

Szostak, E., García-Beyaert, M., Guitart, T., Graindorge, A., Coll, O., and Gebauer, F. (2018). Hrp48 and eIF3d contribute to msl-2 mRNA translational repression. Nucleic Acids Res. *46*, 4099–4113.

Takai, H., Smogorzewska, A., and de Lange, T. (2003). DNA Damage Foci at Dysfunctional Telomeres. Curr. Biol. *13*, 1549–1556.

Tan, D., Marzluff, W.F., Dominski, Z., and Tong, L. (2013). Structure of Histone mRNA Stem-Loop, Human Stem-Loop Binding Protein, and 3'hExo Ternary Complex. Science *339*, 318–321.

Tavana, O., Benjamin, C.L., Puebla-Osorio, N., Sang, M., Ullrich, S.E., Ananthaswamy, H., and Zhu, C. (2010). Absence of p53-dependent apoptosis leads to UV radiation hypersensitivity, enhanced immunosuppression and cellular senescence. Cell Cycle *9*, 3348–3356.

Tinton, S.A., Schepen, B., Bruynooghe, Y., Beyaert, R., and Cornelis, S. (2005). Regulation of the cell-cycle-dependent internal ribosome entry site of the PITSLRE protein kinase: roles of Unr (upstream of N-ras) protein and phosphorylated translation initiation factor eIF-2α. 9.

Tonnessen-Murray, C.A., Lozano, G., and Jackson, J.G. (2017). The Regulation of Cellular Functions by the p53 Protein: Cellular Senescence. Cold Spring Harb. Perspect. Med. *7*, a026112.

Triqueneaux, G., Velten, M., Franzon, P., Dautry, F., and Jacquemin-Sablon, H. (1999). RNA binding specificity of Unr, a protein with five cold shock domains. Nucleic Acids Res. *27*, 1926–1934.

Uhlen, M., Fagerberg, L., Hallstrom, B.M., Lindskog, C., Oksvold, P., Mardinoglu, A., Sivertsson, A., Kampf, C., Sjostedt, E., Asplund, A., et al. (2015). Tissue-based map of the human proteome. Science *347*, 1260419–1260419.

Wajapeyee, N., Serra, R.W., Zhu, X., Mahalingam, M., and Green, M.R. (2008). Oncogenic BRAF Induces Senescence and Apoptosis through Pathways Mediated by the Secreted Protein IGFBP7. Cell *132*, 363–374.

Wang, W.-J., Cai, G.-Y., and Chen, X.-M. (2017). Cellular senescence, senescence-associated secretory phenotype, and chronic kidney disease. Oncotarget *8*, 64520–64533.

Weingarten-Gabbay, S., Elias-Kirma, S., Nir, R., Gritsenko, A.A., Stern-Ginossar, N., Yakhini, Z., Weinberger, A., and Segal, E. (2016).

Systematic discovery of cap-independent translation sequences in human and viral genomes. Science *351*, aad4939.

Whitfield, M.L. (2004). SLBP is associated with histone mRNA on polyribosomes as a component of the histone mRNP. Nucleic Acids Res. *32*, 4833–4842.

Wurth, L. (2012). Versatility of RNA-Binding Proteins in Cancer. Comp. Funct. Genomics *2012*, 1–11.

Wurth, L., Papasaikas, P., Olmeda, D., Bley, N., Calvo, G.T., Guerrero, S., Cerezo-Wallis, D., Martinez-Useros, J., García-Fernández, M., Hüttelmaier, S., et al. (2016). UNR/CSDE1 Drives a Post-transcriptional Program to Promote Melanoma Invasion and Metastasis. Cancer Cell *30*, 694–707.

Xu, Y., Li, N., Xiang, R., and Sun, P. (2014). Emerging roles of the p38 MAPK and PI3K/AKT/mTOR pathways in oncogene-induced senescence. Trends Biochem. Sci. *39*, 268–276.

Yang, X., Purdy, M., Marzluff, W.F., and Dominski, Z. (2006). Characterization of 3′hExo, a 3′ Exonuclease Specifically Interacting with the 3′ End of Histone mRNA. J. Biol. Chem. *281*, 30447–30454.

Yang, X.-C., Sabath, I., Debski, J., Kaus-Drobek, M., Dadlez, M., Marzluff, W.F., and Dominski, Z. (2013). A Complex Containing the CPSF73 Endonuclease and Other Polyadenylation Factors Associates with U7 snRNP and Is Recruited to Histone Pre-mRNA for 3'-End Processing. Mol. Cell. Biol. *33*, 28–37.

Ye, X., Wei, Y., Nalepa, G., and Harper, J.W. (2003). The Cyclin E/Cdk2 Substrate p220NPAT Is Required for S-Phase Entry, Histone Gene Expression, and Cajal Body Maintenance in Human Somatic Cells. Mol. Cell. Biol. *23*, 8586–8600.

Yosef, R., Pilpel, N., Tokarsky-Amiel, R., Biran, A., Ovadya, Y., Cohen, S., Vadai, E., Dassa, L., Shahar, E., Condiotti, R., et al. (2016). Directed elimination of senescent cells by inhibition of BCL-W and BCL-XL. Nat. Commun. *7*, 11190.

Youn, J.-Y., Dunham, W.H., Hong, S.J., Knight, J.D.R., Bashkurov, M., Chen, G.I., Bagci, H., Rathod, B., MacLeod, G., Eng, S.W.M., et al. (2018). High-Density Proximity Mapping Reveals the Subcellular Organization of mRNA-Associated Granules and Bodies. Mol. Cell *69*, 517-532.e11.

Young, A.R.J., Narita, M., Ferreira, M., Kirschner, K., Sadaie, M., Darot, J.F.J., Tavare, S., Arakawa, S., Shimizu, S., Watt, F.M., et al. (2009).

Autophagy mediates the mitotic senescence transition. Genes Dev. *23*, 798–803.

Zerbino, D.R., Achuthan, P., Akanni, W., Amode, M.R., Barrell, D., Bhai, J., Billis, K., Cummins, C., Gall, A., Girón, C.G., et al. (2018). Ensembl 2018. Nucleic Acids Res. *46*, D754–D761.

Zhan, T., Rindtorff, N., and Boutros, M. (2017). Wnt signaling in cancer. Oncogene *36*, 1461–1473.

Zhang, R., Poustovoitov, M.V., Ye, X., Santos, H.A., Chen, W., Daganzo, S.M., Erzberger, J.P., Serebriiskii, I.G., Canutescu, A.A., Dunbrack, R.L., et al. (2005). Formation of MacroH2A-Containing Senescence-Associated Heterochromatin Foci and Senescence Driven by ASF1a and HIRA. Dev. Cell *8*, 19–30.

Zheng, L., Dominski, Z., Yang, X.-C., Elms, P., Raska, C.S., Borchers, C.H., and Marzluff, W.F. (2003). Phosphorylation of Stem-Loop Binding Protein (SLBP) on Two Threonines Triggers Degradation of SLBP, the Sole Cell Cycle-Regulated Factor Required for Regulation of Histone mRNA Processing, at the End of S Phase. Mol. Cell. Biol. *23*, 1590–1601.

Zuckerman, V., Wolyniec, K., Sionov, R.V., Haupt, S., and Haupt, Y. (2009). Tumour suppression by p53: the importance of apoptosis and cellular senescence. J. Pathol. n/a-n/a.